1990-12

Nucleate pool boiling performance of small High Flux and Turbo-B tube bundles in R-114 oil mixtures

Eraydin, Hakan

Monterey, California: Naval Postgraduate School

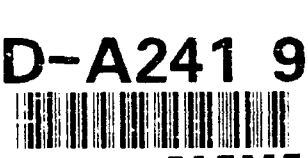

(2)

NAVAL POSTGRADUATE SCHOOL
Monterey, California

THESIS

NUCLEATE POOL BOILING PERFORMANCE
OF SMALL HIGH FLUX AND TURBO-B TUBE BUNDLES
IN R-114/OIL MIXTURES

by

Hakan Eraydin

DECEMBER 1990

Approved for public release; Distribution is unlimited

REPORT DOCUMENTATION PAGE

Form Approved
OMB No 0704-0188

1a REPORT SECURITY CLASSIFICATION: Unclassified	1b RESTRICTIVE MARKINGS
2a SECURITY CLASSIFICATION AUTHORITY	3 DISTRIBUTION / AVAILABILITY OF REPORT: Approved for public release; Distribution is unlimited
2b DECLASSIFICATION / DOWNGRADING SCHEDULE	
4 PERFORMING ORGANIZATION REPORT NUMBER(S)	5 MONITORING ORGANIZATION REPORT NUMBER(S)
6a NAME OF PERFORMING ORGANIZATION: Naval Postgraduate School; 6b OFFICE SYMBOL (If applicable): ME	7a NAME OF MONITORING ORGANIZATION: Naval Postgraduate School
6c ADDRESS (City, State, and ZIP Code): Monterey, CA 93943-5000	7b ADDRESS (City, State, and ZIP Code): Monterey, CA 93943-5000
8a NAME OF FUNDING / SPONSORING ORGANIZATION; 8b OFFICE SYMBOL (If applicable)	9 PROCUREMENT INSTRUMENT IDENTIFICATION NUMBER
8c ADDRESS (City, State, and ZIP Code)	10 SOURCE OF FUNDING NUMBERS: PROGRAM ELEMENT NO; PROJECT NO; TASK NO; WORK UNIT ACCESSION NO

11 TITLE (Include Security Classification)
NUCLEATE POOL BOILING PERFORMANCE OF SMALL HIGH FLUX AND TURBO-B TUBE BUNDLES IN R-114/OIL MIXTURES

12 PERSONAL AUTHOR(S)
HAKAN ERAYDIN

13a TYPE OF REPORT	13b TIME COVERED	14 DATE OF REPORT (Year, Month, Day)	15 PAGE COUNT
Master's Thesis	FROM _____ TO _____	DECEMBER 1990	121

16 SUPPLEMENTARY NOTATION
The views expressed in this thesis are those of the author and do not reflect the official policy or position of the Department of Defense or the U.S. Government

17 COSATI CODES			18 SUBJECT TERMS (Continue on reverse if necessary and identify by block number)
FIELD	GROUP	SUB-GROUP	Heat transfer, pool boiling

19 ABSTRACT (Continue on reverse if necessary and identify by block number)

The U.S. Navy is constantly looking toward using more lightweight and compact heat exchangers. One of the areas of interest is the use of enhanced boiler tubes in the evaporator of a refrigerator plant, thereby cutting down on the number of tubes needed.

The present research is a continuation of work done at NPS concentrating on the boiling characteristics from small tube bundles sitting in a pool of pure R-114, simulating the evaporator in such a heat exchanger. Two types of commercially available enhanced boiler tubes were used, namely High Flux and Turbo-B. In addition, the effect of adding up to 6% of oil to the R-114 (simulating typical amounts found in a real evaporator) during Turbo-B tube experiments was studied to see how much the heat transfer performance of the tubes decreased. All tests were conducted at 2.2 C corresponding to typical working pressures in a Navy evaporator.

The results using pure R-114 indicated that the heat transfer performance for both types of tube were similar and outperformed smooth and finned tube bundles by a factor of up to 5 and 3 respectively. The effectiveness of the Turbo-B tube bundle degraded with increased amounts of oil. At a practical heat flux of $q^{"}=30$ kW/m^2, a 9% and 15% degradation from pure R-114 was observed for 3% and 6% oil concentrations respectively.

20 DISTRIBUTION / AVAILABILITY OF ABSTRACT	21 ABSTRACT SECURITY CLASSIFICATION
☒ UNCLASSIFIED/UNLIMITED ☐ SAME AS RPT ☐ DTIC USERS	unclassified
22a NAME OF RESPONSIBLE INDIVIDUAL: Paul J. Marto	22b TELEPHONE (Include Area Code): (408) 646-2768; 22c OFFICE SYMBOL: ME

DD Form 1473, JUN 86 — Previous editions are obsolete — SECURITY CLASSIFICATION OF THIS PAGE

S/N 0102-LF-014-6603

UNCLASSIFIED

Approved for public release; Distribution is unlimited

Nucleate Pool Boiling Performance
of Small High Flux and Turbo-B Tube Bundles
in R-114/Oil Mixtures

by

Hakan Eraydin
Lieutenant Junior Grade, Turkish Navy
B.S., Turkish Naval Academy, 1983

Submitted in partial fulfillment of the
requirements for the degree of

MASTER OF SCIENCE
IN MECHANICAL ENGINEERING

from the

NAVAL POSTGRADUATE SCHOOL

DECEMBER 1990

Author: [redacted]
Hakan Eraydin

Approved by: [redacted]
Paul J. Marto, Thesis Advisor

[redacted]
Steve Memory, Thesis Co-Advisor

[redacted]
Anthony J. Healey, Chairman
Department of Mechanical Engineering

ABSTRACT

The U.S. Navy is constantly looking toward using more lightweight and compact heat exchangers. One of the areas of interest is the use of enhanced boiler tubes in the evaporator of a refrigerator plant, thereby cutting down on the number of tubes needed.

The present research is a continuation of work done at NPS concentrating on the boiling characteristics from small tube bundles sitting in a pool of pure R-114, simulating the evaporator in such a heat exchanger. Two types of commercially available enhanced boiler tubes were used, namely High Flux and Turbo-B. In addition, the effect of adding up to 6% of oil to the R-114 (simulating typical amounts found in a real evaporator) during Turbo-B tube experiments was studied to see how much the heat transfer performance of the tubes decreased. All tests were conducted at 2.2 C corresponding to typical working pressures in a Navy evaporator.

The results using pure R-114 indicated that the heat transfer performance for both types of tube were similar and outperformed smooth and finned tube bundles by a factor of up to 5 and 3 respectively. The effectiveness of the Turbo-B tube bundle degraded with increased amounts of oil. At a practical heat flux of $q''=30$ kW/m^2, a 9% and 15% degradation from pure R-114 was observed for 3% and 6% oil concentrations respectively.

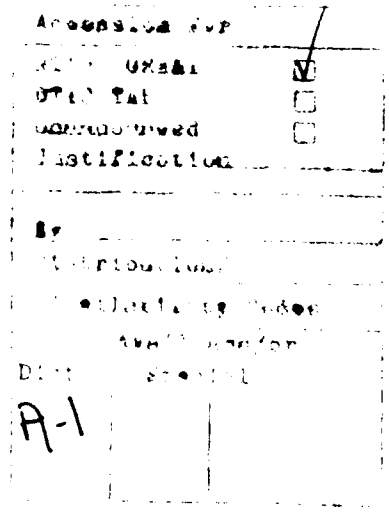

TABLE OF CONTENTS

I. INTRODUCTION 1
A. BACKGROUND 1
B. OBJECTIVES 4

II. LITERATURE SURVEY 5
A. GENERAL INTRODUCTION 5
B. EXPERIMENTAL AND THEORETICAL STUDIES 6

III. EXPERIMENTAL APPARATUS 17
A. TEST APPARATUS OVERVIEW 17
B. DATA ACQUISITION SYSTEM/INSTRUMENTATION 18
C. AUXILIARY EQUIPMENT 19
1. 8-Ton Refrigeration Unit 19
2. Ethylene-Glycol/Water Mixture 19
3. Pumps 19
4. Flowmeters 20
D. GEOMETRY OF ENHANCED SURFACE TUBES USED 20
1. High Flux Tube 20
2. Turbo-B Tube 20

IV. EXPERIMENTAL PROCEDURES 30
A. MANUFACTURE OF INSTRUMENTED EVAPORATOR TUBES 30
B. INSTALLATION OF EVAPORATOR TUBES AND TUBE SUPPORT BLOCK 31
C. SYSTEM LEAKAGE CHECK 32
D. FREON FILL 33
E. FREON REMOVAL 33
F. SYSTEM CLEAN-UP 34
G. GENERAL OPERATION 35
H. OIL ADDITION 36
I. DATA REDUCTION PROCEDURES 37

V. RESULTS AND DISCUSSION 38
A. GENERAL DESCRIPTION 38
B. R-114 BOILING FROM A HIGH FLUX TUBE BUNDLE 39

C. R-114/OIL MIXTURES BOILING FROM A TURBO-B TUBE BUNDLE 45
D. PERFORMANCE COMPARISON OF THE SMOOTH, FINNED, HIGH FLUX AND TURBO-B TUBE BUNDLES 49

VI. CONCLUSIONS AND RECOMMENDATIONS 83
A. CONCLUSIONS 83
B. RECOMMENDATIONS 85

APPENDIX A. LISTING OF DATA FILES 86
APPENDIX B. SAMPLE CALCULATIONS 88
APPENDIX C. UNCERTAINTY ANALYSIS 97
LIST OF REFERENCES 102
INITIAL DISTRIBUTION LIST 105

LIST OF TABLES

TABLE 3.1 EVAPORATOR HEATERS 21

TABLE 3.2 COMPUTER/DATA ACQUISITION ASSIGNMENT 21

TABLE 5.1 BOILING HEAT TRANSFER COEFFICIENTS AND ENHANCEMENT RATIOS FOR SMOOTH TUBE BUNDLE AT A HEAT FLUX OF 30 KW/M^2 51

TABLE 5.2 BOILING HEAT TRANSFER COEFFICIENTS AND ENHANCEMENT RATIOS FOR FINNED TUBE BUNDLE AT A HEAT FLUX OF 30 KW/M^2 51

TABLE 5.3 BOILING HEAT TRANSFER COEFFICIENTS AND ENHANCEMENT RATIOS FOR HIGH FLUX TUBE BUNDLE AT A HEAT FLUX OF 30 KW/M^2 52

TABLE 5.4 BOILING HEAT TRANSFER COEFFICIENTS AND ENHANCEMENT RATIOS FOR TURBO-B TUBE BUNDLE AT A HEAT FLUX OF 30 KW/M^2 52

TABLE A.1 DATA FILE NAMES OF THE TURBO-B AND HIGH FLUX TUBE RUNS 86

TABLE C.1 UNCERTAINTY ANALYSIS RESULTS 101

LIST OF FIGURES

Figure 2.1	Typical Boiling Curve for Refrigerants	13
Figure 2.2	Anderson's [Ref. 7] Smooth Tube Bundle Experiment Results	14
Figure 2.3	Akcasayar's [Ref. 10] Finned Tube Bundle Experiment Results	15
Figure 2.4	Akcasayar's [Ref. 10] High Flux Tube Bundle Experiment Results	16
Figure 3.1	Schematic View of the Apparatus	24
Figure 3.2	Evaporator/Condenser Schematic	25
Figure 3.3	Front View of Evaporator	26
Figure 3.4	Side View of Evaporator	27
Figure 3.5	Sectional View of Evaporator Showing Tube Bundle	28
Figure 3.6	Thermocouple Locations on an Instrumented Boiling Tube and Tube Section View	29
Figure 5.1	Improvement in Heat Transfer Performance with Clean-Up (Decreasing Heat Flux)	53
Figure 5.2	Performance Comparison of a Single High Flux Tube Within a Bundle and Within a Single Tube Apparatus	54
Figure 5.3	Performance Comparison of a Single High Flux Tube Within a Bundle and Within a Single Tube Apparatus (Decreasing Heat Flux)	55

Figure 5.4 Performance Comparison of the Top Tubes of a High Flux, Finned and Smooth Tube Bundle 56

Figure 5.5 Boiling Data for High Flux Tubes 1 and 2 Operating Simultaneously 57

Figure 5.6 Boiling Data for High Flux Tubes 1, 2 and 3 Operating Simultaneously 58

Figure 5.7 Boiling Data for High Flux Tubes 1, 2, 3 and 4 Operating Simultaneously 59

Figure 5.8 Boiling Data for High Flux Tubes 1, 2, 3, 4 and 5 Operating Simultaneously 60

Figure 5.9 Boiling Data for High Flux Tube Bundle 61

Figure 5.10 Boiling Data for High Flux Tube Bundle with Simulation Heaters in Operation 62

Figure 5.11 Boiling Data for High Flux Tube Bundle after Repositioning Tubes 63

Figure 5.12 Boiling Data for Turbo-B Tube 1 as a Single Tube for Increasing and Decreasing Heat Flux 64

Figure 5.13 Performance Comparison of a Single Turbo-B Tube Within a Bundle and Within a Single Tube Apparatus (Decreasing Heat Flux) 65

Figure 5.14 Boiling Data for Turbo-B Tube 1 when Influenced by Increasing Number of Heated Tubes 66

Figure 5.15 Boiling Data for Turbo-B Tube 1 when Influenced by Increasing Number of Heated Tubes (Decreasing Heat Flux) 67

Figure 5.16 Boiling Data for Turbo-B Tubes 1 and 2 Operating Simultaneously 68

Figure 5.17 Boiling Data for Turbo-B Tubes 1, 2 and 3 Operating Simultaneously 69

Figure 5.18 Boiling Data for Turbo-B Tubes 1, 2, 3 and 4 Operating Simultaneously 70

Figure 5.19 Boiling Data for Turbo-B Tube Bundle 71

Figure 5.20 Boiling Data for Turbo-B Tube Bundle with Simulation Heaters in Operation 72

Figure 5.21 Boiling Data for Turbo-B Tubes 1 and 2 Operating Simultaneously (Decreasing Heat Flux) 73

Figure 5.22 Boiling Data for Turbo-B Tubes 1, 2, 3, 4 and 5 Operating Simultaneously (Decreasing Heat Flux) 74

Figure 5.23 Boiling Data for Turbo-B Tube Bundle (Decreasing Heat Flux) 75

Figure 5.24 Boiling Data for Turbo-B Tube Bundle with Simulation Heaters in Operation (Decreasing Heat Flux) 76

Figure 5.25 Boiling Data for Turbo-B Tube 1 with Different Oil Concentrations 77

Figure 5.26 Boiling Data for Turbo-B Tube 1 with Different Oil Concentrations (Decreasing Heat Flux) 78

Figure 5.27 Boiling Data for Turbo-B Tube Bundle with Different Oil Concentrations 79

Figure 5.28 Boiling Data for High Flux, Turbo-B, Finned and Smooth Tube Bundle in Pure R-114 (Decreasing Heat Flux) 80

Figure 5.29 Boiling Data for High Flux, Turbo-B, Finned and Smooth Tube Bundle with 3% Oil (Decreasing Heat Flux) 81

Figure 5.30 Boiling Data for High Flux, Turbo-B, Finned and Smooth Tube Bundle with 6% Oil (Decreasing Heat Flux) 82

NOMENCLATURE

SYMBOL	UNITS	NAME/DESCRIPTION
Aas	V	Voltage output from current sensor
A_c	m^2	Tube-wall cross section area
A_s	m^2	Area of heated surface
c_p	J/kg K	Specific heat
D_i	m	Inside tube diameter
D_o	m	Outside tube diameter
D_{tc}	m	Thermocouple location diameter
g	m/s^2	Gravitational acceleration
h	W/m^2 K	Heat transfer coefficient of enhanced tube surface
h_b	W/m^2 K	Heat transfer coefficient of tube unheated smooth tube ends
h_t	m	Height of Freon column above a heated instrumented tube
k	W/m K	Thermal conductivity of Freon
k_{cu}	W/m K	Thermal conductivity of copper
L	m	Heated length of tube
L_u	m	Unheated length of tube
L_c	m	Corrected unheated length of tube
n	1 /m	Parameter in the calculation of q_f, see equations B.9 and B.13
Pr		Prandtl number
p	m	Perimeter of the tube outside surface

ΔP	Pa	Hydrostatic pressure difference between tube and free surface
q	W	Heat transfer rate
q"	W/m^2	Heat flux
q_f	W	Heat transfer rate from unheated smooth tube ends
T	C	Temperature
t	m	Thickness of tube
ΔT	C	Wall Superheat, $(\bar{T}_{wo} - T_{sat})$
Tfilm	C	Film temperature, $(\bar{T}_{wo} + T_{sat})/2$
$Tfilm_k$	K	Film thermodynamic temperature
Tld1	C	Liquid temperature reading from thermocouple 4
Tld2	C	Liquid temperature reading from thermocouple 5
T_{sat}	C	Saturation temperature
T_{satc}	C	Corrected saturation temperature due to hydrostatic pressure difference
$\bar{T}_{wi}$	C	Average inside wall temperature
$\bar{T}_{wi-K}$	K	Average inside wall thermodynamic temperature
$\bar{T}_{wo}$	C	Average outside wall temperature
Vas	V	Voltage output from voltage sensor
α	m^2/s	Thermal diffusivity
β	1/K	Thermal expansion coefficient

μ	kg/m s	Dynamic viscosity of liquid
ν	m^2/s	Kinematic viscosity of liquid
ρ	kg/m^3	Density of liquid
ϕ	C	Fourier conduction term
ψ		Variable in density calculation

ACKNOWLEDGEMENTS

Above all, I wish to thank my wife and best friend Deniz for her patience and understanding as well as unwavering support throughout this endeavor.

I also wish to thank Dr. Paul Marto and Dr. Steve Memory for their infinite patience and accurate guidance throughout this investigation.

Additionally, the assistance rendered by Thomas McCord and the Machine Shop personnel of the Mechanical Engineering Department was invaluable.

I. INTRODUCTION

A. BACKGROUND

In recent years, the Navy has been increasingly interested in the use of more compact and lighter heating, ventilation and air conditioning systems. To a lesser degree, cost has also been a major influence.

The design of reliable, efficient and compact heat exchangers involves the testing of many different coolants (Freons) and many different enhanced heat transfer surfaces. Today's Navy uses Refrigeration-114 having tried previously R-11 and R-12. Despite being widely used in the refrigeration industry, especially for large refrigeration and air conditioning systems, the use of R-11 has been avoided in the Navy due to internal corrosion caused by acidic attack. On the other hand, prevention of moisture leaking into the system due to moderate operating pressure is the main advantage of R-114. In addition, R-114 is more stable with temperature and relatively non-toxic. Since R-114 is a well-wetting organic liquid, temperature excursion or "boiling hysterisis" is commonly observed in pool boiling of R-114. Nucleation sites at the tube surface are filled with R-114 (due to its very good wetting characteristics), causing an increase in the amount of superheat required to initiate boiling compared with other Freons.

Another variable which can improve the heat transfer is the surface of the heat exchanger itself. Enhanced boiling tubes offer several important advantages

over conventional, plain tube design. As described by Thome [Ref. 1], these include: a shell-side boiling heat transfer coefficient of about 2 to 10 times that of a plain tube bundle; the ability to operate at smaller wall superheats; an improved fouling resistance offered by integral-low finned tubes.

Enhanced boiling tubes, when applied correctly, can make previously impractical temperature approaches not only feasible but also thermally efficient. These tubes can be installed in nearly all the heat exchanger configurations and they are typically used for conventional reboilers and evaporators in service, in the petroleum and chemical processing industries.

Currently, copper finned tubes and/or High Flux tubes are used in Navy refrigeration applications. Despite being available with different fin geometries, only low finned versions are used for boiling applications since the large boiling heat transfer coefficients for medium and high-finned tubes produce an unacceptably low fin efficiency. The finned tubes are made from many different metals. As described by Thome [Ref. 1], the fins are plastically formed by pinching the tube between a plug placed inside and three sets of planetary rings of increasing diameter that compress the outer tube wall and "raise" the fins. Finned tubes exhibit nearly a three-fold increase in heat transfer performance over plain or smooth tubes.

Another type of enhanced tube surface (called High Flux) is the first type of boiling tube other than a low-finned tube to become widely used by the Navy. This tube is fabricated by spraying a specially developed coating (made up of a binder,

a metallic powder and a brazing powder) on its exterior surface to form a thin, rough film. The coated tube is then placed in an oven to melt the brazing powder and to burn off the binding material, leaving behind a thin, porous metallic matrix that is several particle layers thick and has a multitude of random, interconnected passageways. High Flux tubes exhibit a three-fold increase in heat transfer performance over the finned tubes.

Another enhanced surface under consideration is called Turbo-B. On this surface, the exterior boiling enhancement is made by raising integral low fins, cutting longitudinally across these fins,and then rolling the fins to compress them to form mushroom-like pedestals. Re-entrant passageways are thus formed in a rectangular crosshatch pattern. The shape of the fins, when viewed from above, is close to rectangular. This tube is currently available in copper, copper-nickel and low-carbon steel.

The performance of any given tube in a bundle can be significantly different from the performance of a similar tube alone in a large liquid pool. Murphy [Ref. 2] as well as Marto and Memory [Ref. 3] reported that when boiling as a single tube the Turbo-B tube exhibited the best overall performance when compared with a smooth, finned and even a High Flux tube (at low heat fluxes). However, tube bundle boiling characteristics of Turbo-B tubes are currently unavailable; to investigate these characteristics is one of the objectives of this thesis study.

B. OBJECTIVES

Based upon the foregoing discussion, the objectives of this thesis work are:

1. to obtain data for a High Flux tube bundle operating in R-114 using increasing and then decreasing heat flux to analyze "boiling hysterisis,"

2. to fabricate and instrument a Turbo-B tube bundle and take data in different R-114/oil mixtures.

3. to compare data taken with the Turbo-B tube bundle to data taken from smooth, finned and High Flux tube bundles as well as from a single tube apparatus.

II. LITERATURE SURVEY

A. GENERAL INTRODUCTION

Boiling may occur under various conditions. The term "pool boiling" refers to a situation in which the liquid is quiescent; its motion near the surface is due to free convection and mixing induced by bubble growth and detachment. Pool boiling heat transfer is most easily explained with reference to the well-known boiling curve, which represents the functional dependence of heat flux leaving the heated wall on the temperature difference between the surface of the heated wall and the surrounding bulk liquid. The pool boiling curve is divided into four distinct heat transfer regimes; natural convection (single phase), nucleate pool boiling, transition boiling and film boiling.

As the wall superheat is increased, natural convection is in effect until nucleation occurs and the first bubbles form on the heated wall. At point B on Figure 2.1, natural convection is complete and the onset of nucleate boiling starts; it is the presence of sufficient wall superheat that activates nucleate boiling. Curve B-C exhibits the overshoot, which is sometimes referred to as the temperature excursion. This may or may not be seen depending upon the wetting characteristics of the fluid used. The coolant, currently used by the Navy, R-114, typically exhibits this overshoot behavior. Between points C and D, nucleate pool boiling is attained. In this regime, heat transfer rates and convection coefficients

are high and it is thus desirable to operate many engineering devices in this boiling regime. Presently, most of the data available for enhanced surfaces have been taken in this region. During nucleate boiling, the difference in behavior between increasing and decreasing heat flux is referred to as boiling "hysterisis." Following departure from nucleate pool boiling (point E), the critical heat flux (CHF) is reached. This maximum is thought to occur as a result of hydrodynamic instability in the vapor jets leaving the heated wall, which in turn causes a vapor film to form over portions of the heated wall. Since the vapor formation is very rapid, a vapor film begins to form on the surface. At any point on the surface, conditions may oscillate between film and nucleate boiling. Finally, complete film boiling is reached (F-H). This regime is characterized by a stable vapor film that covers the whole tube surface. The heat must be conducted or convected through this vapor blanket to reach the bulk fluid. This additional resistance causes smaller heat transfer coefficients and larger wall superheats. This regime is avoided in design considerations due to its poor thermal capability. The reduced heat flux is marked by the solid line. The dashed curve indicates the transition boiling regime.

B. EXPERIMENTAL AND THEORETICAL STUDIES

Today's Navy already uses finned and High Flux tubes in its shipboard heat exchangers. Replacement of these kind of tubes, in place of plain, drawn tubes, are the results of extensive experimental research. Initial experiments with a single tube apparatus showed that improvements in performance up to a factor of 10-20

could be obtained with the use of enhanced surfaces. Some of these single tube experiments were repeated in a tube bundle to provide more realistic results. To date, in tube bundle experiments, smooth, finned, cold worked finned surface (i.e., Gewa-T and Thermoexcel-E) and porous coated surfaces have been tested using different refrigerants. Tube bundle experiments showed that bundle performance primarily depends not only upon the type of enhancement but also on the operating conditions (e.g., pressure, saturation temperature, etc.).

Yilmaz and Palen [Ref. 4] obtained data for an integral low-finned tube bundle using a hydrocarbon. They pointed out that finned tube bundles normally give higher heat fluxes and therefore much higher heat duty per unit length than identical plain tube bundles at very low wall superheat. This is where the finned tube bundle is more likely to be economically feasible. According to Yilmaz and Palen [Ref. 4], the presence of fins can increase heat transfer in nucleate boiling due to increased surface area. On the other hand, at high wall superheats, the finned tubes may experience some partial vapor blanketing, thus causing the bundle heat transfer coefficients to be less than those for a single finned tube.

Hahne and Müller [Refs. 5, 6] conducted experiments on a low integral-fin tube bundle using R-11. They found that the heat transfer coefficients varied with position within the bundle and heat flux. At low heat fluxes, the heat transfer coefficient increased significantly as one moved up the bundle; as the heat flux increased, the boiling curve of each tube converged to a single curve which was representative of a single finned tube.

Anderson [Ref. 7] made measurements for boiling of refrigerants from smooth and finned tube (19 fins per inch) bundles. The bundle, similar to the presented thesis work, contained 15 heated tubes arranged in an equilateral triangular pitch of 19.1 mm. The smooth tube bundle was tested in R-113 and R-114. Heat transfer performance was more than doubled for the finned tubes when compared to that for the smooth tubes. The results of Anderson's [Ref. 7] smooth tube bundle experiments are shown in Figure 2.2.

The second type of enhanced surface commonly tested in bundles includes Thermoexcel-E and Gewa-T tubes. Yilmaz, Palen and Taborek [Ref. 8] point out that a single Gewa-T tube outperforms a plain smooth tube by a factor of 10 at low wall superheats. However the enhancement of the Gewa-T tube bundle relative to a single Gewa-T tube is much smaller than the corresponding enhancement of a plain tube-bundle compared to a single plain tube. Experiments with Thermoexcel-E tubes also agreed with this Gewa-T tube performance.

Another enhancement technique which is aimed at improving the nucleation characteristics of a surface is the bonding of a porous, sintered metallic matrix to the base tube; these are called High Flux tubes which are fabricated by Union Carbide. This type of enhanced surface has not only been tested in a single tube apparatus, but also in a variety of tube bundles. Reilly [Ref. 9] investigated a single High Flux tube in R-114 at a boiling temperature of -2.2 C. The same enhanced surface was also tested by Akcasayar [Ref. 10] in a 15-tube triangular pitched bundle. The average bundle heat transfer performance approached the single tube

performance since all the individual instrumented tubes within the bundle performed similarly for different operations. Akcasayar [Ref. 10] pointed out that the reason for this behavior was the elimination of the convective effect of the rising bubbles due to the bubble coating around the surface which produced density populated nucleation sites. Another explanation for this behavior was given by Fujita [Refs. 11, 12]. He points out that, since the nucleation and convective effects each have their own area of influence, if the nucleation site density is small, then the area available for convective effects will be large. As a result of the excellent nucleation characteristics of a porous coated surface, very large nucleation site density leaves very little area for convective effects resulting in an unnoticeable effect when comparing bundle with single tube performance. Akcasayar [Ref. 10] repeated the finned tube experiment that was done by Anderson [Ref. 7], using the same finned tubes (19 fins per inch) and the same refrigerant (R-114). Akcasayar's [Ref. 10] High Flux tube and finned tube experiment results are shown in Figures 2.3 and 2.4.

Another concern about tube bundle studies is the effect of oil contamination on these enhanced surfaces. Refrigeration systems having hermetically sealed compressors always allow a certain amount of oil to leak into the evaporator section; the effect of this oil contamination on the boiling performance of these surfaces must therefore be clearly established. The boiling process, especially when oil is present, is extremely complex and is almost impossible to treat theoretically.

Stephan [Ref. 13] reported the influence of oil on the boiling heat-transfer coefficient of R-12 and R-22 using a smooth horizontal plate as the boiling surface. He reported up to a 50% reduction in the boiling coefficient with 9% oil by weight, while 50% oil caused a 90% reduction. Henrici and Hesse [Ref. 14] conducted experiments involving boiling of R-114 in the presence of oil from a smooth copper tube. They reported a decrease of up to 20% (depending upon the heat flux) in the boiling coefficient with 1% oil. Danilova and Dyundin [Ref. 15] found that oil contamination had an adverse effect on the heat-transfer in finned tube bundles. Depending upon the operating temperature, 8% oil (by weight) caused up to a 50% decrease in heat-transfer.

Anderson [Ref. 7] reported that the presence of oil (up to 3% by mass) improved the heat transfer performance of smooth and finned tube bundles. Furthermore, at an oil concentration of 10%, only a slight degradation of heat-transfer (when compared to the pure R-114 case) was found. He obtained maximum performance at an oil concentration of around 2% in the case of the smooth tube bundle and around 3% in the case of finned tube bundle. Anderson's [Ref. 7] oil contaminated smooth tube bundle experiment results are shown in Figure 2.2.

For a single High Flux tube, Reilly [Ref. 3] found that the presence of oil delayed considerably the onset of nucleate boiling, while this delay was quite small for a single smooth tube. The presence of oil resulted in a reduction of up to a 35% in the boiling heat-transfer coefficient of the High Flux tube at a practical heat

flux of 30 kW/m^2. The boiling heat-transfer coefficient of the High Flux tube was about seven times greater than that of the smooth tube with up to 10% oil over the practical range of heat flux.

Akcasayar [Ref. 10] reported that oil addition affected the finned tube bundle performance positively, particularly at high heat fluxes. Bundle performance increased 1.8 times with 3% oil contamination compared to pure R-114 at the maximum heat flux level. At low heat flux applications, the positive effect is diminished. For 6% and 10% oil concentrations, the performance of the bundle decreased to a value slightly below the pure R-114 condition. Akcasayar's [Ref. 10] finned tube experiment results with oil contamination are shown in Figure 2.3.

On the other hand, during High Flux tube bundle experiments, Akcasayar [Ref. 10] found that the effectiveness of the High Flux tube bundle degraded with increased amounts of oil. The degradation was especially significant at high heat fluxes with 6% and 10% oil concentrations. He pointed out that, at a heat flux of 30 kW/m^2, a 28% and 47% degradation of pure R-114 was found at 6% and 10% oil concentrations respectively. Above a heat flux of 30 kW/m^2, the High Flux tube degraded so much that the performance of the finned tube bundle became better for a 6% or greater oil concentration. His High Flux tube bundle results with oil contamination are shown in Figure 2.4.

Marto and Memory [Ref. 3] and Murphy [Ref. 2] tested a single Turbo-B tube at various oil concentrations in R-114. They found out that, at a practical heat flux of 30 kW/m^2, the Turbo-B tube showed essentially the same pool-boiling

enhancements as the previously tested High Flux tube. However, the Turbo-B tube outperformed the High Flux tube at lower heat fluxes, while the High Flux tube showed superior performance at higher heat fluxes with oil concentrations of 6% or less. There is currently no data available in the literature for Turbo-B tubes performing in a bundle.

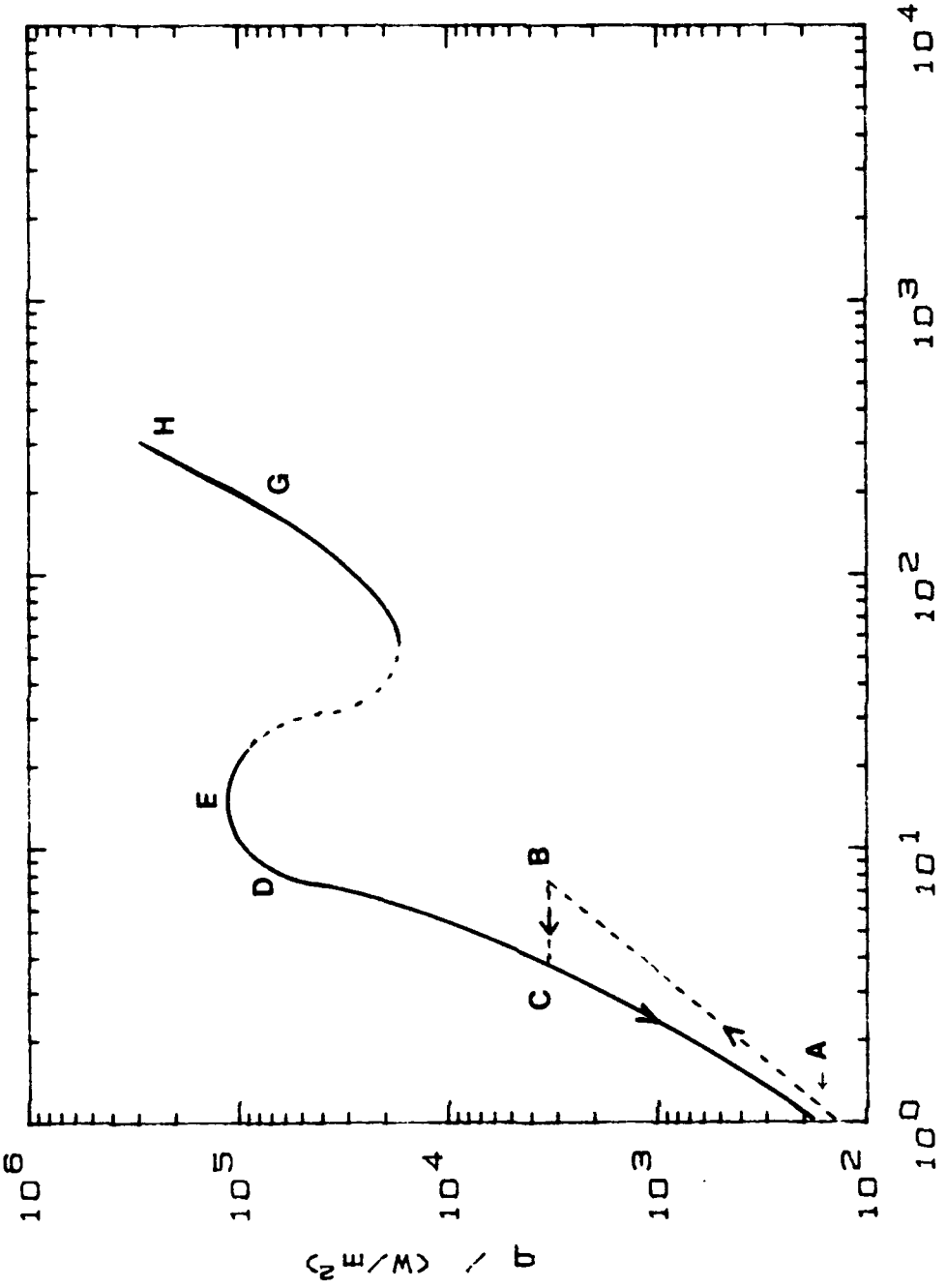

Figure 2.1. Typical Boiling Curve for Refrigerants.

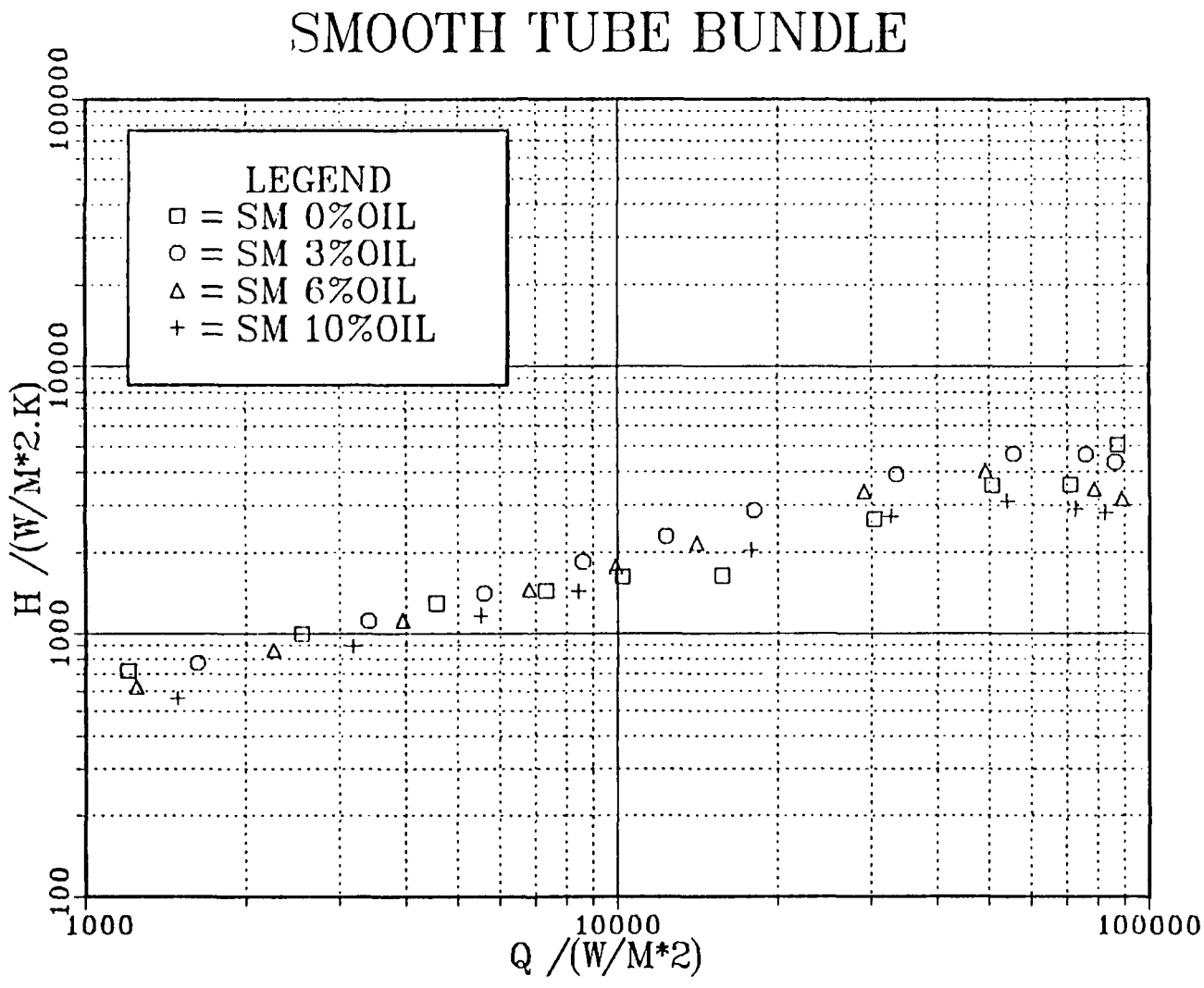

Figure 2.2. Anderson's [Ref. 7] Smooth Tube Bundle Experiment Results.

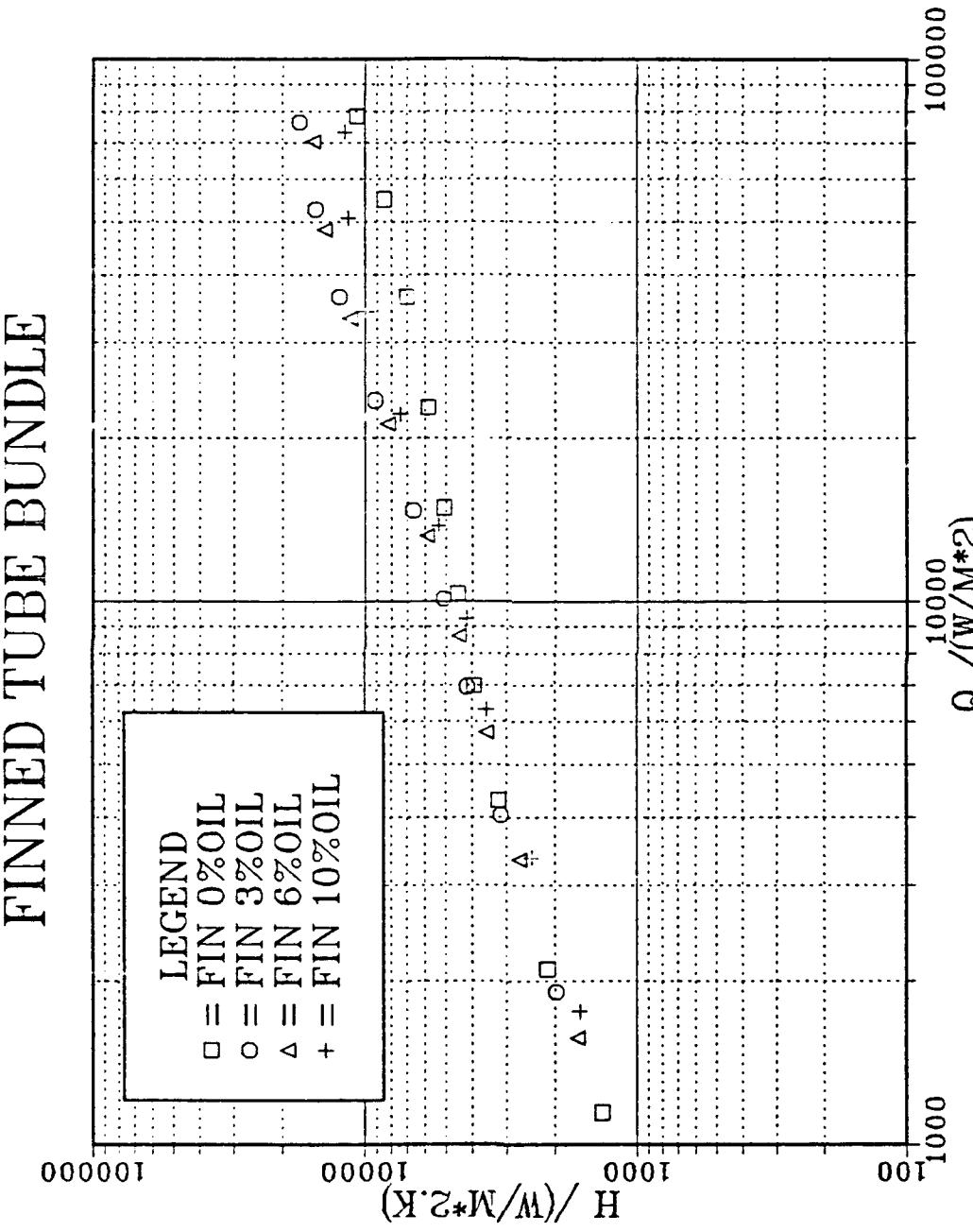

Figure 2.3. Akcasayar's [Ref. 10] Finned Tube Bundle Experiment Results.

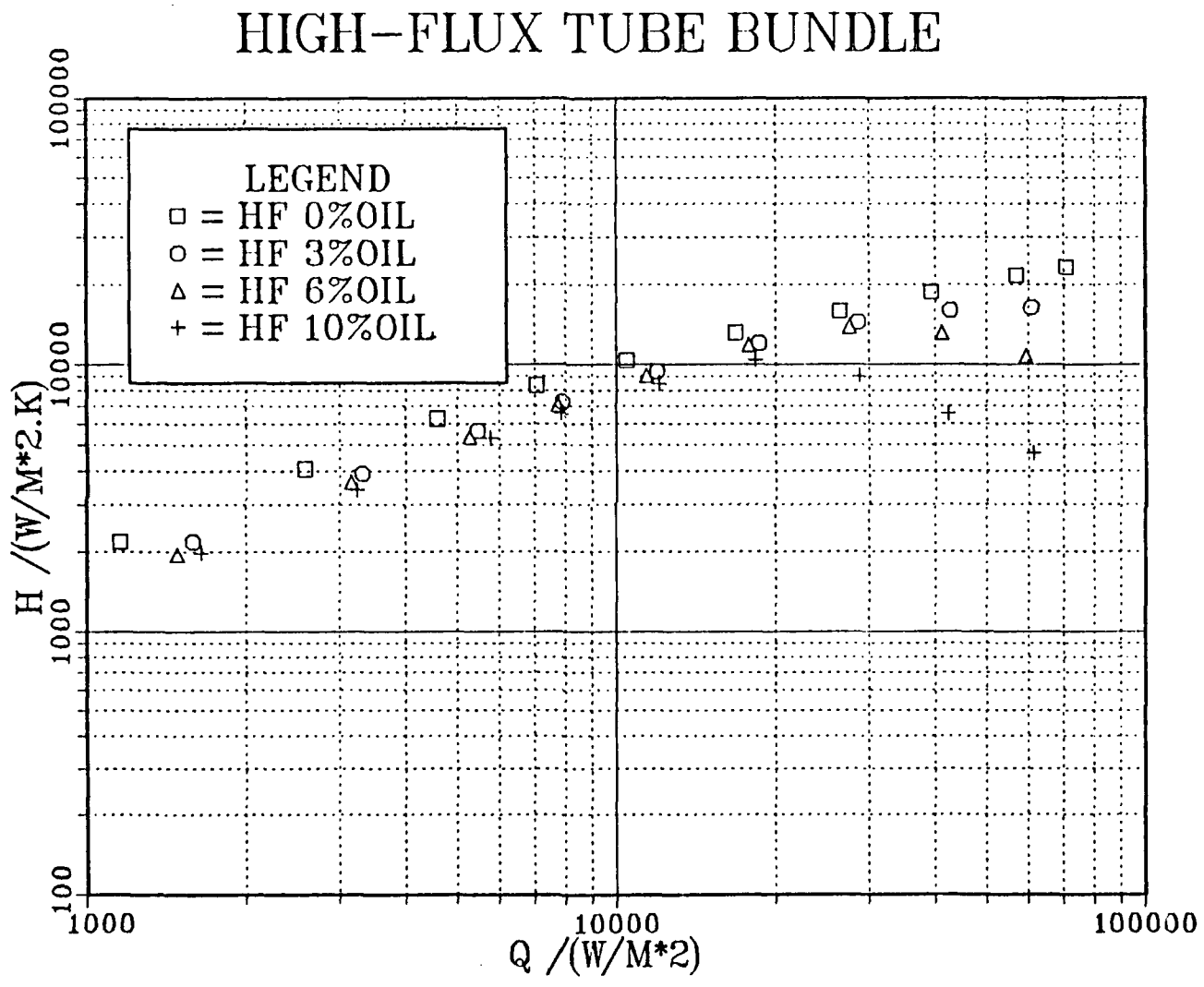

Figure 2.4. Akcasayar's [Ref. 10] High Flux Tube Bundle Experiment Results.

III. EXPERIMENTAL APPARATUS

A. TEST APPARATUS OVERVIEW

The test apparatus was designed by Zebrowski [Ref. 16], and built by Murphy [Ref. 2] for both boiling and condensation experiments. The schematic view of the experimental apparatus is shown in Figure 3.1; the details of the system were given in the references mentioned above. Consequently, only a brief description of the apparatus, concentrating on the evaporator section itself is given here.

As seen in Figures 3.1 and 3.2, the condenser consists of four instrumented horizontal condenser tubes and five auxiliary copper coils, all cooled by a mixture of water and ethylene glycol. Each of the tubes and coils can be operated separately when required. Vapor from the evaporator enters the condenser section through a "riser" and is guided both axially and circumferentially to the top of the condenser by a vapor shroud. After condensation, the condensate returns to the evaporator by gravity. Coolant flow rate to the condenser is varied to maintain the system pressure near atmospheric conditions. Other schematics of the system are given in Figures 3.3 to 3.5.

The evaporator was designed to simulate a small portion of a flooded refrigerant evaporator. It has a kettle reboiler type of design and consists of four

individually-controlled sets of heaters. The description of these heaters is given in Table 3.1.

Power is supplied separately to each set of heaters by using a STACO 240V, 23.5 KVA rheostat controller. Depending upon the requirements, they could also be powered altogether. Desired numbers of auxiliary, simulation, instrumented or active tube bundle heaters could also be operated independently by using circuit breakers.

The instrumented tubes were manufactured locally. They consist of an outer test tube shell (with the enhanced surface), an inner copper cylindrical sleeve and a cartridge heater push-fitted in the center. The outer diameter of the copper sleeve was machined 0.005 in smaller than the inner diameter of the outer test tube shell. The copper sleeve had six equally spaced 1mm square channels machined at 60 degree increments around its circumference. Figure 3.6 shows the position of the thermocouple grooves in addition to the position of one evaporator tube in the tube block. The copper sleeve and tube were bonded together with eutectic lead-tin (50:50) solder. This solder was chosen for its strength, low melting temperature, and favorable heat-transfer characteristics. The evaporator and condenser both have glass windows to permit easy viewing.

B. DATA ACQUISITION SYSTEM/INSTRUMENTATION

A Hewlett-Packard HP-349A Data Acquisition System and HP-9125 Computer were used for data collection. As described by Akcasayar [Ref. 10], Type-T

copper-constantan thermocouple measurements (mvolts) were made on the HP-349A with the relay multiplexer/assembly equipped with thermocouple compensation. A 20-channel relay multiplexer card was used to measure voltage taken from separate sensors measuring tube bundle, simulation and auxiliary heater potential. Auxiliary and simulation heater (total) amperages were each measured using an American Aerospace Control (AAC) current sensor. The currents of each instrumented tube heater were measured using five identical current sensors.

Computer channel assignments for data acquisition and array assignments are given in Table 3.2.

C. AUXILIARY EQUIPMENT

1. 8-Ton Refrigeration Unit

This refrigeration unit was used to cool a 1.8m^3 reservoir sump of ethylene-glycol/water (60:40 by volume) and bring it to the desired working temperature (less than -10 C).

2. Ethylene-Glycol/Water Mixture

This mixture was used as coolant to remove heat from the condenser.

3. Pumps

Two pumps were used in the coolant system to pump the coolant from the sump into the condenser. Condenser tubes were fed by pump #1 while condenser coils were fed by pump #2. The coils in the refrigerant storage tanks

were also fed by pump #2. They were especially needed during the transfer of refrigerant from the evaporator to the storage tank.

4. Flowmeters

Four calibrated float-type flowmeters, connected to pump #1, were used to control the coolant flow rate passing through the four condenser tubes. Another flowmeter was used to control the total coolant flow rate passing through the condenser coils supplied by pump #2.

D. GEOMETRY OF ENHANCED SURFACE TUBES USED

1. High Flux Tube

Outside diameter = 15.8 mm

Inside diameter = 11.6 mm

Porous metal film thickness = 0.025 mm (approximately)

Enhanced surface length = 203.2 mm

2. Turbo-B Tube

Outside diameter = 14.15 mm

Inside diameter = 12.7 mm

Enhanced surface length = 203.2 mm

TABLE 3.1. EVAPORATOR HEATERS

HEATERS	NUMBER	POWER/(EACH)
Instrumented Heater Tubes	5	1000 Watts
Active Bundle Heaters	10	1000 Watts
Auxiliary Heaters	4	4000 Watts
Simulation Heaters	5	4000 Watts

TABLE 3.2. COMPUTER/DATA ACQUISITION ASSIGNMENT

Thermocouple Description	Channel	Array in code
Vapor	00	T(0)
Vapor	01	T(1)
Vapor	02	T(2)
Liquid	03	T(3)
Liquid	04	T(4)
Tube 1, No. 1	40	T(5)
Tube 1, No. 2	41	T(6)
Tube 1, No. 3	42	T(7)
Tube 1, No. 4	43	T(8)
Tube 1, No. 5	44	T(9)
Tube 1, No. 6	45	T(10)
Tube 2, No. 1	46	T(11)
Tube 2, No. 2	47	T(12)
Tube 2, No. 3	48	T(13)
Tube 2, No. 4	49	T(14)
Tube 2, No. 5	50	T(15)
Tube 2, No. 6	51	T(16)
Tube 3, No. 1	52	T(17)

TABLE 3.2 (cont.)

Tube 3, No. 2	53	T(18)
Tube 3, No. 3	54	T(19)
Tube 3, No. 4	55	T(20)
Tube 3, No. 5	56	T(21)
Tube 3, No. 6	57	T(22)
Tube 4, No. 1	58	T(23)
Tube 4, No. 2	59	T(24)
Tube 4, No. 3	60	T(25)
Tube 4, No. 4	61	T(26)
Tube 4, No. 5	62	T(27)
Tube 4, No. 6	63	T(28)
Tube 5, No. 1	64	T(29)
Tube 5, No. 2	65	T(30)
Tube 5, No. 3	66	T(31)
Tube 5, No. 4	67	T(32)
Tube 5, No. 5	68	T(33)
Tube 5, No. 6	69	T(34)
Tube 1	30	Amp(0)
Tube 2	31	Amp(1)
Tube 3	32	Amp(2)
Tube 4	33	Amp(3)
Tube 5	34	Amp(4)
Active	35	Amp(5)
Active	36	Amp(6)
Active	37	Amp(7)
Active	38	Amp(8)

TABLE 3.2 (cont.)

Active	39	Amp(9)
Auxiliary Heaters	25	Amp(10)
Simulation Heaters	26	Amp(11)
Voltage Sensor Description	Channel	Array
Instrumented Active	27	Volt(0)
Simulation Heaters	28	Volt(1)
Auxiliary Heaters	29	Volt(2)

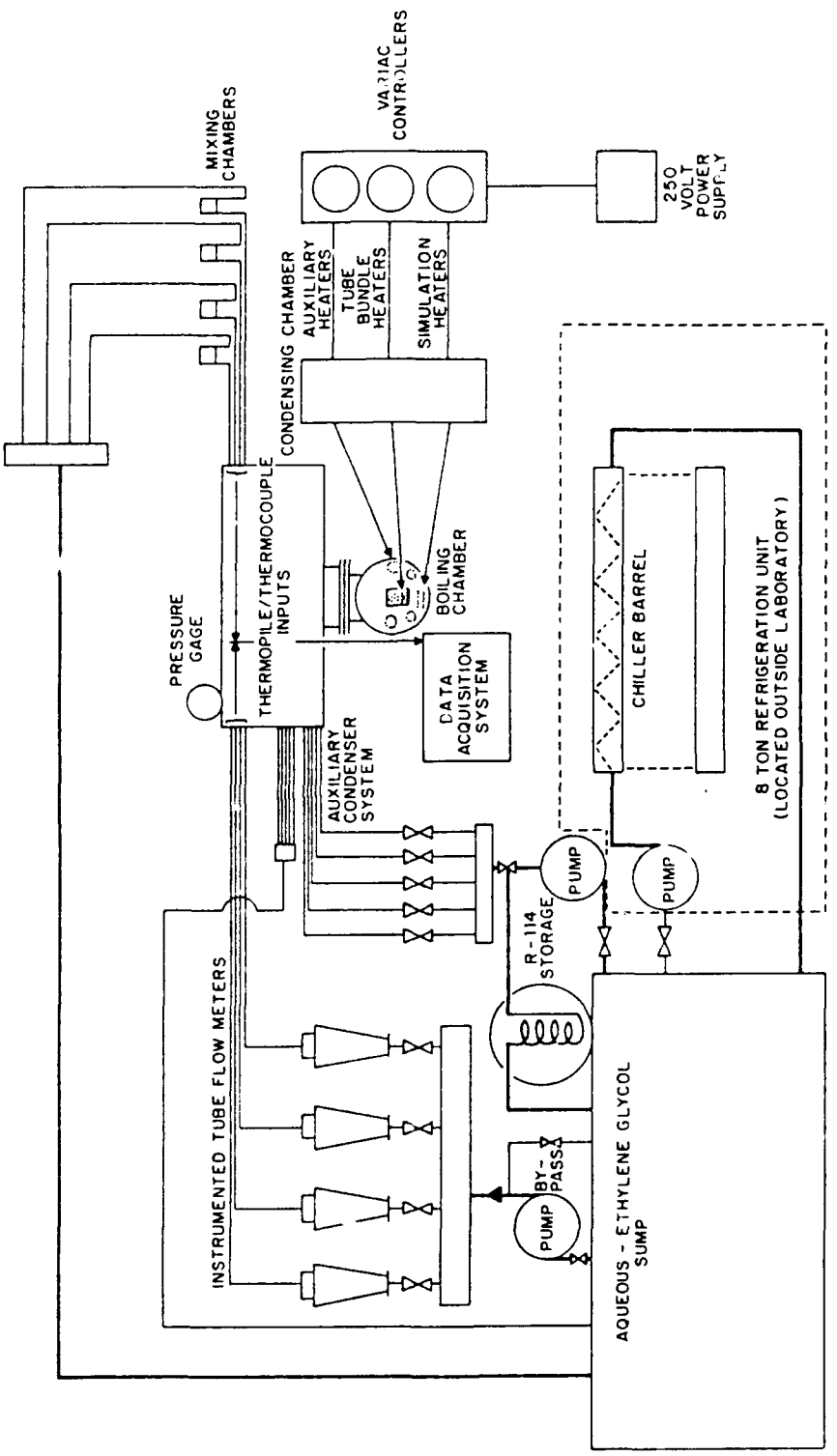

Figure 3.1. Schematic View of the Apparatus.

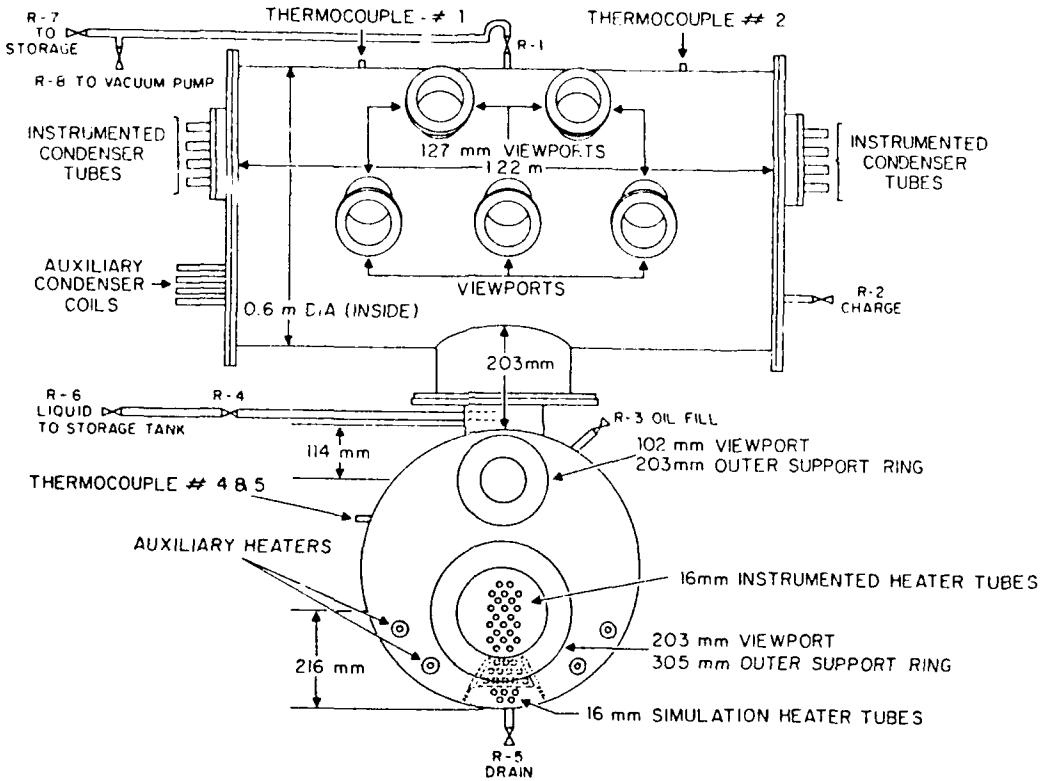

Figure 3.2. Evaporator/Condenser Schematic.

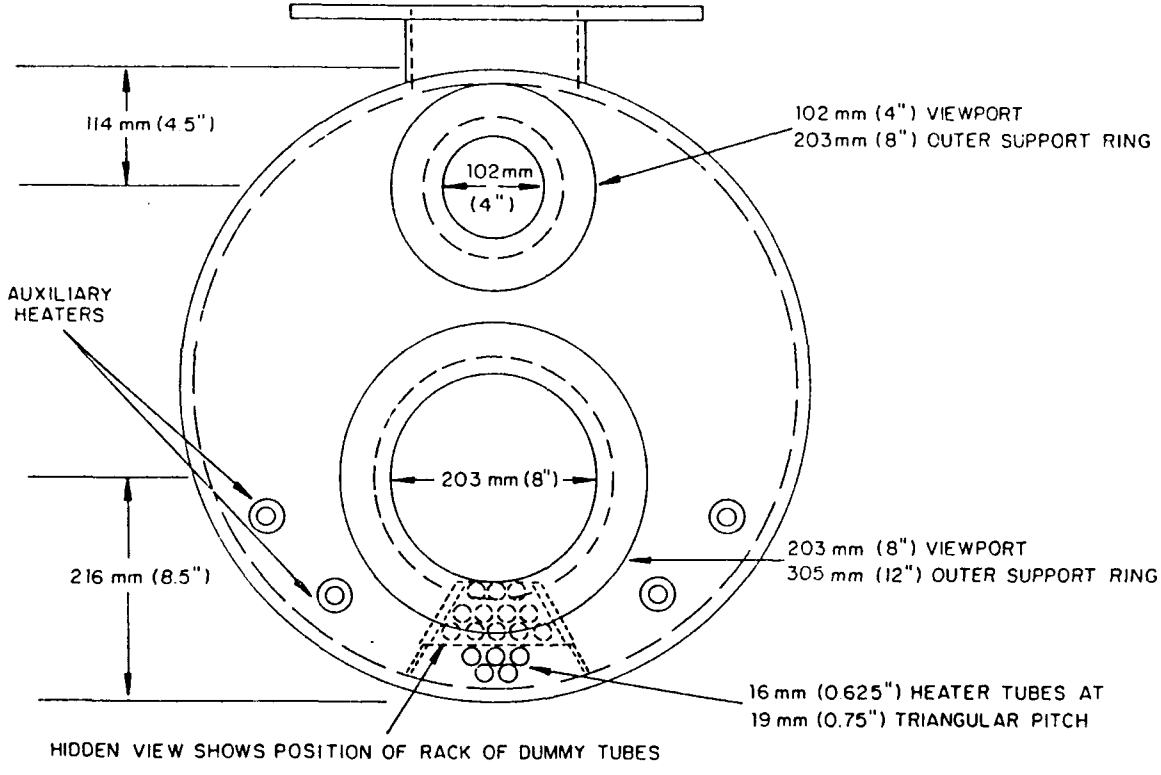

Figure 3.3. Front View of Evaporator.

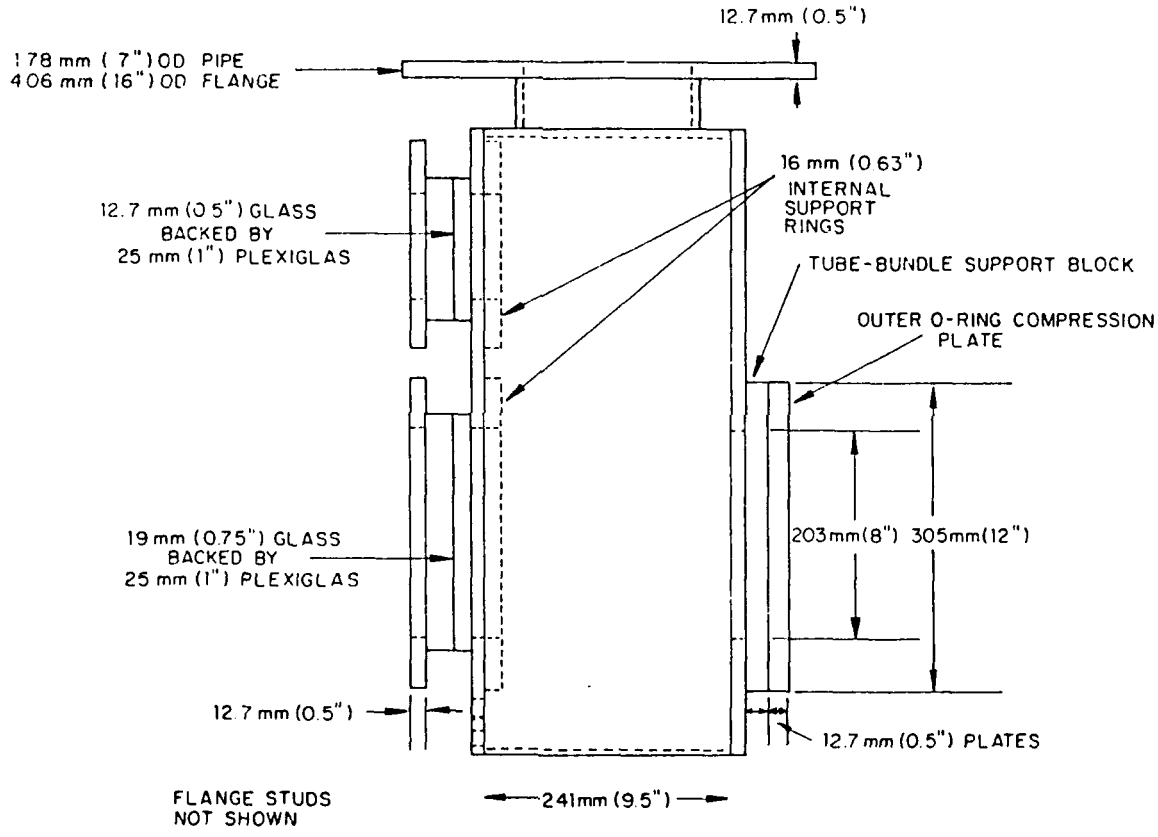

Figure 3.4. Side View of Evaporator.

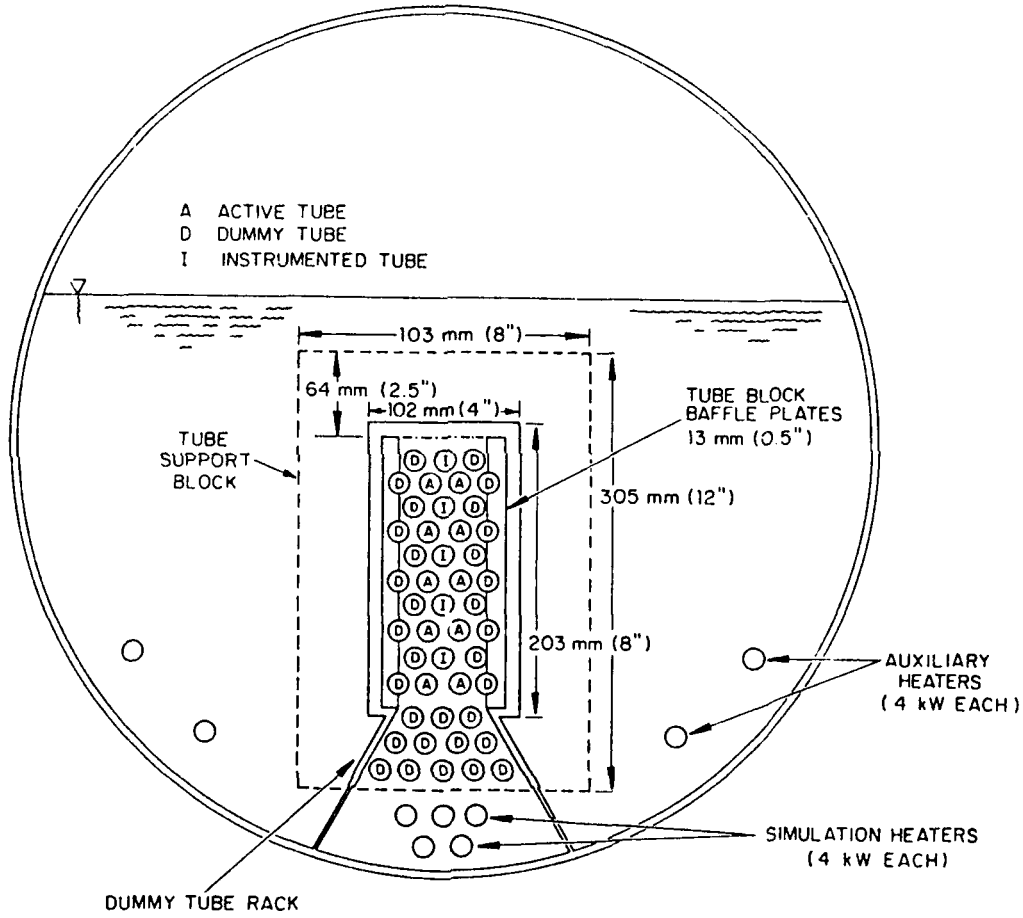

Figure 3.5. Sectional View of Evaporator Showing Tube Bundle.

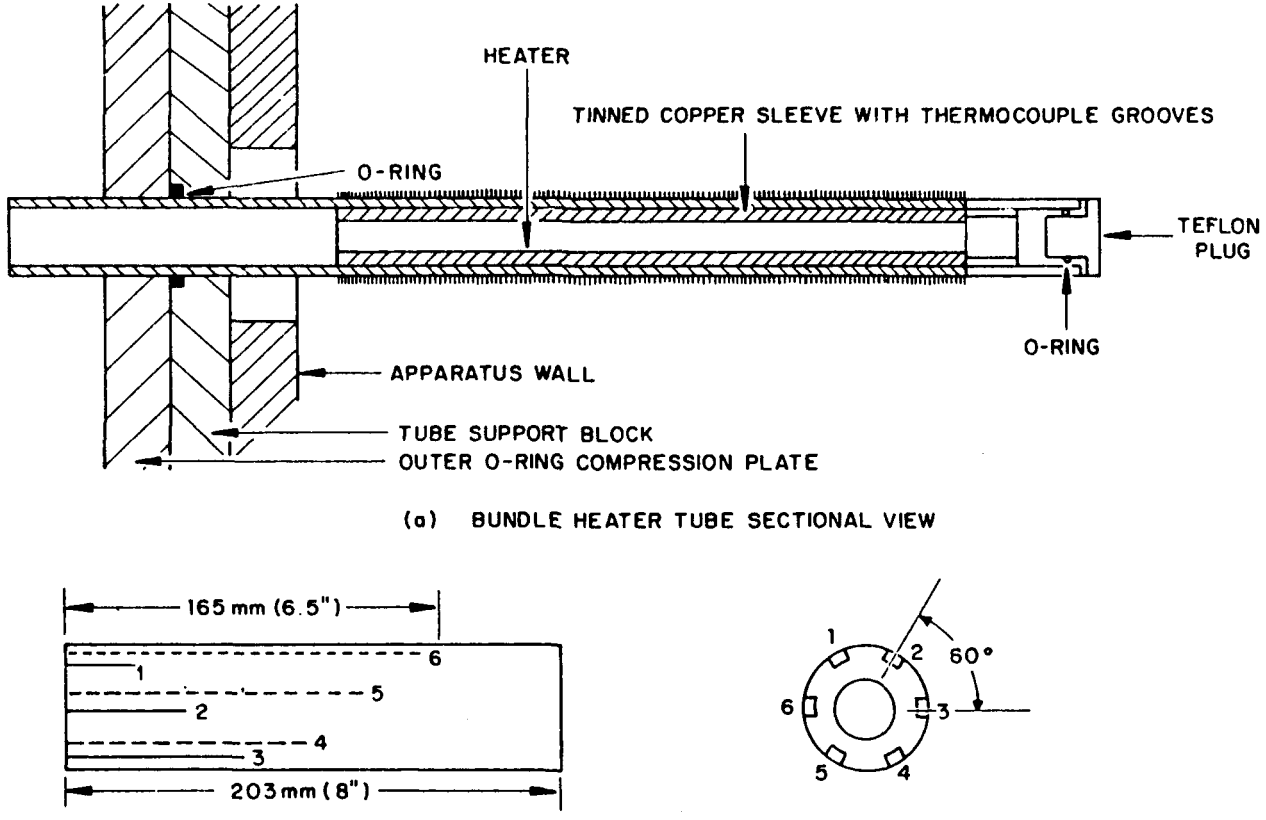

Figure 3.6. Thermocouple Locations on an Instrumented Boiling Tube and Tube Section View.

IV. EXPERIMENTAL PROCEDURES

A. MANUFACTURE OF INSTRUMENTED EVAPORATOR TUBES

The tubes used for the High Flux tube bundle experiments were manufactured by Akcasayar [Ref. 10]. As he pointed out, even though the same manufacturing technique was used, the wall temperature variations for the finned tubes were more homogenous than the High Flux tubes. As a result of this, large uncertainties were associated with the High Flux tube data. Keeping this in mind after a couple of different methods were tried, the temperature distribution obtained with the following technique was accepted as satisfactory and used for resoldering the High Flux tubes and manufacturing the Turbo-B tubes.

As a first step, type-T copper-constantan thermocouples were positioned in 1mm x 1mm grooves machined on the outer surface of the copper sleeve. A cartridge heater was inserted into the copper sleeve using a push fit. The thermocouples were secured in place by peening over the edges of the grooves in different locations using a blunt punch. The resulting imperfections were then removed with fine (400 grit) sand paper.

The copper sleeve, having been instrumented with thermocouples and a cartridge heater, was placed on two wooden blocks. The thermocouple channels were filled with the solder flux (50% tin and 50% lead). Great care was exercised to fill the channels entirely. The outer surface of the sleeve was then brushed with

solder flux to insure good wetting. The tube was placed vertically on top of a 0.5 inch long aluminum plug (to provide proper placement of the copper sleeve inside the tube case) and the copper sleeve was inserted from the top until it touched the aluminum plug. The tube, containing the copper sleeve, was placed horizontally in a cylindrical oven, open at both ends. The thermocouples were attached to a Newport temperature indicator to monitor the temperature increase when the oven was heated. The heat was then applied making sure that the wall temperature did not exceed 500 F which was the melting temperature of the thermocouple sheath. At 400 F, the solder started to melt and the tube was taken out of the oven and quenched from the bottom using a wet cloth. The oven was then placed vertically between two supports, keeping the bottom of the oven clear. The tube was inserted into the oven from underneath keeping the bottom section quenched. When the tube temperature reached 400 F, the solder started to re-melt and flow down inside the tube. Further solder was then applied from the top of the tube to a designated level. At this point, the tube was removed and quenched over its entire length using a wet cloth. After this initial quenching, the tube was left to cool down in air.

B. INSTALLATION OF EVAPORATOR TUBES AND TUBE SUPPORT BLOCK

Before removing the tube bundle from the evaporator, the support block, backing plate and front glass viewing window were carefully removed. The tube bundle was taken out from the back of the boiler. It consisted of five instrumented

evaporator tubes, 10 actively heated evaporator tubes, and 20 dummy smooth tubes. The seal was provided by O-rings compressed between the tube support block and the stainless-steel backing plate. Once the evaporator tubes were installed in the support block, without tightening the backing plate nuts, the block was guided into the evaporator section. The block was then levelled and all bolts were tightened appropriately. To replace the front window, very small, equal torques were applied circumferentially to each nut, in turn, in the outer ring support. Each heated tube was pushed forward so as to touch the front-viewing window. The backing plate was then tightened and the O-rings compressed, providing a good vacuum in the system.

C. SYSTEM LEAKAGE CHECK

After the system was isolated from the atmosphere and system integrity was restored, a Seargent Welch 10 SCFM vacuum pump was turned on and the pressure in the system was taken down to 29 in-Hg vacuum. The valves R-1 and R-8 (Figure 3.2) were kept open in order to achieve this vacuum. These valves were then secured and the system was left untouched for at least 10 hours to see if there was any leakage. If there was significant leakage, then the system was pressurized with air to 15 psi (through valve R-2). Large leaks were then detected by simply listening to the air coming from the system. If the leaks were small, the system was charged with R-114 vapor at a pressure of 5-7 psi through valve R-2. A freon detector was then used to find any minor leaks. After all leaks had been

secured, the system was again subjected to a vacuum for 10 hours. When the system passed the above vacuum test, Freon fill from the reservoir was started.

D. FREON FILL

A Freon storage tank was used to store the R-114 during experiments. Storage prevented discharge of the R-114 into the atmosphere and made experimentation less costly. To fill the evaporator with R-114 from the storage tank, the ethylene glycol/water mixture was first cooled to a temperature less than -10 C. Both condenser pumps were put into operation thus allowing coolant to flow through the condenser section. Valves (connecting the storage tank to the evaporator) were opened and Freon fill started. At the start of the fill, the pressure in the storage tank was about 13-14 psig; the system was under 29 in-Hg vacuum. Due to this pressure difference, the liquid (R-114) flowed from the storage tank into the evaporator. Approximately 20 to 30 minutes later, when the pressures were equalized, the transfer of Freon was complete. Then valves R-4 and R-6 were closed. Additional Freon could be added from a Freon cylinder using valve R-2 if required (there was always a small loss of Freon when transferring from the storage tank to the evaporator or vice-versa).

E. FREON REMOVAL

For tube replacement, maintenance or clean-up purposes, the R-114 was removed to the storage tank. The ethylene glycol/water mixture temperature was

cooled to less than -10 C: valves R-7 and R-8 were opened and the vacuum pump was turned on to put the storage tank under vacuum. Then, R-114 flowed from the evaporator to the storage tank because of pressure difference.

F. SYSTEM CLEAN-UP

After removal of the R-114 from the evaporator, valve R-5 was opened and any leftover R-114/oil mixture was drained into a container and dumped. A fan was on at all times during this operation to disperse the small quantity of R-114 vapor still in the system.

To clean the system, Freon R-113 (due to its higher boiling temperature compared with R-114), acetone and water were used.

For the first phase of clean-up, the boiler was filled with R-113 to a level 5 cm above the tube bundle and was boiled for 30 minutes. After boiling, air was put into the system via valve R-2. Using this excess pressure, the R-113 (and any residual oil) was drained to a waste drum through valve R-5. The mixture was then taken from the drum and placed in a distillation bottle. Heat was applied and R-113 was boiled off and collected for re-use. The oil which accumulated at the bottom of the distillation bottle was then dumped. This distillation process was then repeated.

After completing the R-113 clean, all electrical connections to the system were disconnected and the front-viewing glass window was removed. The tube bundle and dummy tube rack were then taken out. The inside surface of the boiler

Excess acetone was removed through valve R-5 and stored in a waste container. The system was then air dried with a blower.

Having removed the tubes from the tube bundle, bundle and rack were individually washed with water and then acetone. Tubes were also cleaned using acetone and a soft bristled toothbrush, exercising care not to interfere with the tube surface.

After cleaning all pieces of the system separately, the R-114 was transferred into the evaporator through standard procedures mentioned earlier (keeping the tube bundle outside). The storage tank was then opened and cleaned using water and acetone. The R-114 was then transferred back to the storage tank by slow boiling using the simulation heaters. This second transfer was complete within five hours. Any oil left in the evaporator (which was a small amount) was drained and dumped. The entire clean-up procedure was then repeated to make sure that the oil quantity in the evaporator was negligible.

G. GENERAL OPERATION

After the system had been cleaned, the boiler was filled with R-114 to a level of 10 cm above the top tube in the bundle, corresponding to a mass of 60.3 kg of R-114 at -15 C. Prior to operating the system, the 8-ton refrigeration unit was run for an hour to reduce the ethylene-glycol/water mixture temperature in the sump to a value of less than -10 C. The pressure in the evaporator was 12 to 14 psig. When the sump temperature was sufficiently low, the data acquisition system

psig. When the sump temperature was sufficiently low, the data acquisition system and computer were turned on. The system pressure was slowly lowered by allowing the coolant to pass through the condenser tubes. This slow cooling is especially important for runs using "increasing heat flux" from a secured condition (as explained in Chapter V, Surface Preparation Technique -C) to ensure that the nucleation sites were not activated prematurely.

Boiling in the evaporator initially started due to the pressure drop without applying any heat flux. At the required saturation temperature of 2.2 C, the heaters were switched on to the desired setting and data were taken. The heat flux was then slowly increased by adjusting the rheostat. For observation of "boiling hysterisis" effect, the data were taken with very small heat flux increments, waiting at least 5 minutes at each heat flux to attain steady conditions. At critical regions such as the onset of nucleate boiling, at least two readings were taken. The bundle was continuously monitored through the glass window and compared to the data printout to observe trends.

H. OIL ADDITION

During the Turbo-B tube bundle experiments, successive amounts of oil were added into the evaporator. Since the weight of the refrigerant in the evaporator was 60.3 kg, the amount of oil corresponding to 1% by weight was measured as 670 ml, 2% as 1340 ml etc. The oil was syphoned into the evaporator from a storage drum through valve R-3 by reducing the system pressure to less than 15

in-Hg vacuum. Ensuring that no air entered the system, the scale of the measuring container was observed to see that the appropriate amount of oil was added to the refrigerant. Valve R-3 was secured after oil addition.

I. DATA REDUCTION PROCEDURES

The data reduction program "DRP4" was used during the experiments for processing the data collected. The program was written in HP Basic 3.01 and run on an HP-9000 series computer. The characteristics and capabilities of this software and the entire listing of the program is provided by Anderson [Ref. 7].

V. RESULTS AND DISCUSSION

A. GENERAL DESCRIPTION

During the experiments, both the High Flux and Turbo-B tubes were tested at a saturation temperature of 2.2 C. All runs were conducted using refrigerant (R-114) at slightly under atmospheric pressure.

The onset of nucleate boiling was observed through the front glass viewing window; this was linked to the sudden change in the wall superheat value given by the thermocouples embedded in the tube and indicated on the computer printout. During these experiments, the data were taken from five instrumented tubes, numbered consecutively 1 to 5 from the top downward.

The data taken by Akcasayar [Ref. 10] simulated a continuously operating air-conditioning system by using surface preparation technique-D as described in the next section. During this thesis study, however, surface preparation technique-C was used, simulating the initial start-up of a refrigeration system.

Naming of the files used for data storage is similar to that of Akcasayar [Ref. 10]. Each file name is comprised of five sets of alpha-numeric characters, split up as follows:

First set	- tube type	- HF (High Flux) - TB (Turbo-B)
Second set	- H	- H (H. Eraydin data)
Third set	- surface preparation	- C (Increasing q") - D (Decreasing q")

Fourth set	- % of oil in Freon (by weight)	- 0, 1, 2, 3, 6, 10
Fifth set	- number of activated tubes	- 1 (one tube activated) - 2 (two tubes activated) - 3 (three tubes activated) - 4 (four tubes activated) - 5 (five tubes activated) - 6 (entire bundle activated) - 7 (bundle and simulation heaters activated)

To give an example, the file name "TBHC62" indicates that Turbo-B tubes, data taken by H. Eraydin, increasing heat flux, 6% oil and two tubes activated. Exception to this file naming method is the data set of "TBHCD01." This file contained the data for both increasing the decreasing heat flux.

Filenames used on the figures start with the letter of "p" to indicate that they are plotting files.

B. R-114 BOILING FROM A HIGH FLUX TUBE BUNDLE

The first set of data using a High Flux tube with R-114 was obtained by Reilly [Ref. 9] in an apparatus designed for a single tube. These experiments were then repeated in the bundle apparatus by Akcasayar [Ref. 10]. Comparison of the results showed that the performance enhancement due to bundle operation was not significant (see Ref. 10). The average bundle heat-transfer performance approached the single tube performance since all instrumented tube performances remained nearly the same for different operations in the bundle.

Data were obtained by Akcasayar [Ref. 10] using surface preparation-D to simulate a continuously operating air-condition system. This surface preparation

entailed initially boiling of the R-114 for 30 minutes at a maximum heat flux of 75-100 kW/m^2. Data were then taken in decreasing steps of heat flux down to a minimum value of 1 kW/m^2. In this way, nucleation sites within the bundle remained active, thus preventing any "boiling hysterisis."

During this thesis study, surface preparation-C was used to simulate the initial start-up of a refrigeration system. This surface preparation required securing the evaporator power for 24 hours and then slowly attaining saturation conditions by cooling the R-114. Data were then taken in small increasing heat flux increments. After the maximum heat flux was reached, data were then also taken for decreasing heat flux.

The first stage of the experiments was to determine the effect of contamination on the heat-transfer capability of High Flux tubes. The apparatus was cleaned first by simply distilling the oil by boiling off the R-114. The oil was removed, the evaporator refilled and data taken. The system was then cleaned more thoroughly using the full procedure laid out in Chapter IV. The evaporator was recharged with R-114 and data taken. Figure 5.1 shows a noticeable difference between the two data sets and demonstrates the importance of the lengthy (and somewhat arduous) cleaning procedure that was subsequently employed.

Figures 5.2 and 5.3 show the data for tube 1 operating alone within the bundle for increasing and decreasing heat flux respectively. In the same figures, the data taken by Reilly [Ref. 9] for a High Flux tube in the single tube apparatus

are also included. The boiling curves of these two separate experiments agree closely for both increasing and decreasing heat flux, with the single tube apparatus results giving slightly better heat transfer performance at low and intermediate heat flux. The differences seen between the curves are probably due to different bubble circulation patterns experienced by each apparatus. Notice also in Figure 5.2 the scatter obtained by Reilly [Ref. 9] at low fluxes. This demonstrates the difficulty in taking data in this sensitive region at very low wall superheats (less than 0.5 K), where the inaccuracies in the wall temperature distribution (due to thermocouple error, or the fabrication/soldering process) may be as large as the temperature difference being measured.

In Figure 5.4, the performance of tube 1 operating alone in High Flux, finned [Ref. 10] and smooth [Ref 7] tube bundles are compared for increasing heat flux. The comparison clearly exhibits the enhancement of nucleate boiling obtained with the High Flux tubes. Note, however, in the natural convection region High Flux tube has the smallest heat transfer coefficient comparing to other tubes. The small value of wall superheat of around 1-3 K obtained with the High Flux tube during nucleate boiling should be noted. This compares with values of 5-8 K and 8-20 K for the finned and smooth tubes respectively. Furthermore, the onset of nucleate boiling occurs at a heat flux of 1200 W/m^2 for the High Flux tube, compared to much higher values of 20,000 W/m^2 and 7500 W/m^2 for the finned and smooth tubes respectively. Also, the temperature overshoot for the finned tube is almost 15 K while for the High Flux tube a value of 6 K is seen. This behavior indicates the

earlier (i.e., lower heat flux) activation of nucleation sites for the High Flux surface. Also, the very low values of wall superheat associated with the High Flux tube indicate that the number of nucleation sites is much greater, thereby increasing the amount of heat that can be removed from the surface.

Figure 5.5 shows the results when tubes 1 and 2 are activated together, again for increasing heat flux. The presence of another tube vertically below does not seem to noticeably affect the performance of the upper tube either in the natural convection or nucleate boiling regimes. Clearly, however, the natural convection heat-transfer coefficient for tube 2 is less than tube 1, whereas the nucleate boiling heat-transfer coefficient is slightly greater. Similar behavior to that found in Figure 5.5 was observed for smooth tubes by Marto and Anderson [Ref 20]. They pointed out that this behavior might be explained by the close proximity of the tubes influencing the velocity and temperature fields in the wake of a heated tube. In addition, it should be noted that the start of nucleate boiling of the upper tube increases the natural convection heat transfer coefficient of the lower tube due to bubble pumping from the upper one.

Figure 5.6 shows the data when three tubes are activated. As with Figure 5.5, the top tube in the bundle starts nucleating first: this causes a slight reduction in wall superheat for tubes 2 and 3 which continue in the natural convection regime. At a higher heat flux, tubes 2 and 3 start to nucleate at the same time. The existence of two tubes vertically below tube 1 does not seem to influence the natural convection behavior of this top tube. However, the presence of tube 3 does

cause a slightly earlier transition to nucleate boiling for tube 1 and a slight delay for tube 2. In addition, as shown in Figure 5.5, during nucleate boiling tube 2 gives the best results.

As seen in Figures 5.7 and 5.8, an increase in the number of activated tubes to 4 and 5 does not noticeably affect the bundle behavior over that seen with three activated tubes.

For example, Figure 5.8 shows that tube 1 starts to nucleate first. This causes a slight reduction in wall superheat for the other four tubes (probably due to the bubble pumping action on tube 1 in turn causing a greater liquid circulation around the bundle). The tubes then start nucleating in order, although it appears that tubes 2, 3 and 4 start nucleate at a similar heat flux. As further tubes nucleate, the wall superheats of the remaining tubes below reduce slightly. It can also be seen from Figure 5.8 that the nucleate boiling curve is not the same for each tube: tube 2 has the highest heat-transfer coefficient with tube 5 having a significantly lower value. This behavior was repeated at all oil concentrations and also found by Akcasayar [Ref. 10]. It should be noted here that as each tube nucleated, the performance of the other tubes already nucleating was not altered.

Figures 5.9 and 5.10 show the data for the complete tube bundle (15 tubes activated-test number 6) and the bundle plus simulation heaters (test number 7) respectively. In the natural convection region, the behavior is much the same as described above. However, it can be seen that the performance of tubes 3 and 4 deteriorate significantly in the nucleate boiling regime. It was presumed that this

deterioration could either be a bundle effect or a temperature distribution/soldering problem. The first possibility was further examined by altering the positioning of the tubes. Each tube was moved down by 2 positions, i.e., 1 to 3, 2 to 4, 3 to 5, etc. However, in this new arrangement, where tubes 3 and 4 became tubes 5 and 1, it became evident that it was not a bundle effect (see Figure 5.11) as each tube number (and not position) performed as before. Consequently, the reason for the differences seen the figures had to be due to individual tubes. Similar behavior had also been reported by Akcasayar [Ref. 10] who pointed out that the differences in measured wall superheat could be due to increased temperature differences between thermocouple readings around the tube (note that due to the low values of wall superheat, poor temperature distribution around the tube could lead to significant error).

The poor temperature distribution could be due to a number of reasons:

1. poor soldering technique (the soldering should have been carried out either in a vacuum or inert atmosphere, but no such facilities were available) resulting in an oxide layer or even air gaps around thermocouple junction.
2. poor heater cartridge resulting in a non-uniform heat flux,
3. insufficient wall thickness (the tubes may not have sufficient wall thickness to provide a uniform temperature distribution),
4. poor tube surface characteristics.

It was considered that reasons 2 and 3 were not likely. Reason 1 was investigated further by using the new soldering technique described in Chapter IV.

All the existing instrumented High Flux tubes were resoldered. Despite being resoldered, these tubes still exhibited a significant deterioration in performance.

Consequently, it was felt that any maldistribution in the tube wall temperature readings did not cause the behavior seen in the figures. It is more likely to be the enhanced surface itself and it is planned to make up a new set of High Flux tubes and retest this bundle in the future.

An interesting point is the fact that the deterioration seen in tubes 3 and 4 on Figures 5.9 and 5.10 only occurs when the entire bundle is activated. This problem does not occur when auxiliary and simulation heaters are not activated. The reasons for this is not known.

Very little information is available in the literature regarding the onset of nucleate boiling in a tube bundle, especially hysterisis effects and the influence of surface preparation (past history) upon the incipient boiling condition. It is therefore very difficult to draw a definite conclusion explaining the behavior seen. More data are needed using these enhanced surfaces with other fluids, different bundles, pool (i.e., liquid height) geometries and inlet qualities.

C. R-114/OIL MIXTURES BOILING FROM A TURBO-B TUBE BUNDLE

The performance of tube 1 activated alone, in pure R-114 within the bundle is shown in Figure 5.12 for both increasing and decreasing heat flux. Above a heat flux of 15 kW/m^2 the results are almost identical. The temperature overshoot for increasing heat flux is not as significant in magnitude as the High Flux tube. Since

the nucleation sites remain active, overshoot is not seen for decreasing heat flux, thus creating the classic hysterisis curve. Despite not having a striking overshoot, the value of gradual overshoot is about 1 K for increasing heat flux.

Marto and Memory [Ref. 3] and Murphy [Ref. 2] tested the Turbo-B tube in pure R-114 and R-114/oil mixtures using the single tube apparatus. Their results for pure R-114 are plotted in Figure 5.13 for decreasing heat flux and are compared with the present data. Although the boiling curves are parallel, it can be seen the single tube apparatus data result in better heat transfer performance. This improvement could be due either to slightly different tube manufacturing techniques or the different flow patterns set up in the more confined single tube apparatus.

The influence of lower tubes on the performance of tube 1 is shown in Figures 5.14 and 5.15 for increasing and decreasing heat flux respectively. Apart from the natural convection region seen in Figure 5.14 (where there seems to be no regular "pattern"), the boiling curves are nearly parallel for the entire heat flux range in both figures. It appears that the activation of successive tubes below the top tube increases the heat transfer coefficient by an equal amount. This increase is probably attributed to better flow circulation within the bundle. For the natural convection region, the wall superheat varies significantly depending on the number of tubes activated (this behavior was very repeatable). However, this variation is quite irregular and the reason for this is not known at the moment, but could be an oscillatory bundle effect.

Figure 5.16 shows the boiling characteristics of tubes 1 and 2 activated together for increasing heat flux. The observed behavior is very similar to the High Flux tube results in that initially the upper tube starts nucleating, causing a noticeable increase in heat transfer coefficient of the lower tube, even though this lower tube remains in the convection region. The onset of nucleate boiling on the lower tube does not, however, affect the heat-transfer coefficient for the upper tube already nucleating. It is thought that the start of nucleate boiling on the upper tube before the lower tube is due to the influence of the closely-spaced tubes upon the velocity and temperature fields in the wake region of a heated tube. Notice also that in the nucleate boiling region, both tubes perform very similarly with the lower tube slightly better at high heat flux (more than 20 kW/m^2), but slightly worse at intermediate heat flux.

As seen in Figure 5.17 for increasing heat flux, the activation of tube 3 seems to cause a significant reduction in the wall superheat of tube 1 in the natural convection regime. However, when Figure 5.17 is compared to Figure 5.18 (4 tubes activated), this behavior is not repeated and suggests that there is no regular pattern in this region. It appears that the convection region is heavily affected by operating conditions.

The operation of the whole bundle (15 tubes activated) and bundle plus simulation heaters (Figures 5.19 and 5.20) does reduce the temperature overshoot of tube 1 dramatically. However, the remaining tubes still clearly exhibit a temperature overshoot. This is probably due to significant flow circulation within

the bundle triggering an early change to nucleation for tube 1. The behavior of the Turbo-B tubes in pure R-114 for decreasing heat flux is shown in Figures 5.21 through 5.24. These figures verify the increasing heat flux behavior: for a heat flux greater than 20 kW/m^2, tube 2 gives the best heat transfer performance whereas at low heat fluxes, tube 1 prevails. Lower tubes (3, 4 and 5) showed poorer performance for the whole range of heat flux, with tube 4 giving the largest values of wall superheat (lowest heat transfer coefficient). This is probably due (as with the High Flux tubes) to a nonhomogeneous tube wall temperature distribution as indicated by the relatively high wall thermocouple values for this tube.

Figures 5.25 and 5.26 show the performance variation of the top tube (tube 1) with various oil concentrations added to the R-114 for increasing and decreasing heat flux respectively. Figure 5.26 shows that with decreasing heat flux, even 1% oil addition causes a significant amount of degradation especially at low heat flux. The performance curve stays almost the same for 2% oil addition, but deteriorates further for 3% oil at low heat flux. As seen in Figure 5.25 it is very difficult to observe the effect that oil contamination has in the natural convection region on a Turbo-B tube within a bundle. The presence of 3% oil seems to cause a significant degradation in natural convection regime. On the other hand, the addition of 6% oil gives significant increase in heat transfer coefficient comparing to that of pure R-114: there seems again to be no regular pattern for the convection region.

Marto and Memory [Ref. 3] and Murphy [Ref. 2] also investigated the effect of oil contamination on Turbo-B tubes boiling in the single-tube apparatus. They reported very similar behavior to that mentioned above.

The effect of oil on pool-boiling performance of R-114 from enhanced surfaces was investigated by Wanniaroichchi, Marto and Reilly [Ref. 17] in detail. They reported that, when boiling occurs within large re-entrant cavities, channels or pores (such as High Flux and Turbo-B tube surfaces), the more volatile R-114 liquid evaporates leaving behind an oil rich mixture in the vicinity of tube surface where the actual evaporation takes place. The presence of this oil-rich layer within the cavities creates a resistance to further heat-transfer, thereby degrading the boiling performance.

In Figure 5.27, the performance of the Turbo-B tube bundle (15 tubes activated) is shown for different oil concentrations. Here the heat transfer coefficient is plotted against the heat flux. The addition of 3% and 6% oil causes a noticeable decrease in the heat transfer coefficient at all levels of heat flux: however, the degradation is much more noticeable and significant at low heat flux.

D. PERFORMANCE COMPARISON OF THE SMOOTH, FINNED, HIGH FLUX AND TURBO-B TUBE BUNDLES.

The boiling curves (i.e., heat transfer coefficient vs heat flux) for the smooth, finned, High Flux and Turbo-B tube bundles (15 tubes activated) are shown in Figures 5.28 through 5.30. The first thing to notice (as pointed out by Marto and

Memory [Ref. 3]) is that there appear to be three distinct types of surface: smooth, ordinary integral finned and restructured finned/porous surfaces. The results using pure R-114 indicate that the heat transfer performance for both High Flux and Turbo-B tube bundles are similar and outperform both smooth and finned tube bundles by a factor of up to 5 and 3 respectively. Despite having slightly lower heat transfer coefficients at low heat flux, the High Flux tube bundle exhibits a higher heat-transfer performance than the Turbo-B tube bundle at the more practical high heat flux values.

Average bundle heat-transfer coefficients of each individual tube type are tabulated for various oil concentrations in Table 5.1 through 5.4 for a practical heat flux of 30 kW/m^2. As seen in Figure 5.29 the addition of 3% oil causes the boiling curves of High Flux, Turbo-B and finned tubes to merge at high heat fluxes. With 6% oil addition, the performance of High Flux tubes degrade significantly, especially at high heat flux greater than 40 kW/m^2. Consequently both Turbo-B and finned tube bundles outperform the High Flux tube bundle for high fluxes and for oil concentrations equal or greater than 6%. The reason for large degradation in performance of the High Flux tubes at high heat flux and high oil concentration is probably due to the fact that diffusion of oil from the surface is overwhelmed by the oil migration into the surface (caused by boiling mechanism), leaving a thick oil-rich layer within the numerous pores of the tube. For the Turbo-B tubes, diffusion from the surface is easier, and although some degradation (over the pure

R-114 case) is seen at high oil concentrations, it is not as severe as with the High Flux tubes.

TABLE 5.1. BOILING HEAT TRANSFER COEFFICIENTS AND ENHANCEMENT RATIOS FOR SMOOTH TUBE BUNDLE AT A HEAT FLUX OF 30 KW/M².

% Oil	Bundle h (kW/m²K)	Enhancement Ratio
0	2.59	1.00
1	3.21	1.24
2	3.72	1.44
3	3.60	1.39
6	3.19	1.23
10	2.57	0.99

TABLE 5.2. BOILING HEAT TRANSFER COEFFICIENTS AND ENHANCEMENT RATIOS FOR FINNED TUBE BUNDLE AT A HEAT FLUX OF 30 KW/M².

% Oil	Bundle h (kW/m²K)	Enhancement Ratio
0	6.56	1.00
1	8.31	1.27
2	10.38	1.58
3	10.80	1.65
6	10.52	1.60
10	9.03	1.38

TABLE 5.3. BOILING HEAT TRANSFER COEFFICIENTS AND ENHANCEMENT RATIOS FOR HIGH FLUX TUBE BUNDLE AT A HEAT FLUX OF 30 KW/M².

% Oil	Bundle h (kW/m²K)	Enhancement Ratio
0	16.61	1.00
1	14.17	0.85
2	14.40	0.87
3	14.50	0.87
6	13.72	0.82
10	8.75	0.53

TABLE 5.4. BOILING HEAT TRANSFER COEFFICIENTS AND ENHANCEMENT RATIOS FOR TURBO-B TUBE BUNDLE AT A HEAT FLUX OF 30 KW/M².

% Oil	Bundle h (kW/m²K)	Enhancement Ratio
0	13.85	1.00
1	13.20	0.95
2	12.70	0.92
3	12.60	0.91
6	11.82	0.85

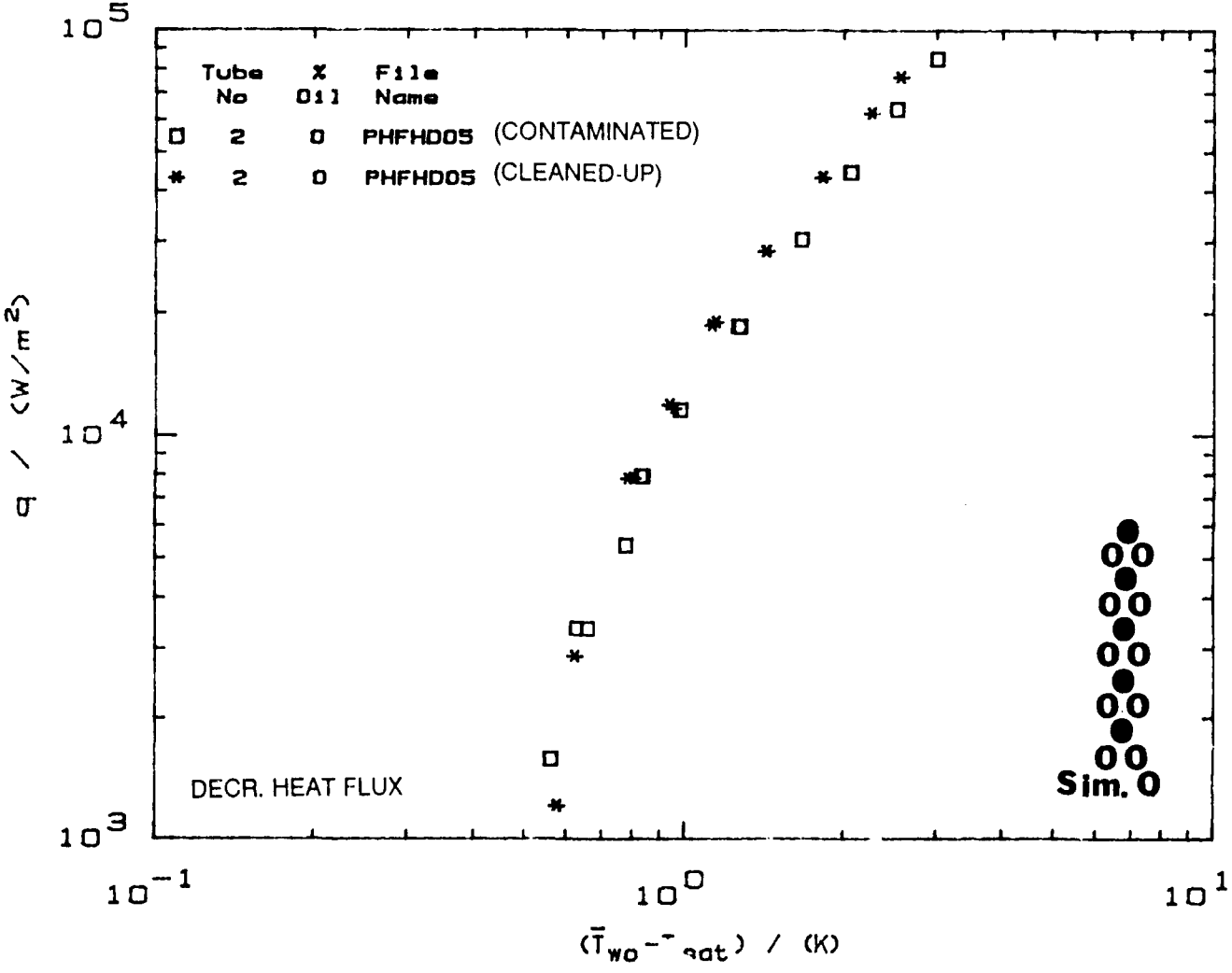

Figure 5.1. Improvement in Heat Transfer Performance with Clean-up (Decreasing Heat Flux).

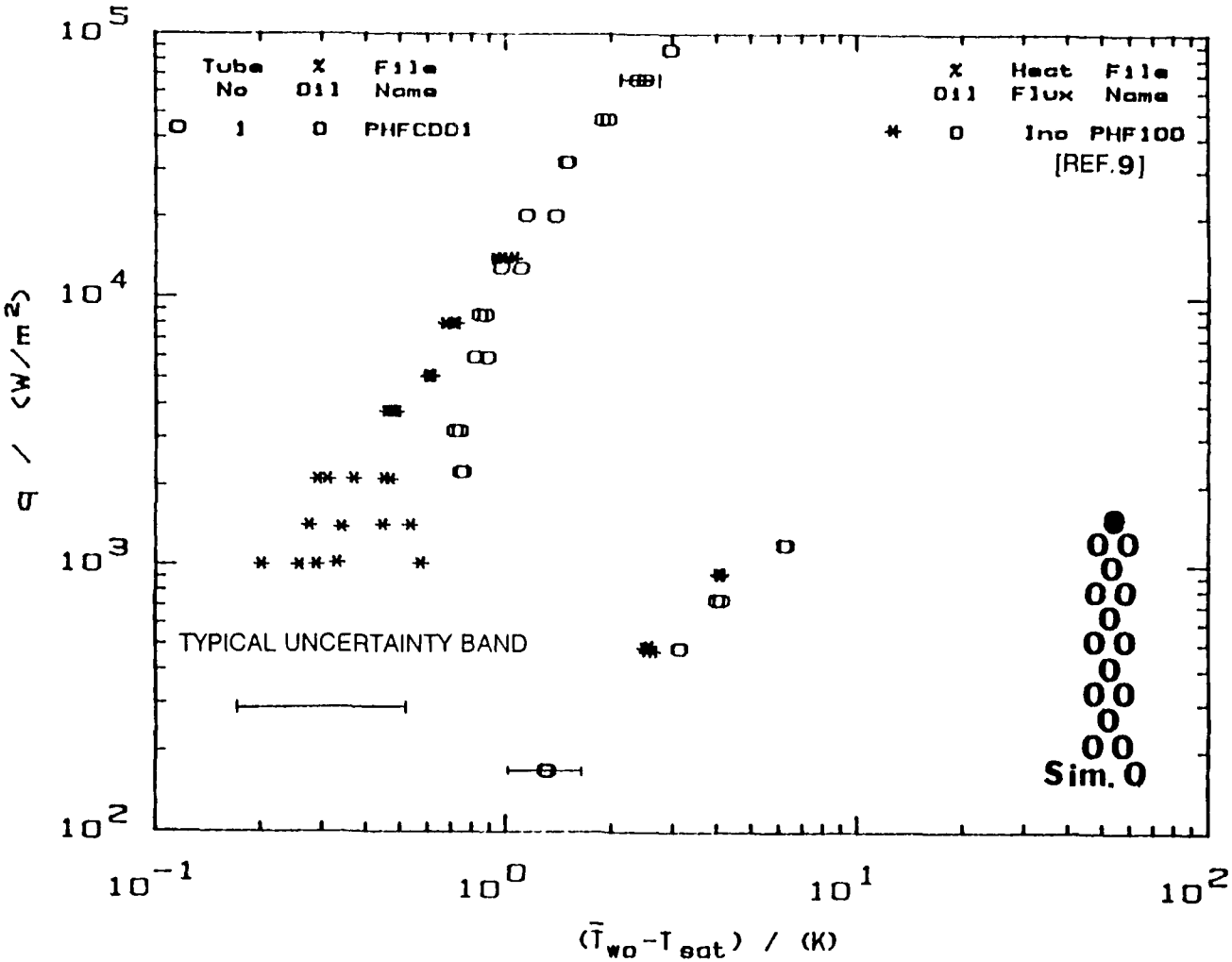

Figure 5.2. Performance Comparison of a Single High Flux Tube Within a Bundle and Within a Single Tube Apparatus.

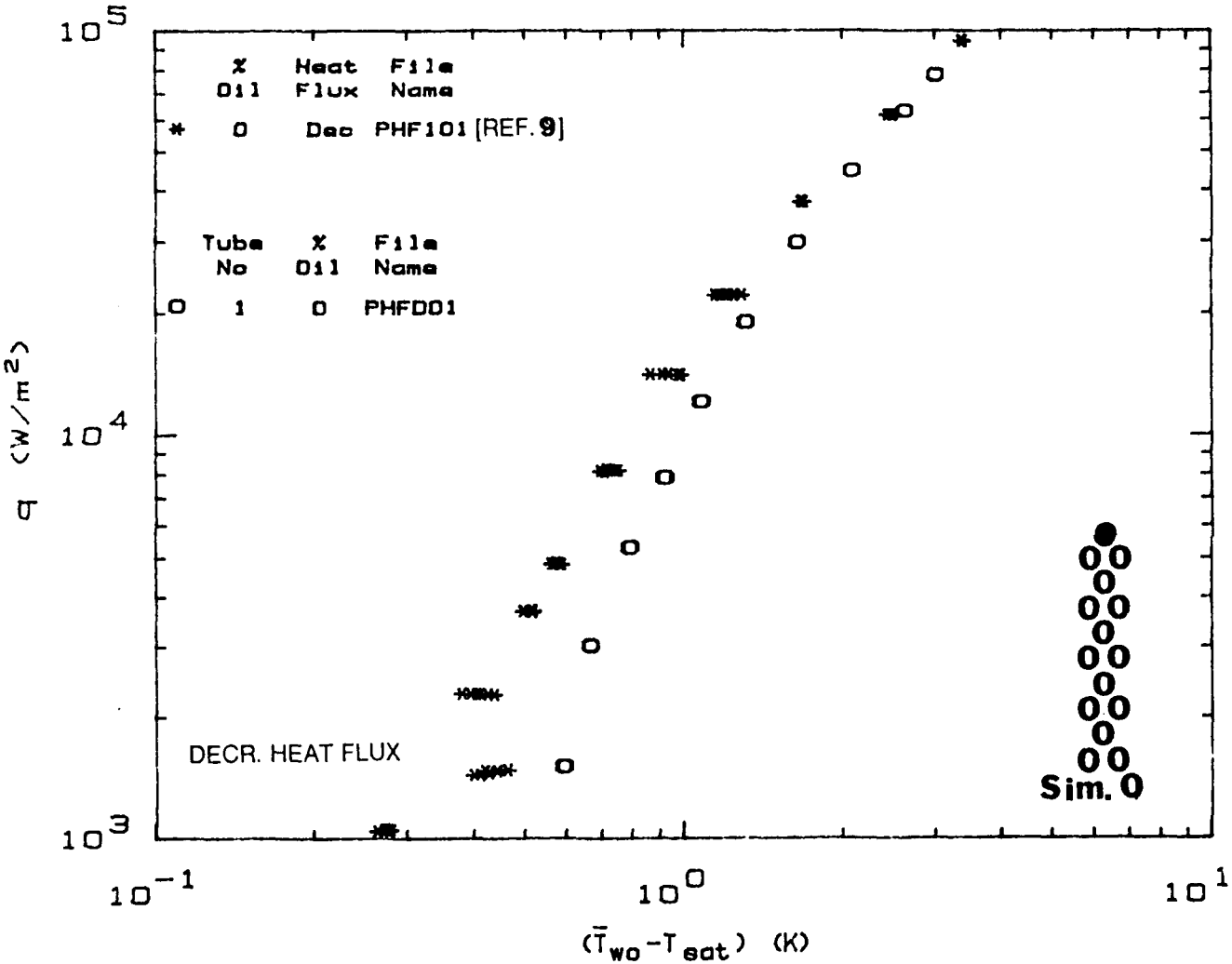

Figure 5.3. Performance Comparison of a Single High Flux Tube Within a Bundle and Within a Single Tube Apparatus (Decreasing Heat Flux).

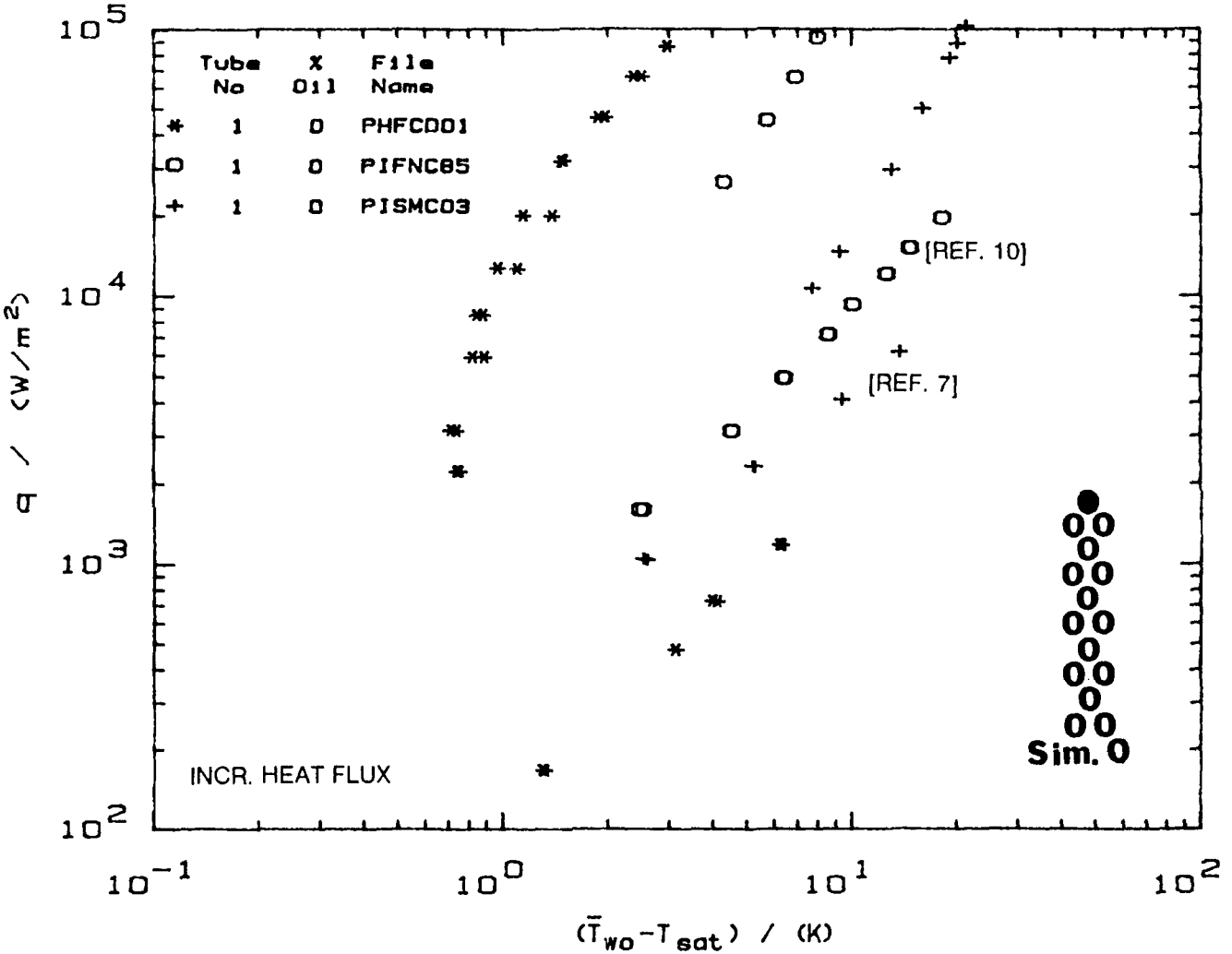

Figure 5.4. Performance Comparison of the Top Tubes of a High Flux, Finned and Smooth Tube Bundle.

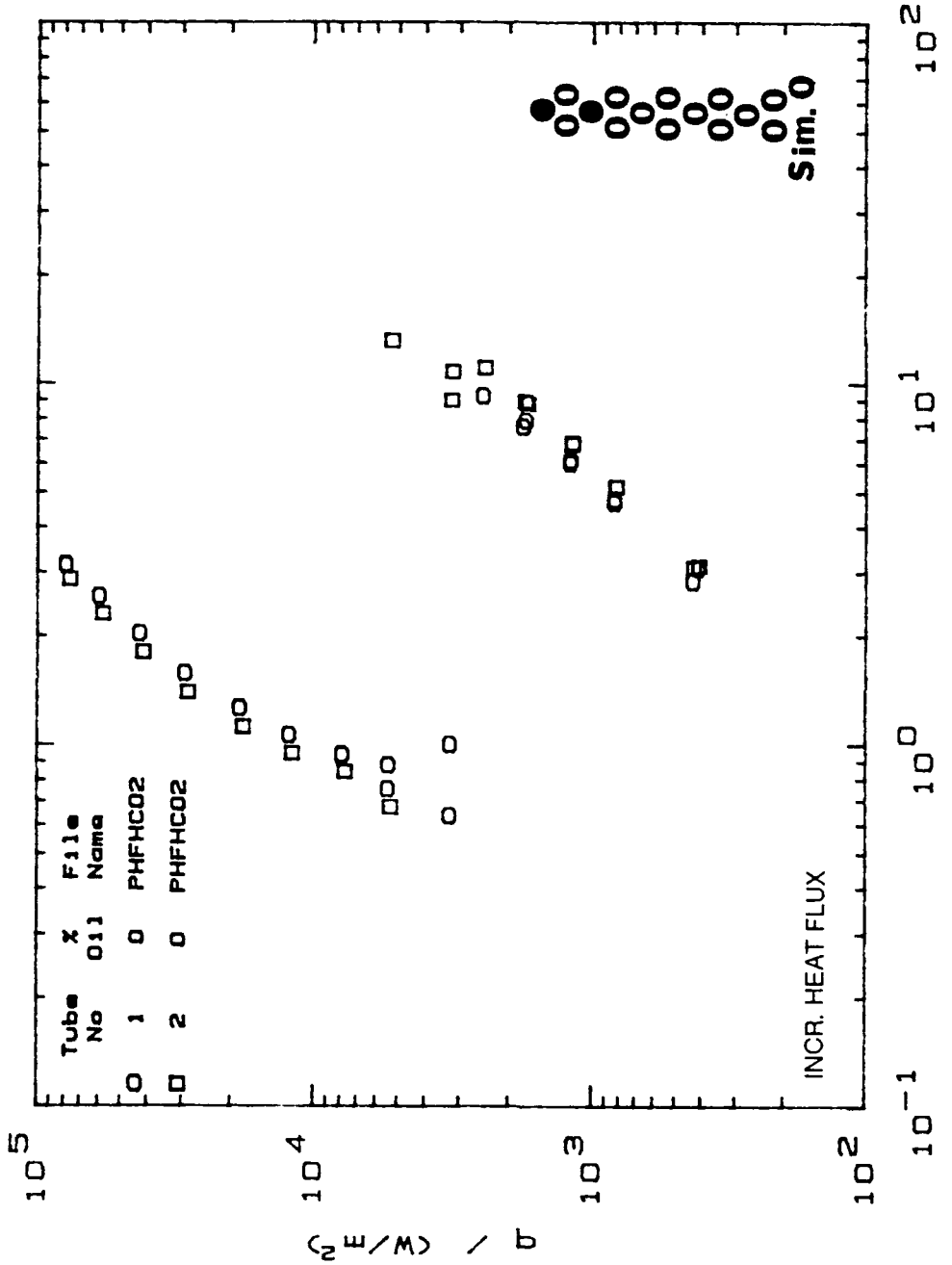

Figure 5.5. Boiling Data for High Flux Tubes 1 and 2 Operating Simultaneously.

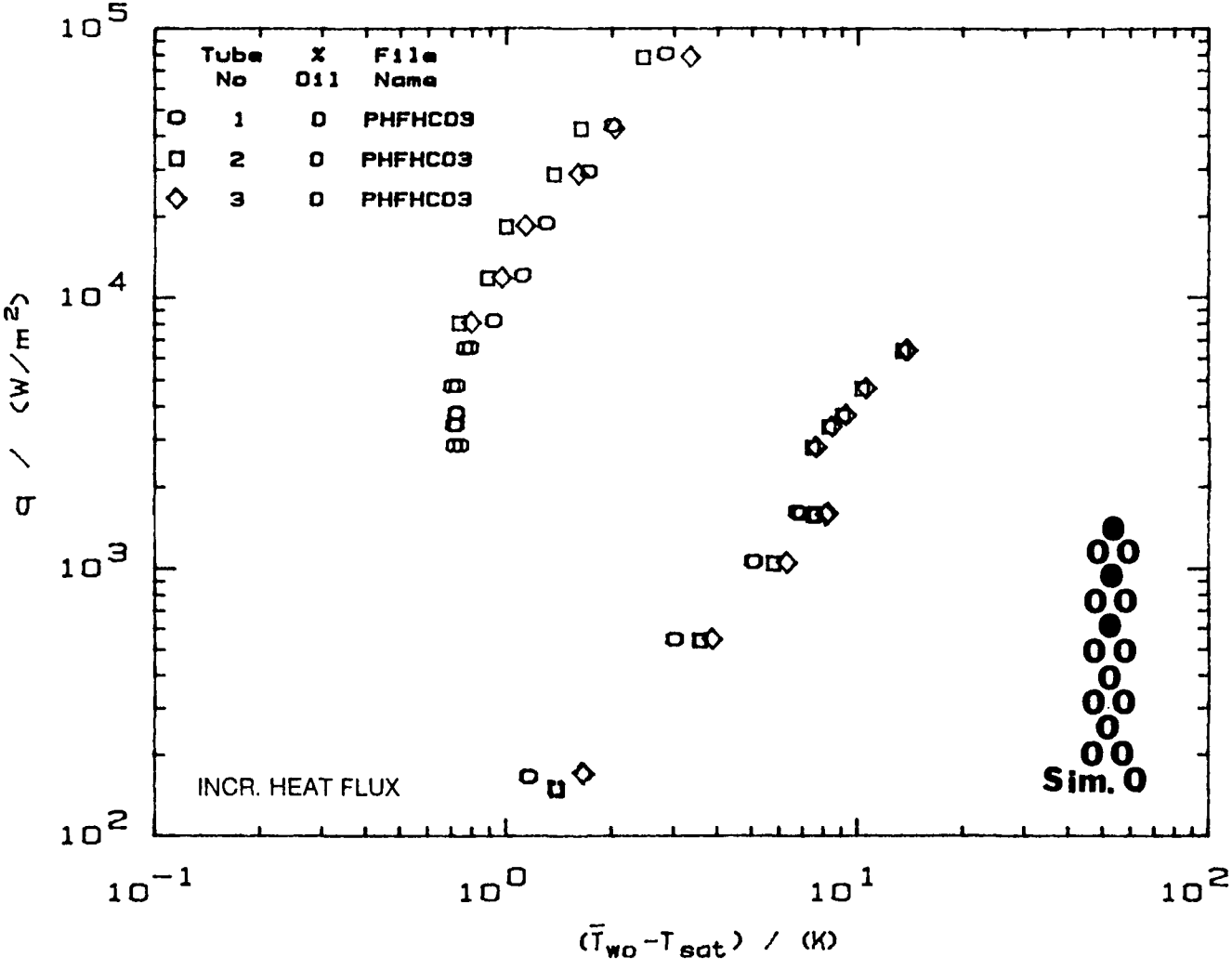

Figure 5.6. Boiling Data for High Flux Tubes 1, 2 and 3 Operating Simultaneously.

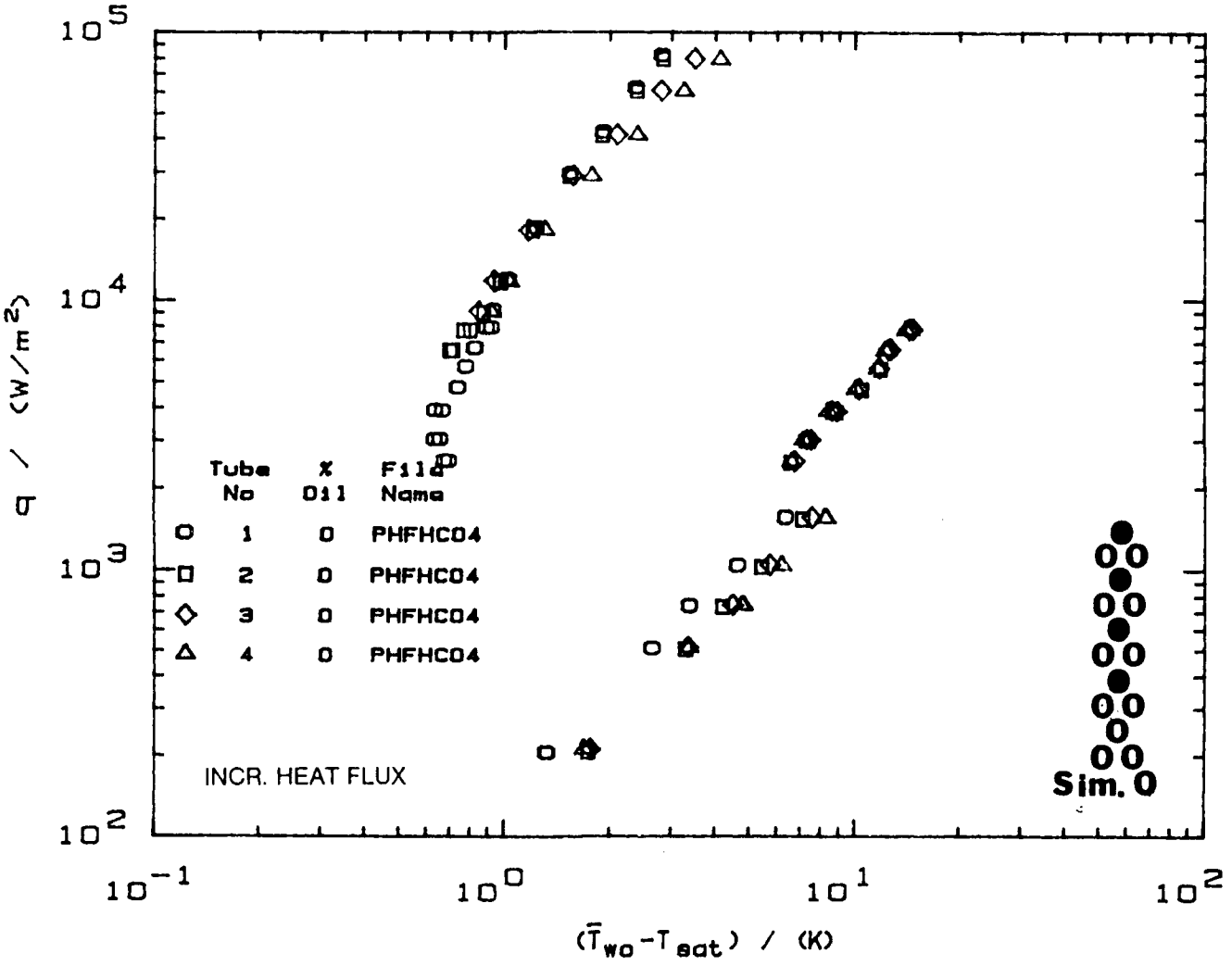

Figure 5.7. Boiling Data for High Flux Tubes 1, 2, 3 and 4 Operating Simultaneously.

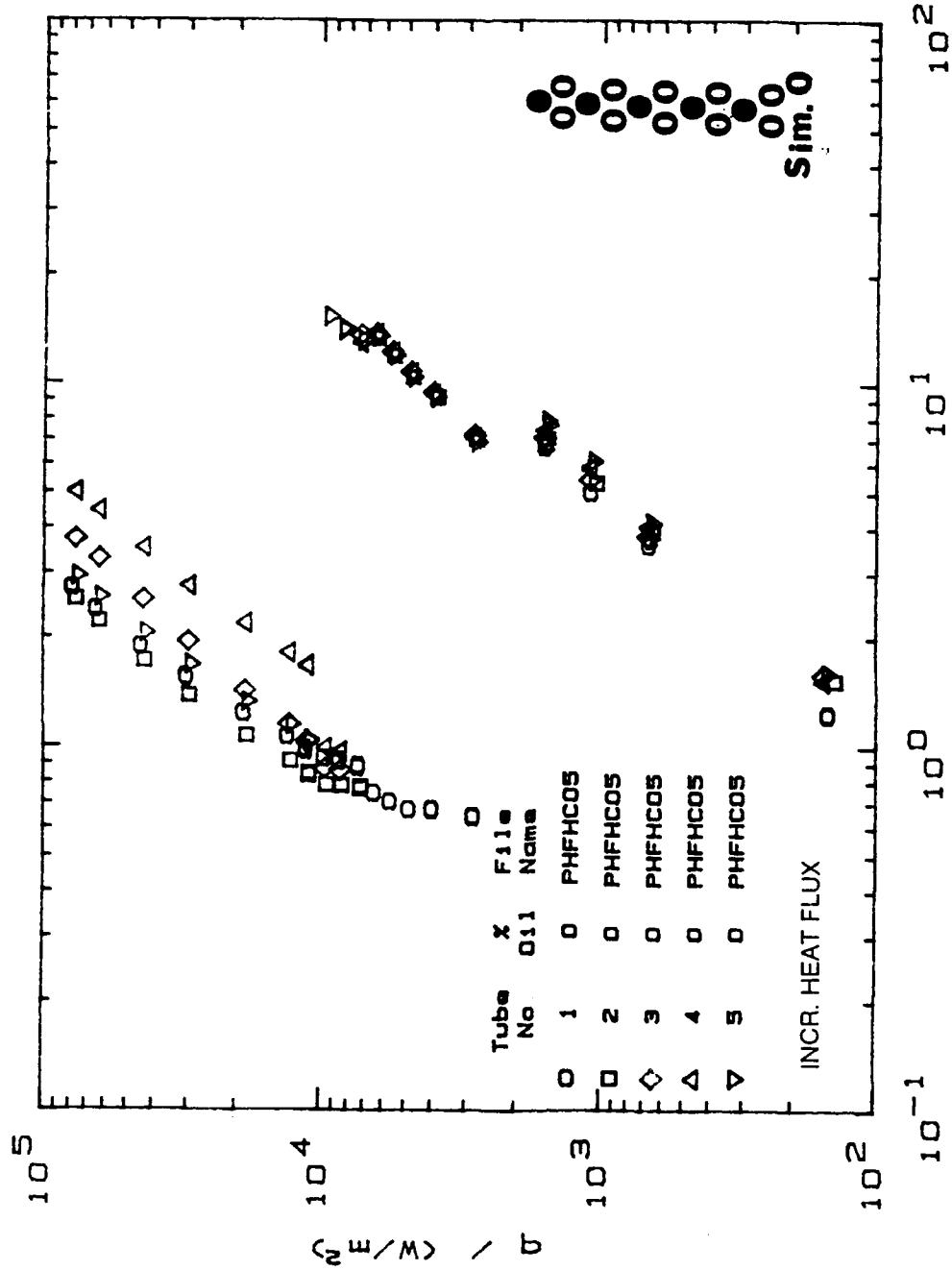

Figure 5.8. Boiling Data for High Flux Tubes 1, 2, 3, 4 and 5 Operating Simultaneously.

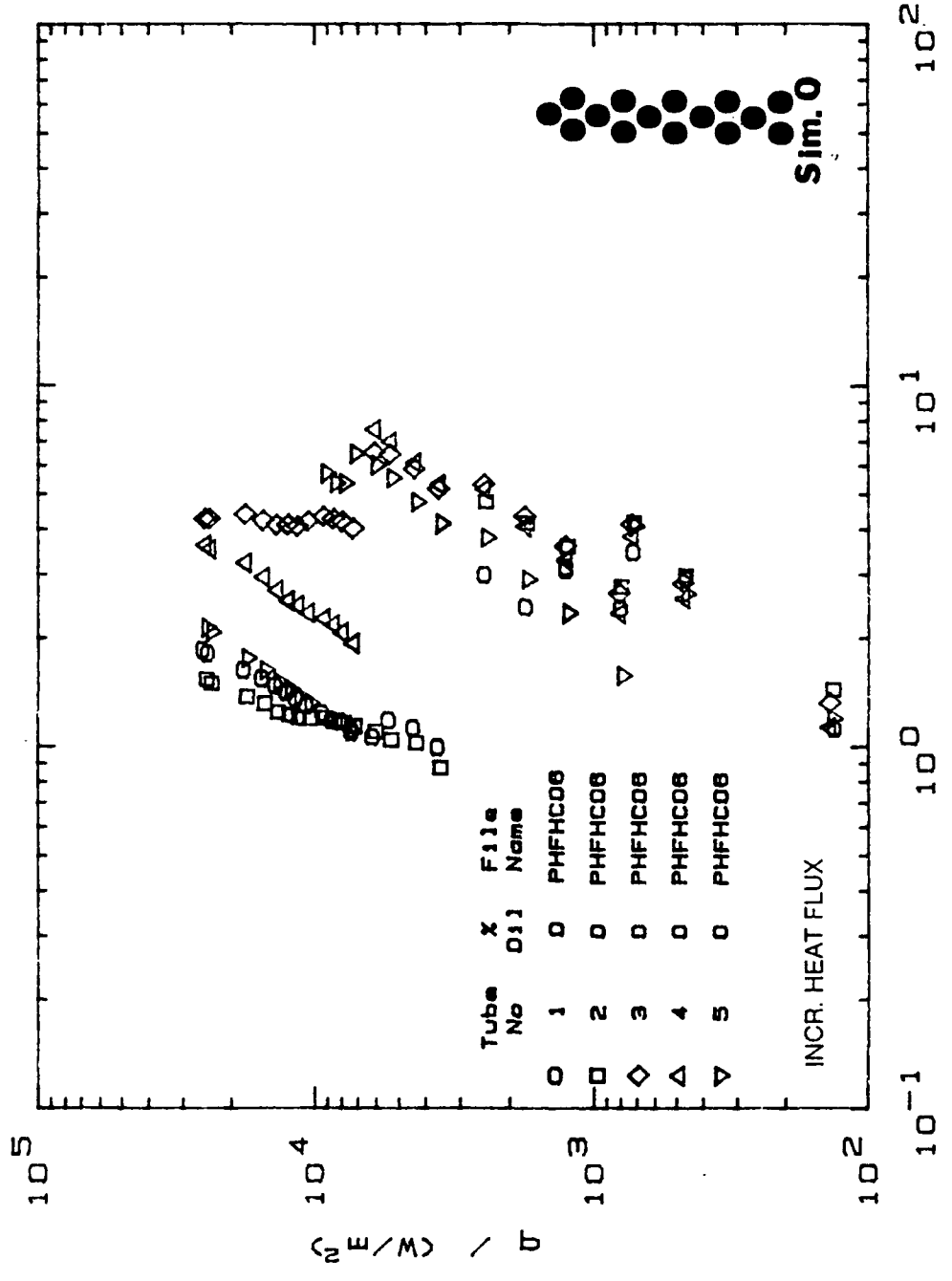

Figure 5.9. Boiling Data for High Flux Tube Bundle.

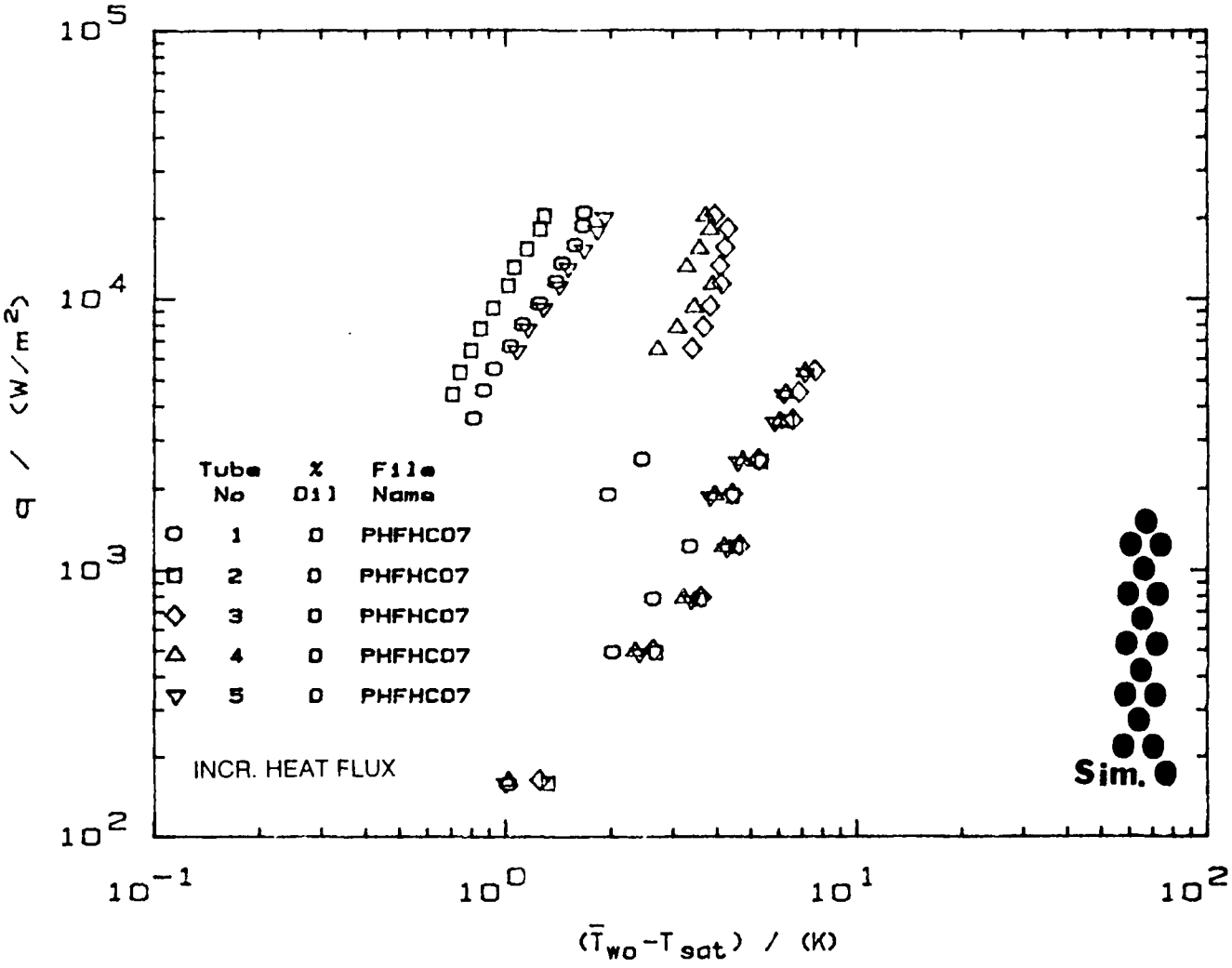

Figure 5.10. Boiling Data for High Flux Tube Bundle with Simulation Heaters in Operation.

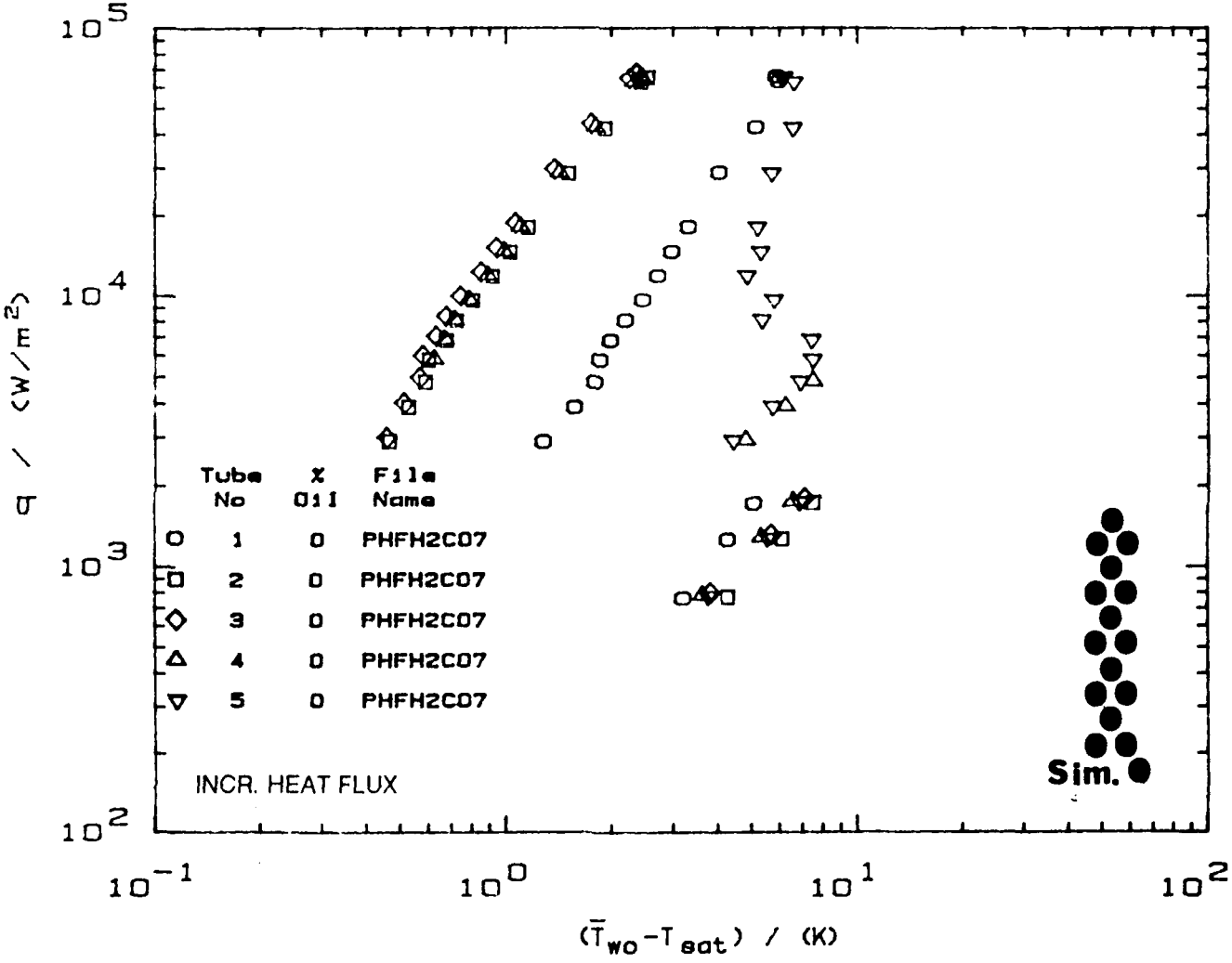

Figure 5.11. Boiling Data for High Flux Tube Bundle After Repositioning Tubes.

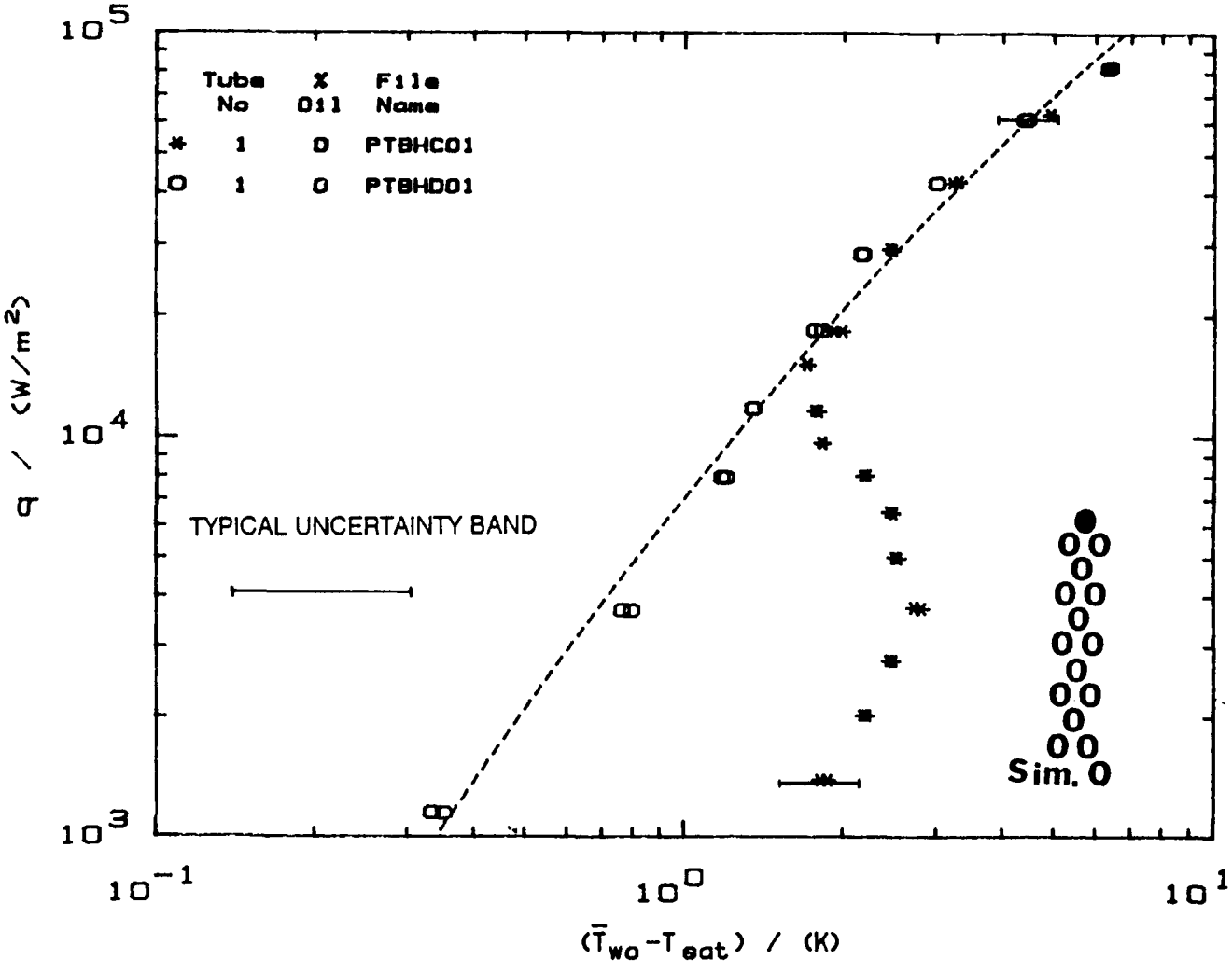

Figure 5.12. Boiling Data for Turbo-B Tube 1 as a Single Tube for Increasing and Decreasing Heat Flux.

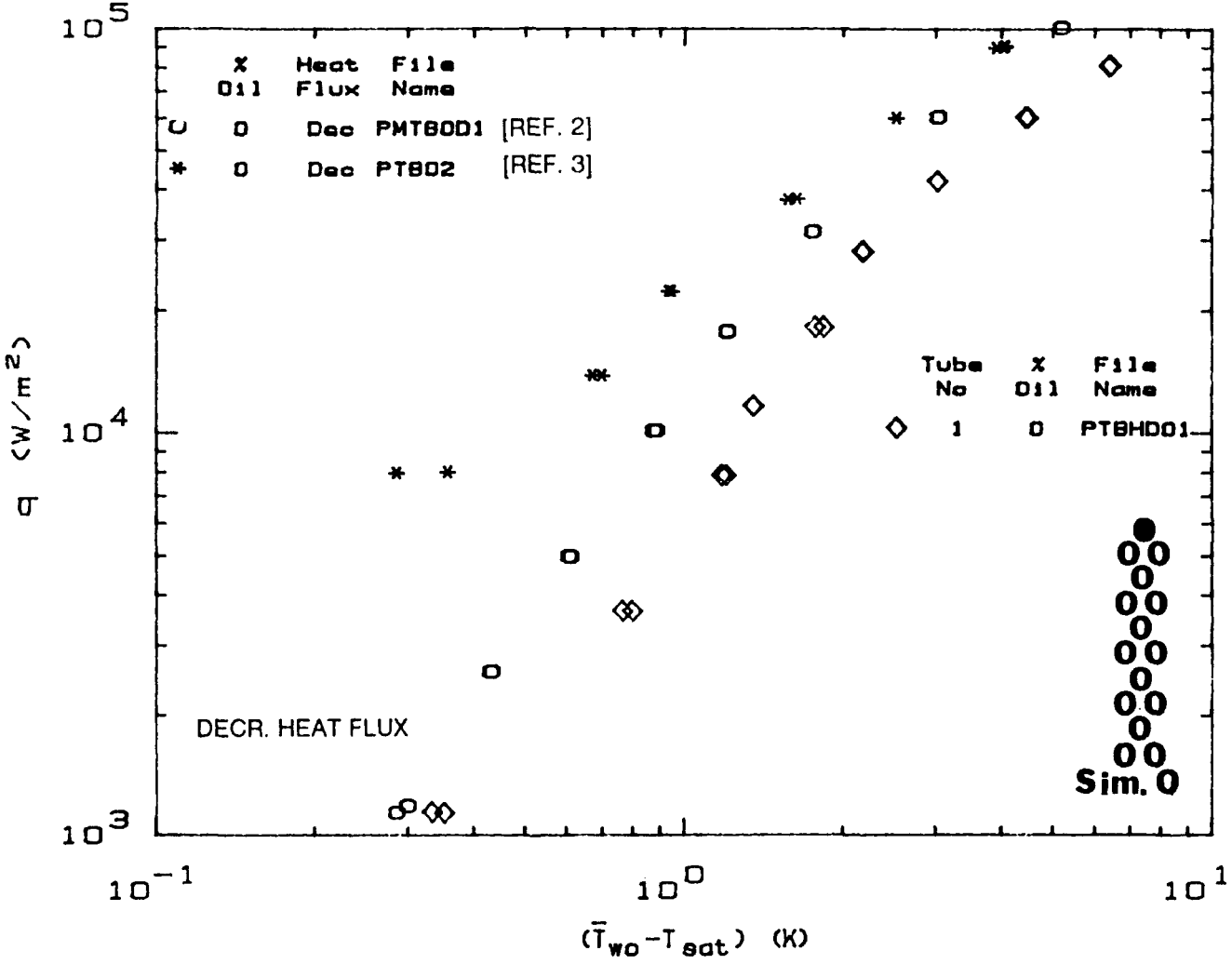

Figure 5.13. Performance Comparison of a Single Turbo-B Tube Within a Bundle and Within a Single Tube Apparatus (Decreasing Heat Flux).

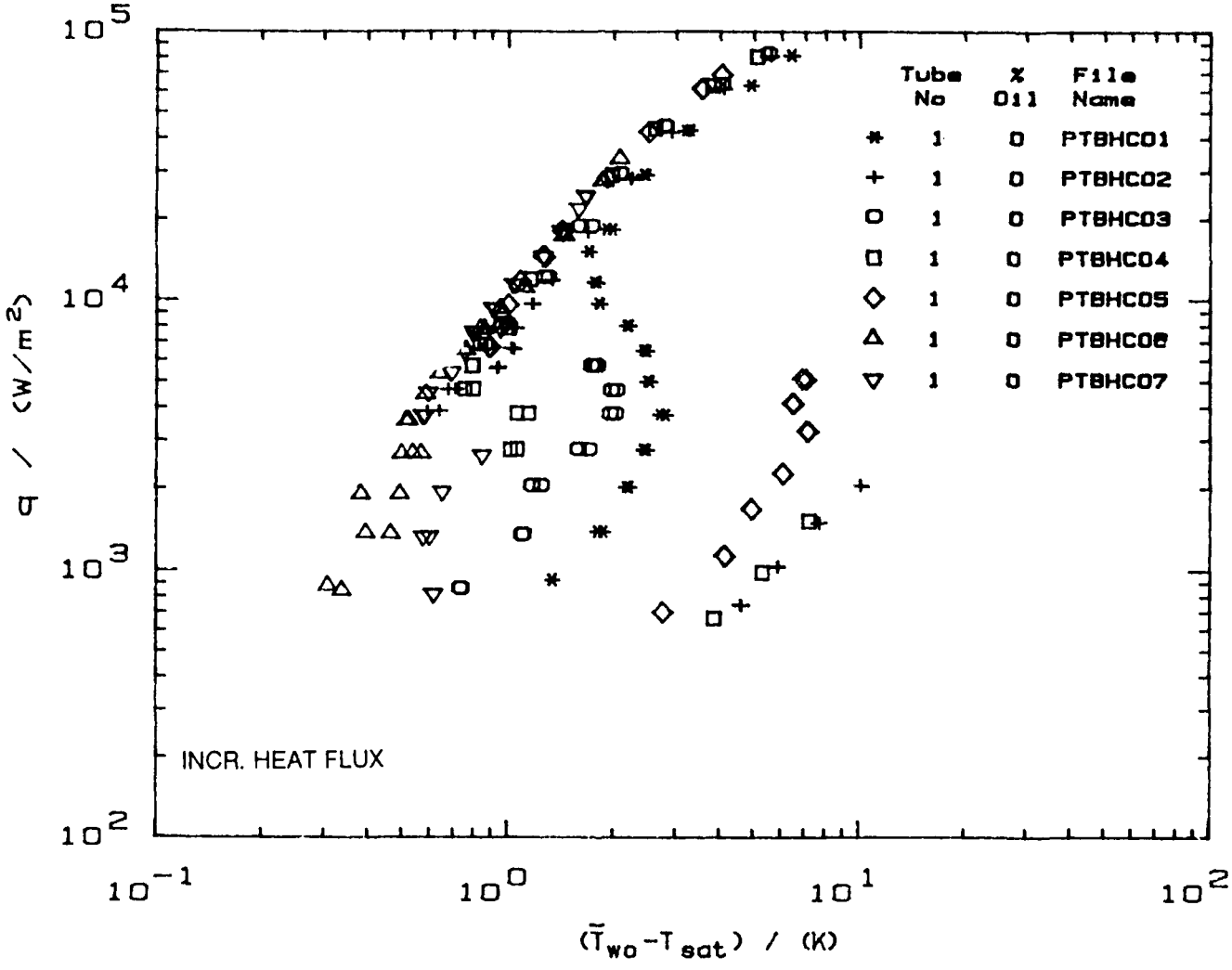

Figure 5.14. Boiling Data for Turbo-B Tube 1 when Influenced by Increasing Number of Heated Tubes.

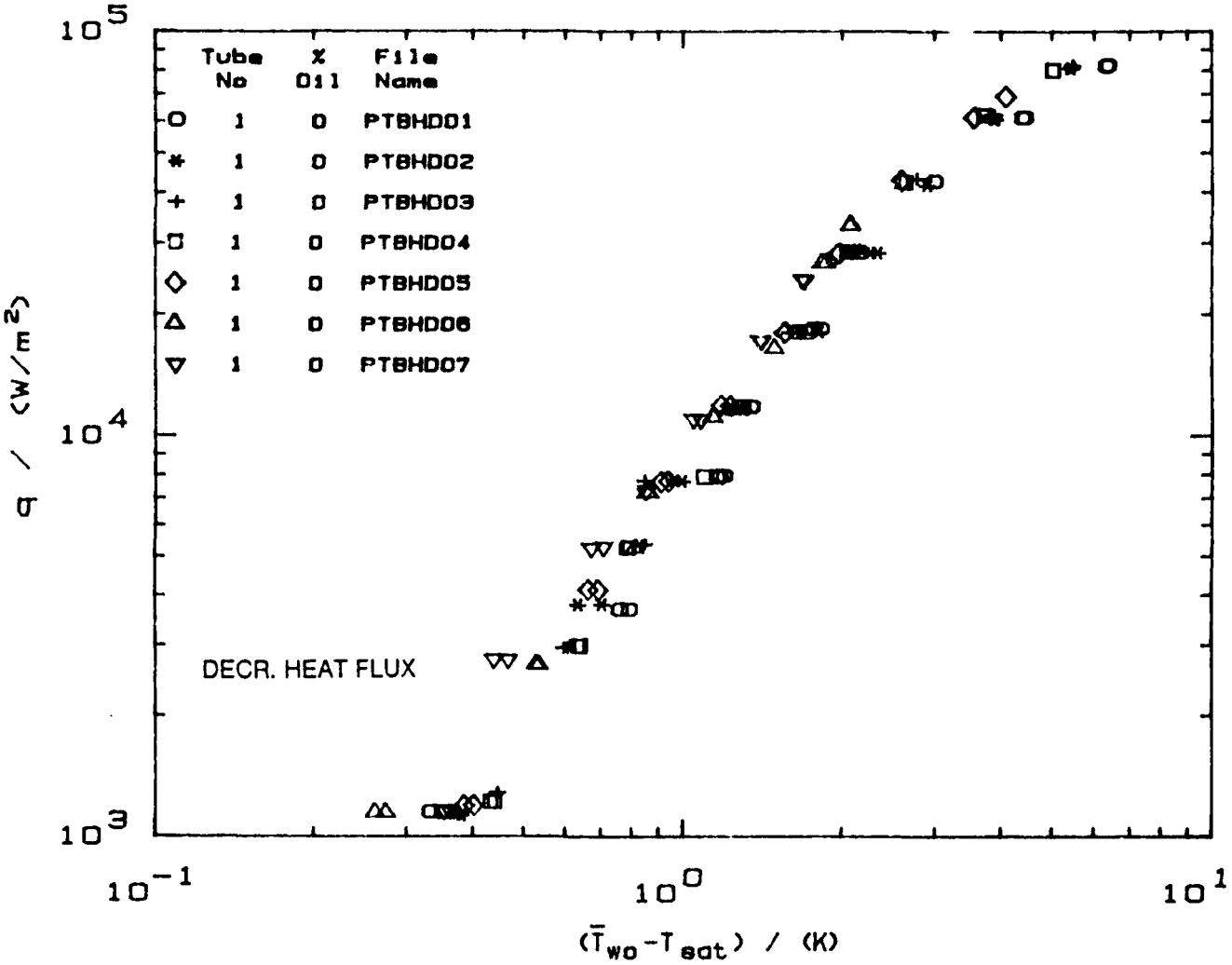

Figure 5.15. Boiling Data for Turbo-B Tube 1 when Influenced by Increasing Number of Heated Tubes (Decreasing Heat Flux).

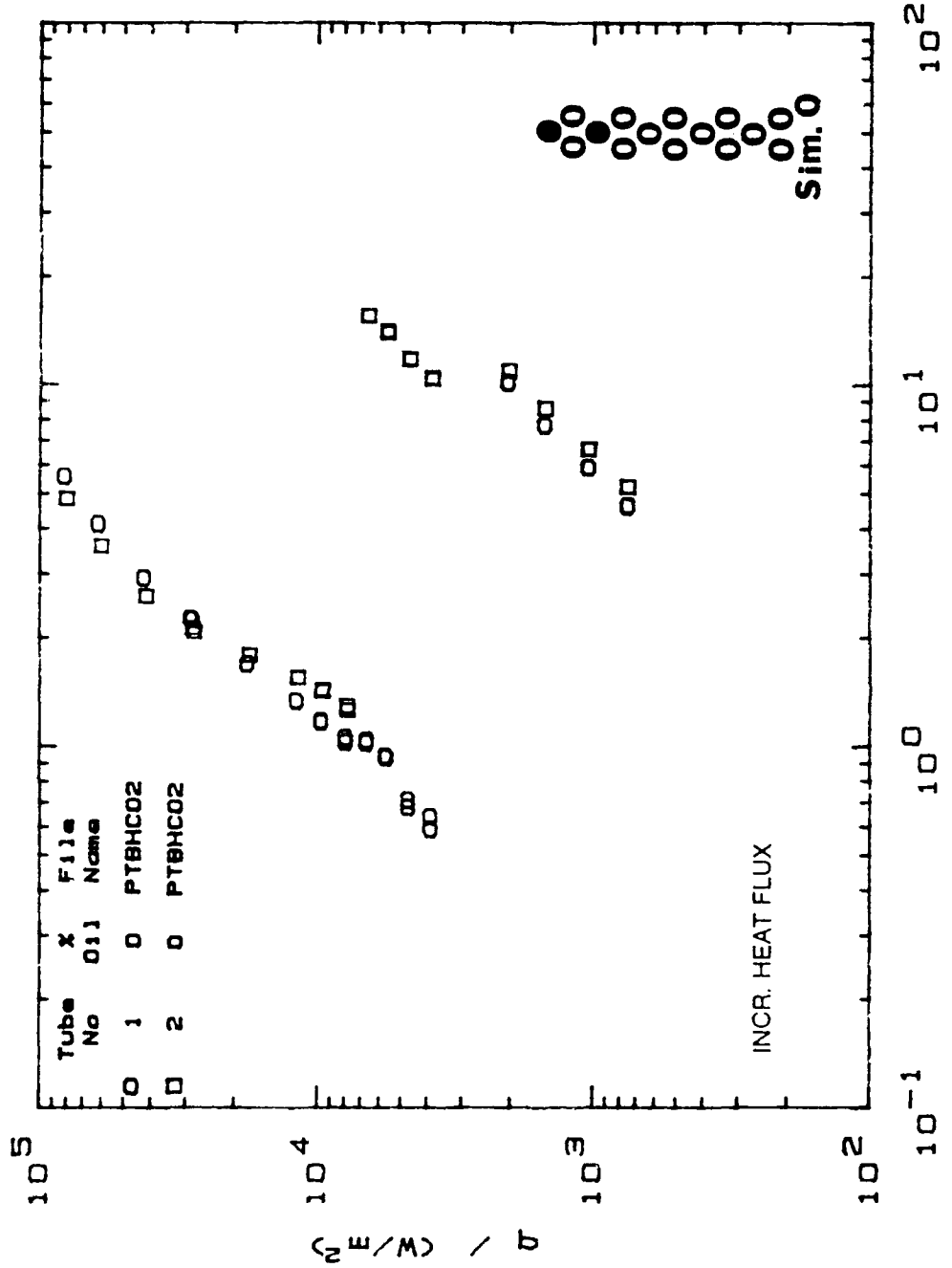

Figure 5.16. Boiling Data for Turbo-B Tubes 1 and 2 Operating Simultaneously.

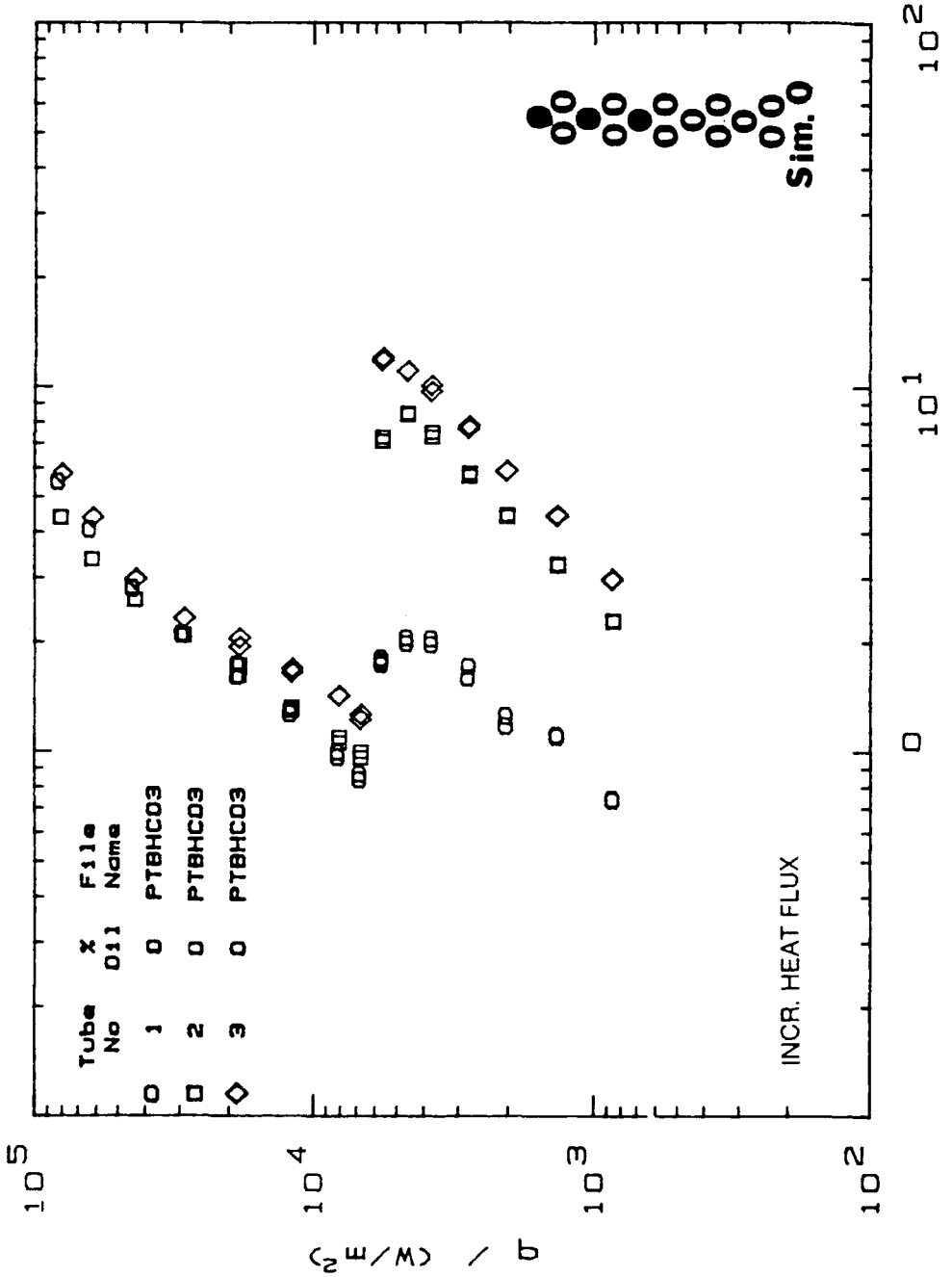

Figure 5.17. Boiling Data for Turbo-B Tubes 1, 2 and 3 Operating Simultaneously.

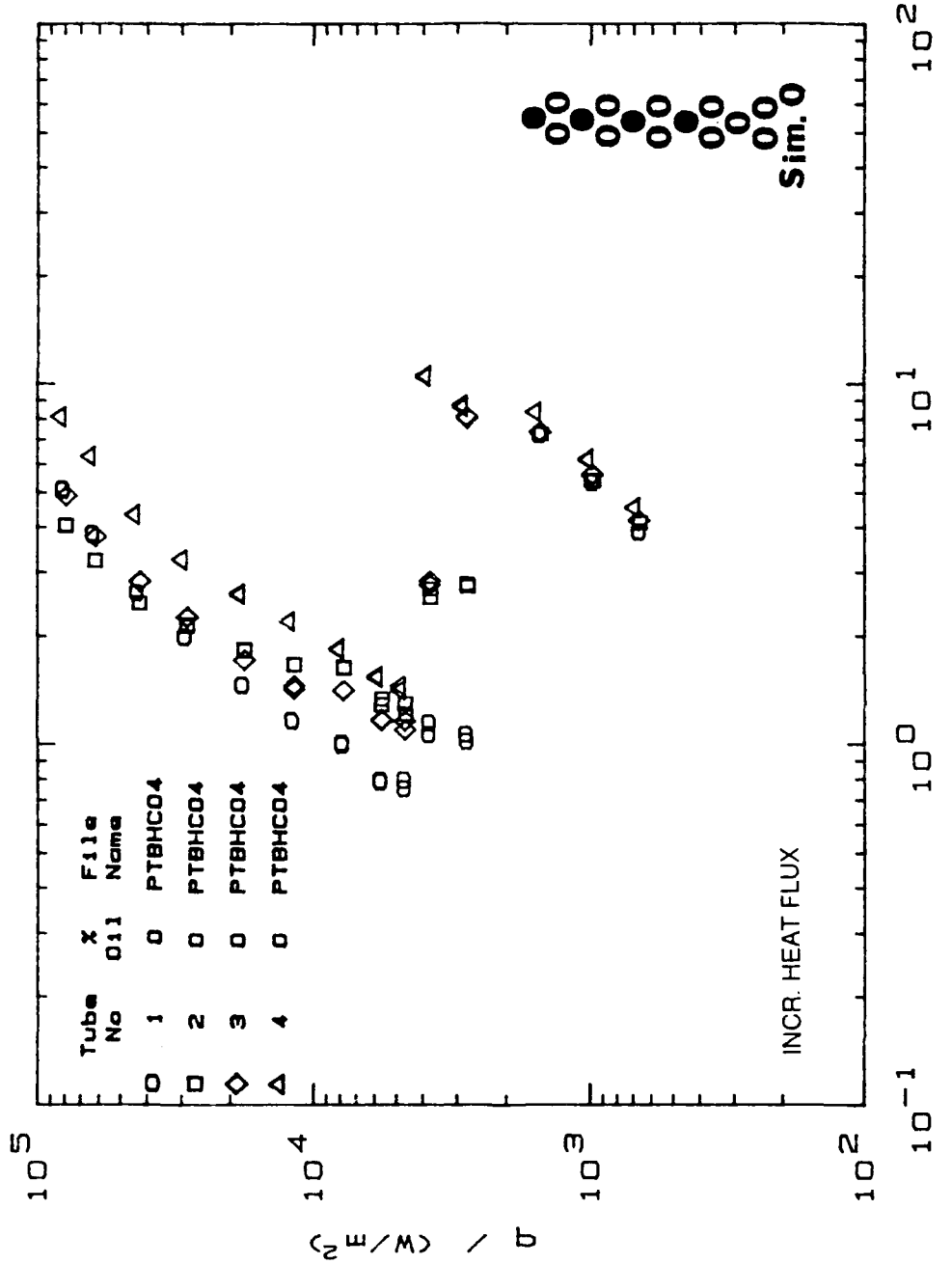

Figure 5.18. Boiling Data for Turbo-B Tubes 1, 2, 3 and 4 Operating Simultaneously.

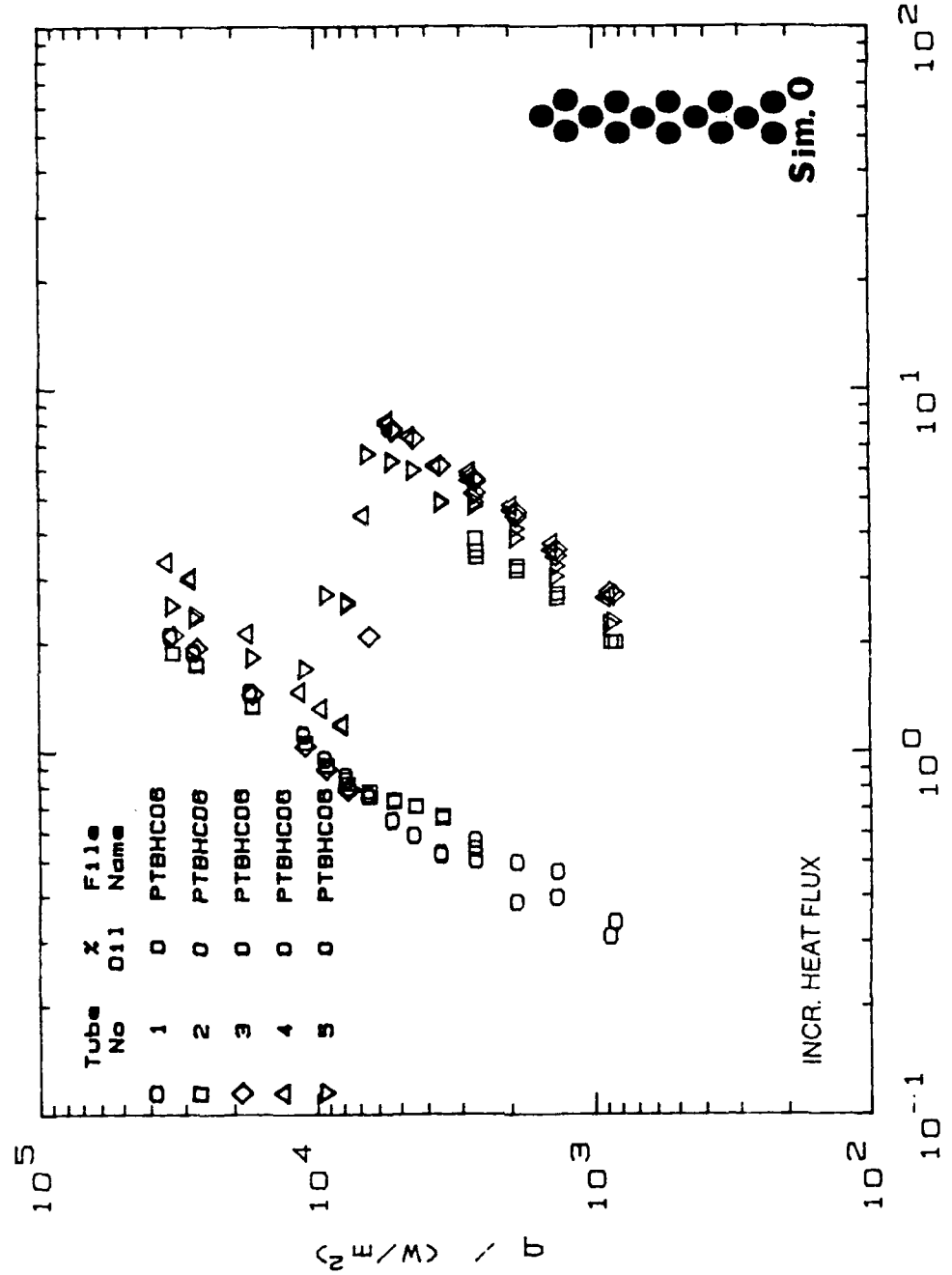

Figure 5.19. Boiling Data for Turbo-B Tube Bundle.

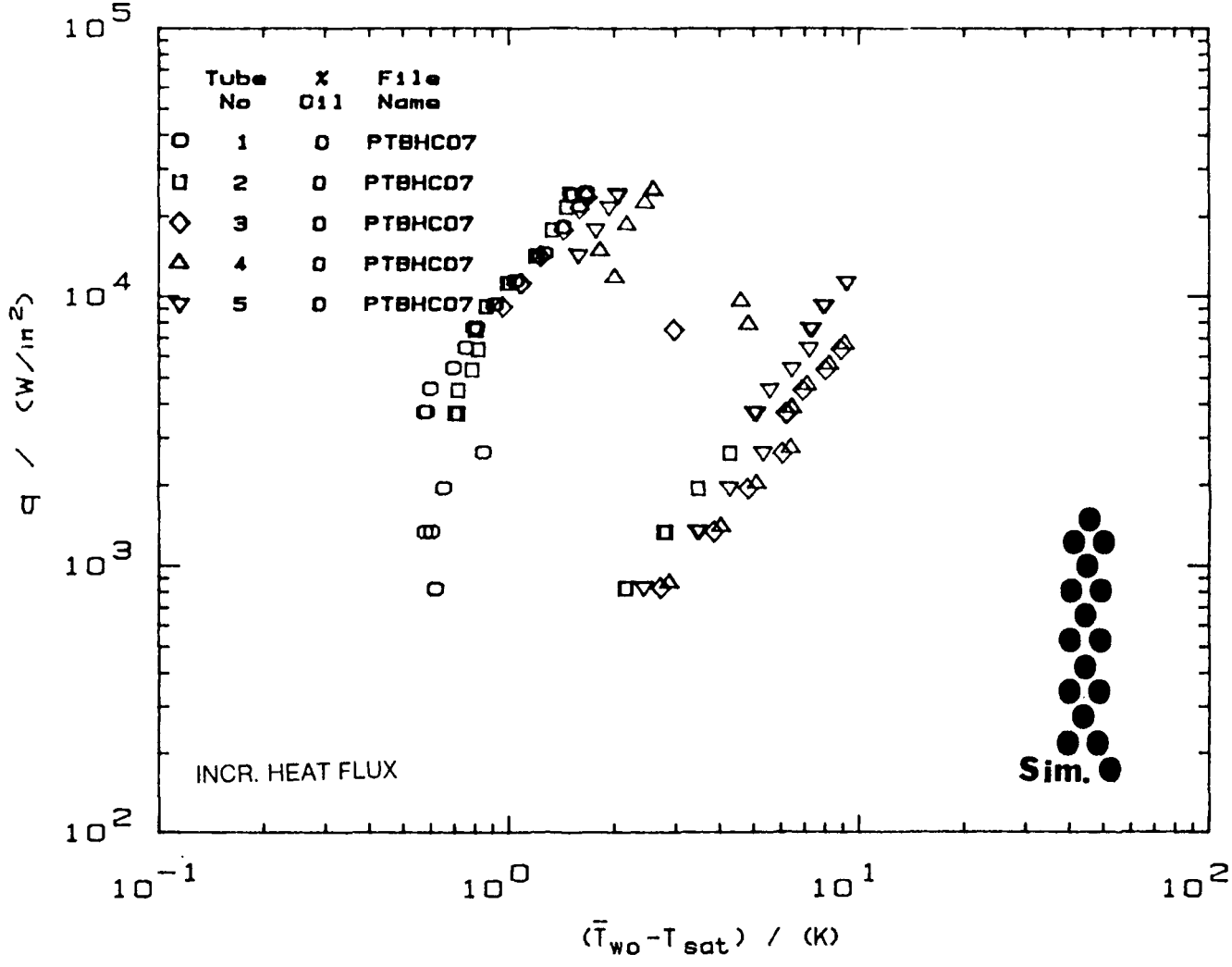

Figure 5.20. Boiling Data for Turbo-B Tube Bundle with Simulation Heaters in Operation.

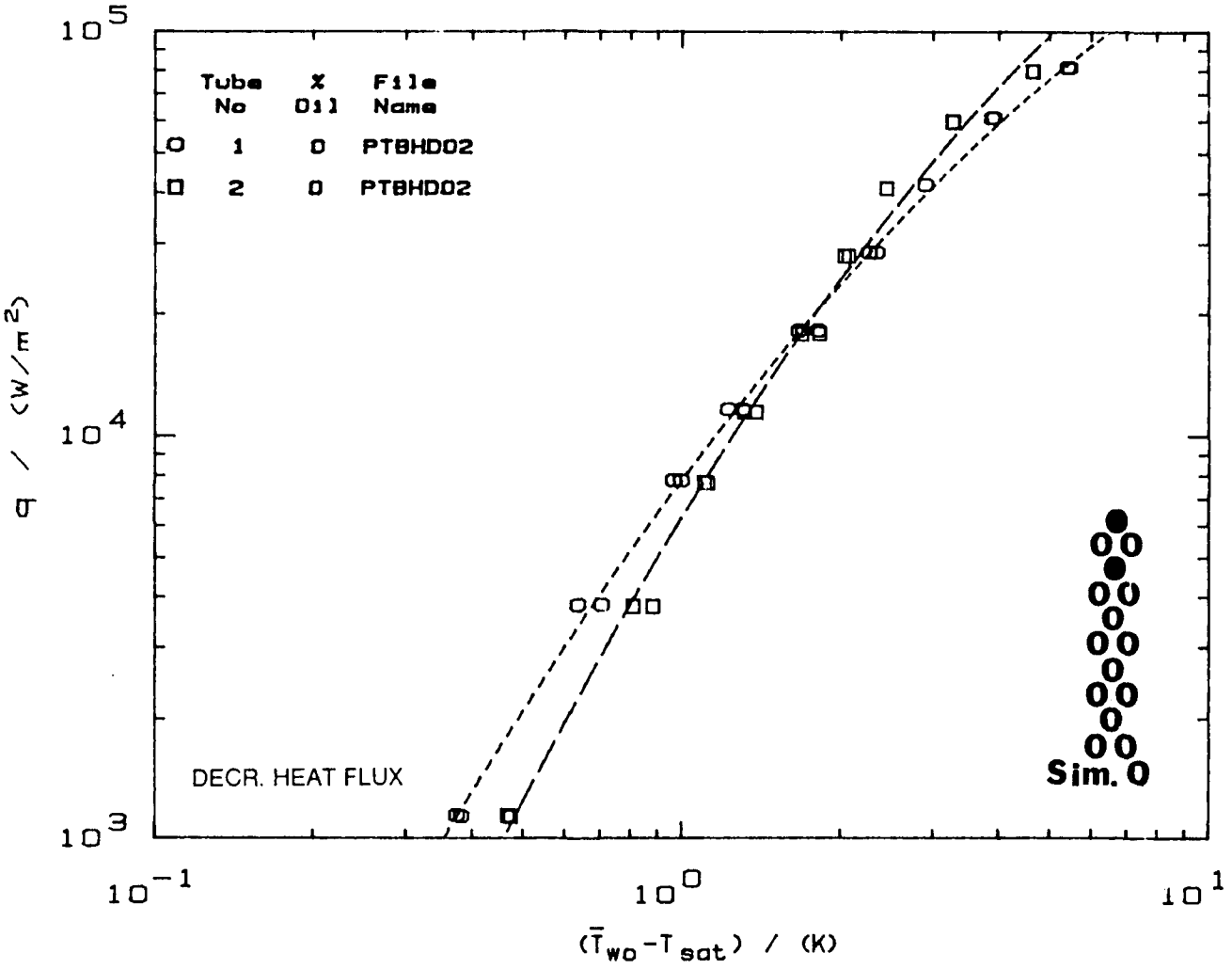

Figure 5.21. Boiling Data for Turbo-B Tubes 1 and 2 Operating Simultaneously (Decreasing Heat Flux).

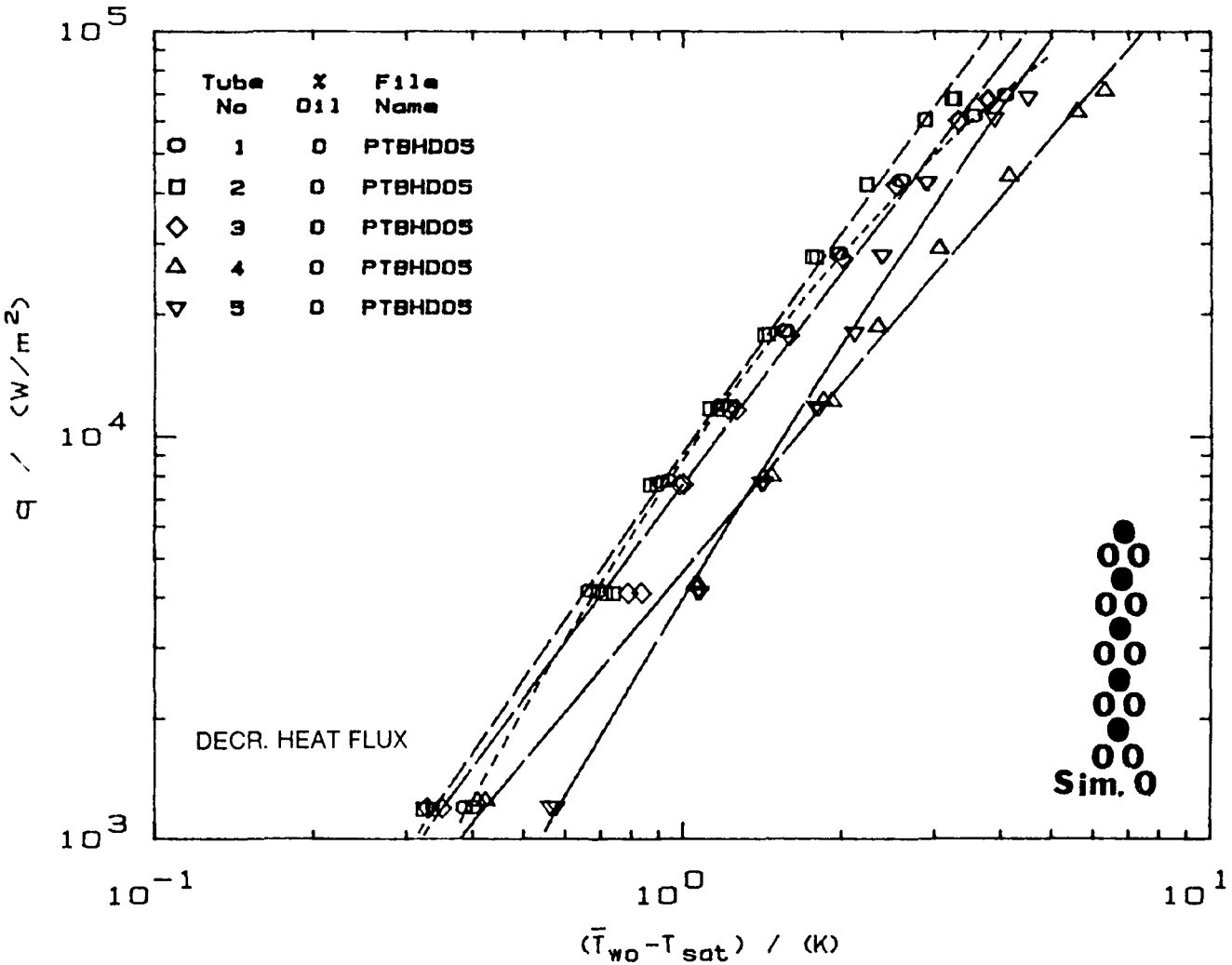

Figure 5.22. Boiling Data for Turbo-B Tubes 1, 2, 3, 4 and 5 Operating Simultaneously (Decreasing Heat Flux).

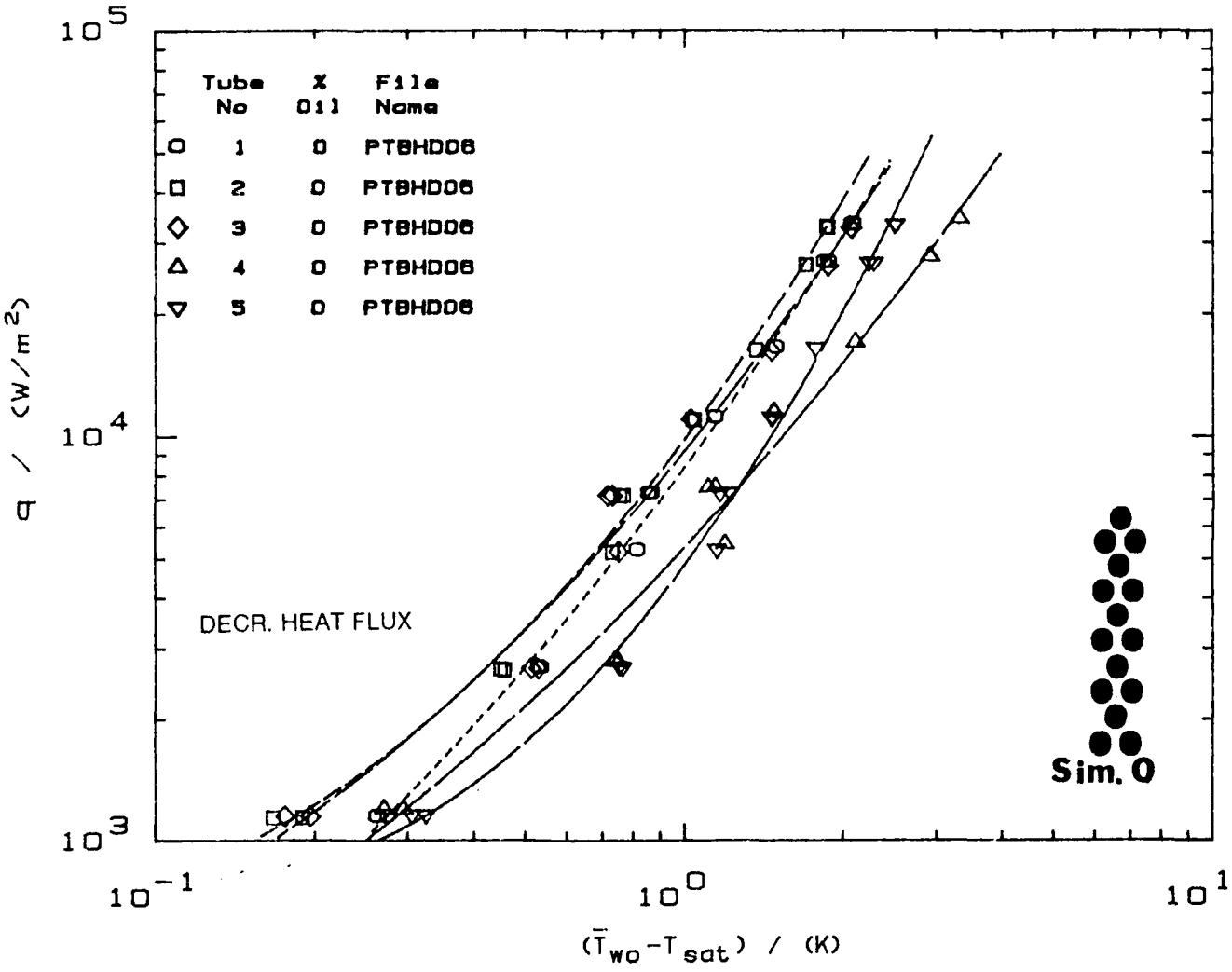

Figure 5.23. Boiling Data for Turbo-B Tube Bundle (Decreasing Heat Flux).

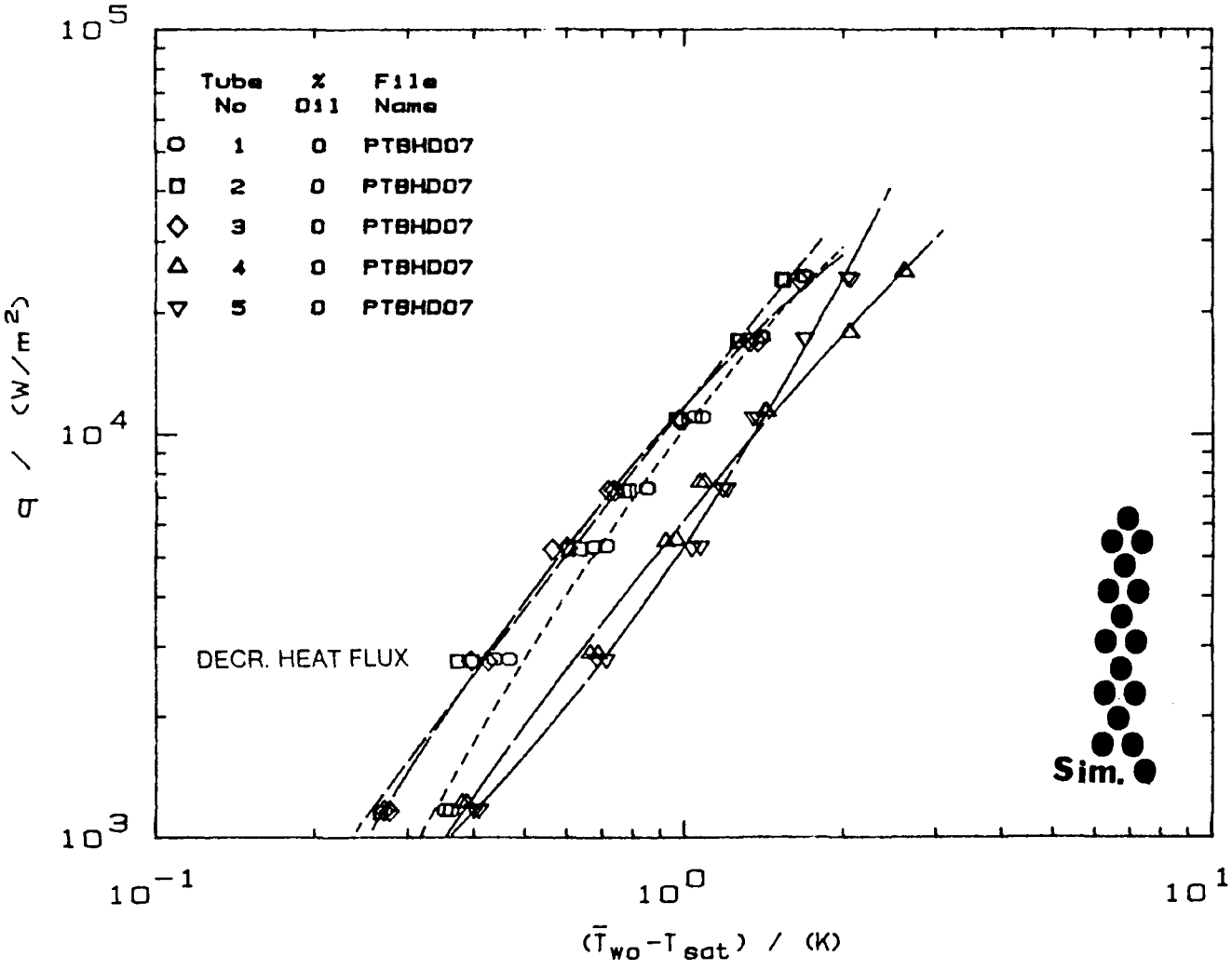

Figure 5.24. Boiling Data for Turbo-B Tube Bundle with Simulation Heaters in Operation (Decreasing Heat Flux).

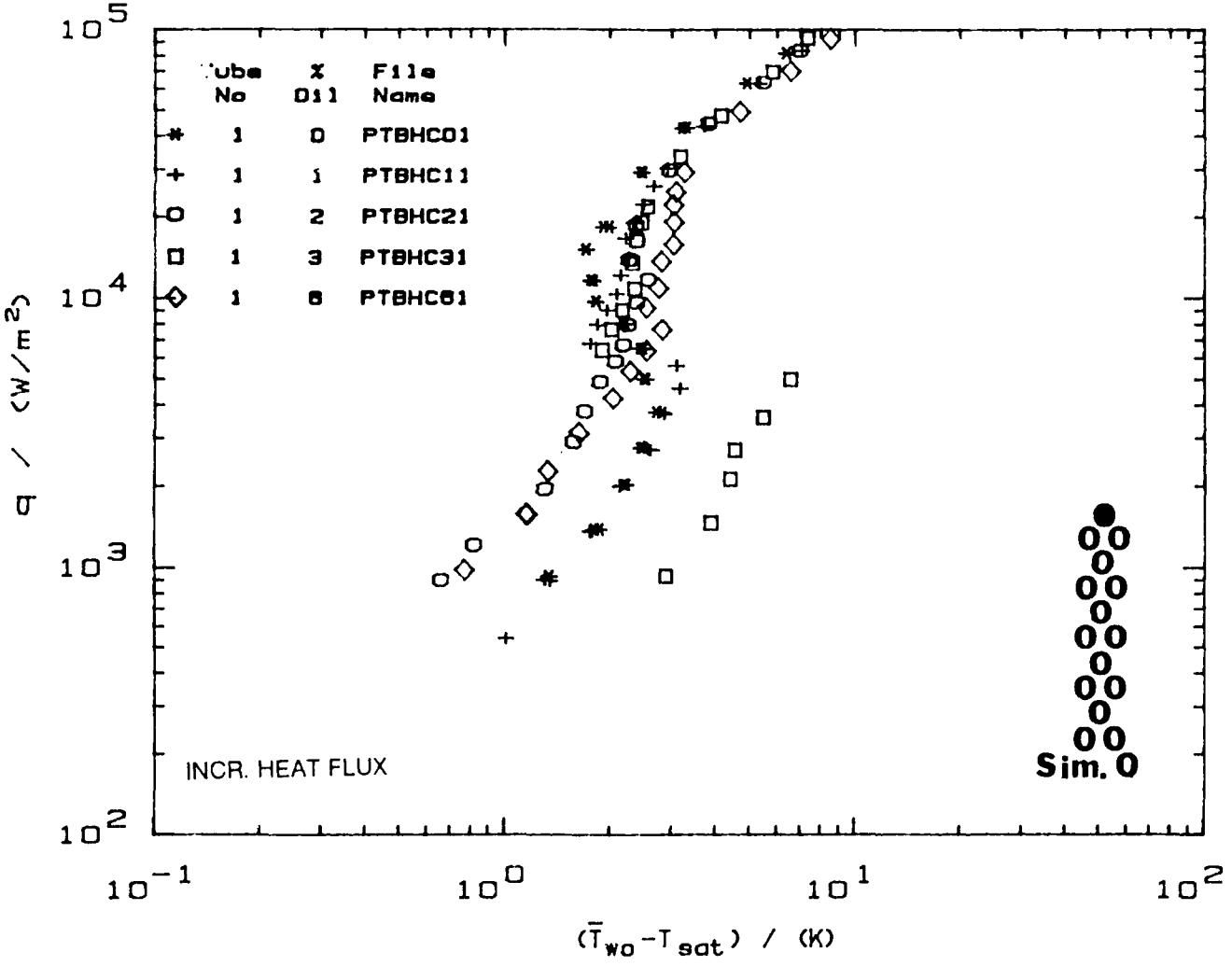

Figure 5.25. Boiling Data for Turbo-B Tube 1 with Different Oil Concentrations.

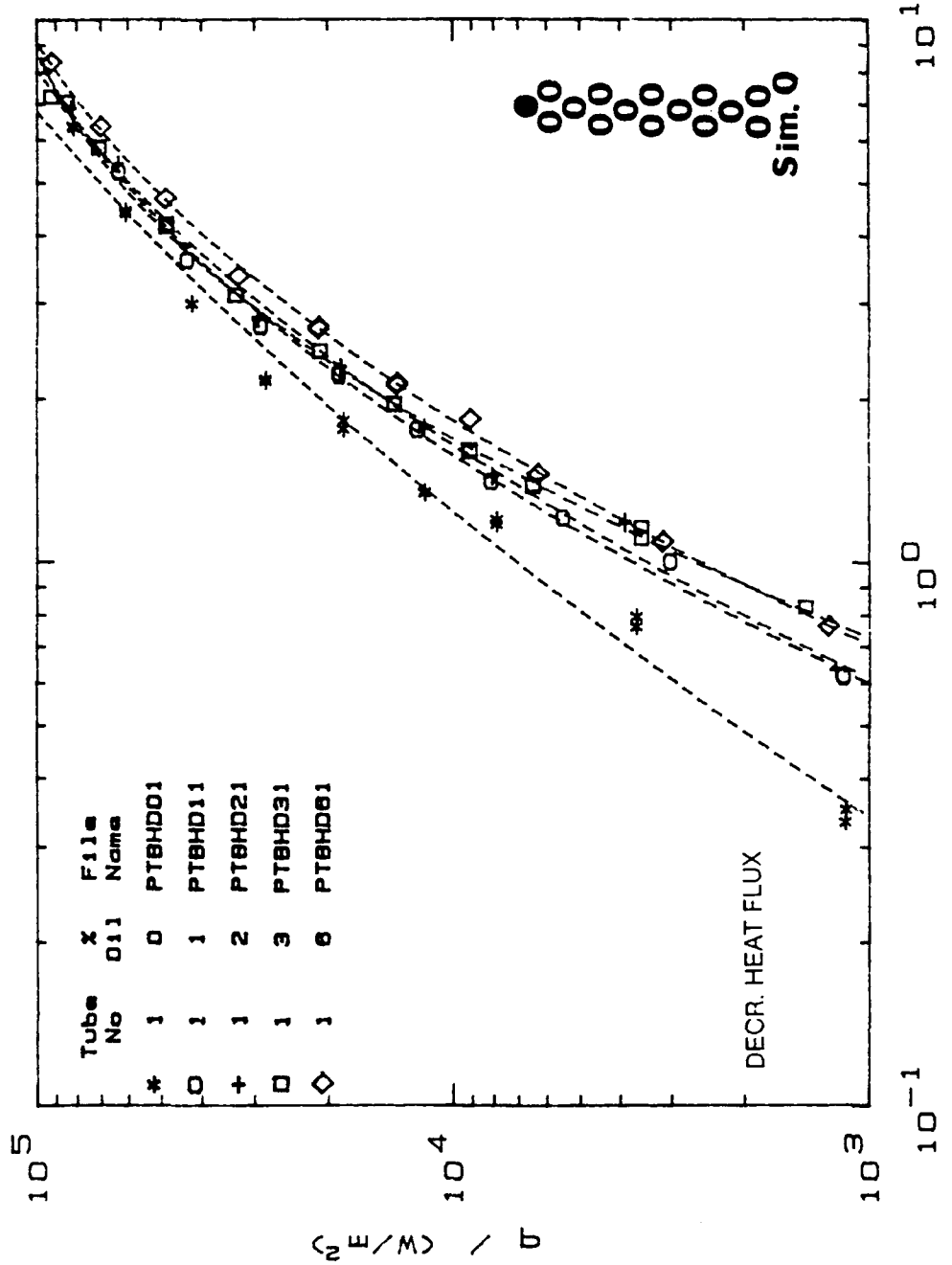

Figure 5.26. Boiling Data for Turbo-B Tube 1 with Different Oil Concentrations (Decreasing Heat Flux).

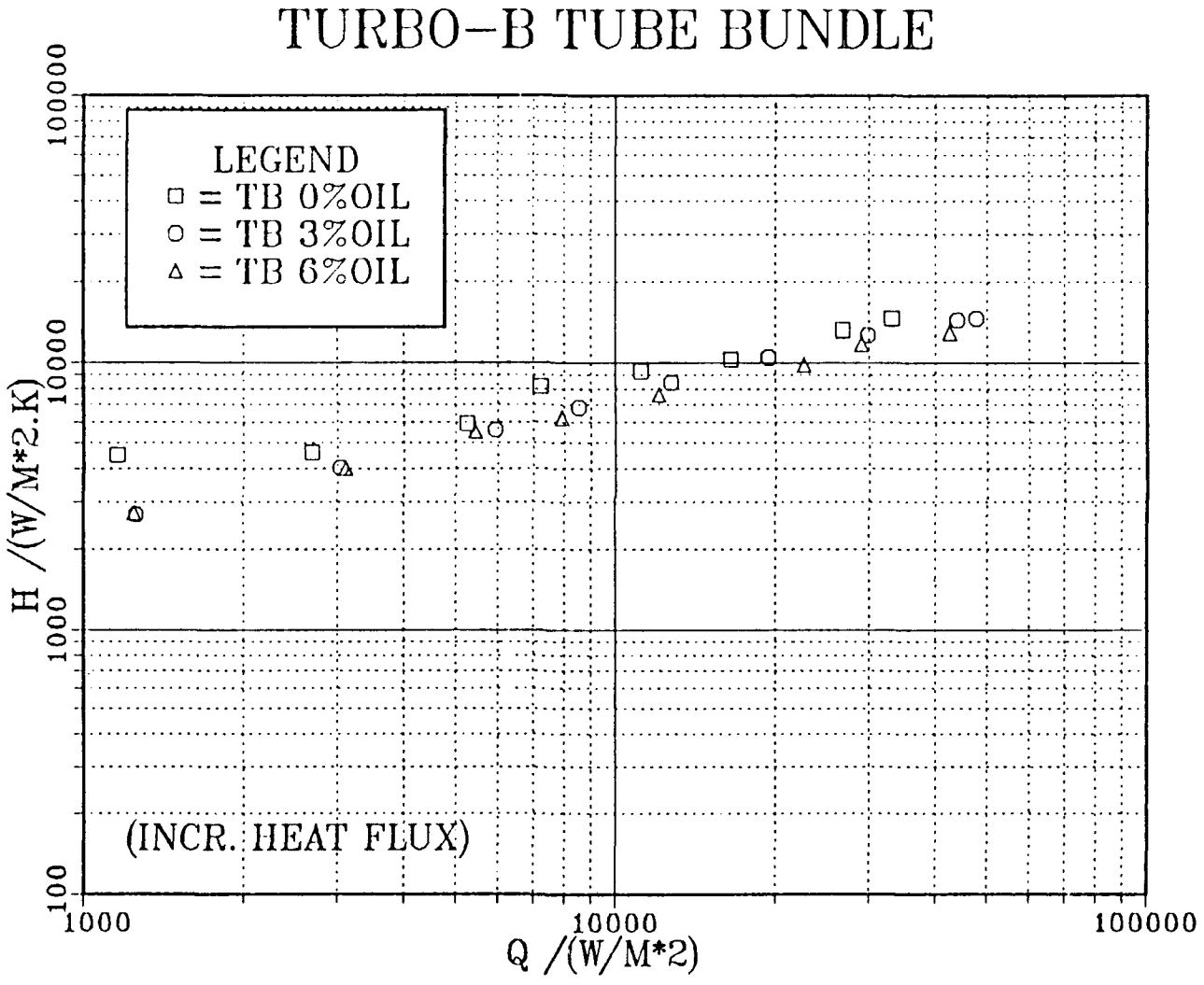

Figure 5.27. Boiling Data for Turbo-B Tube Bundle with Different Oil Concentrations.

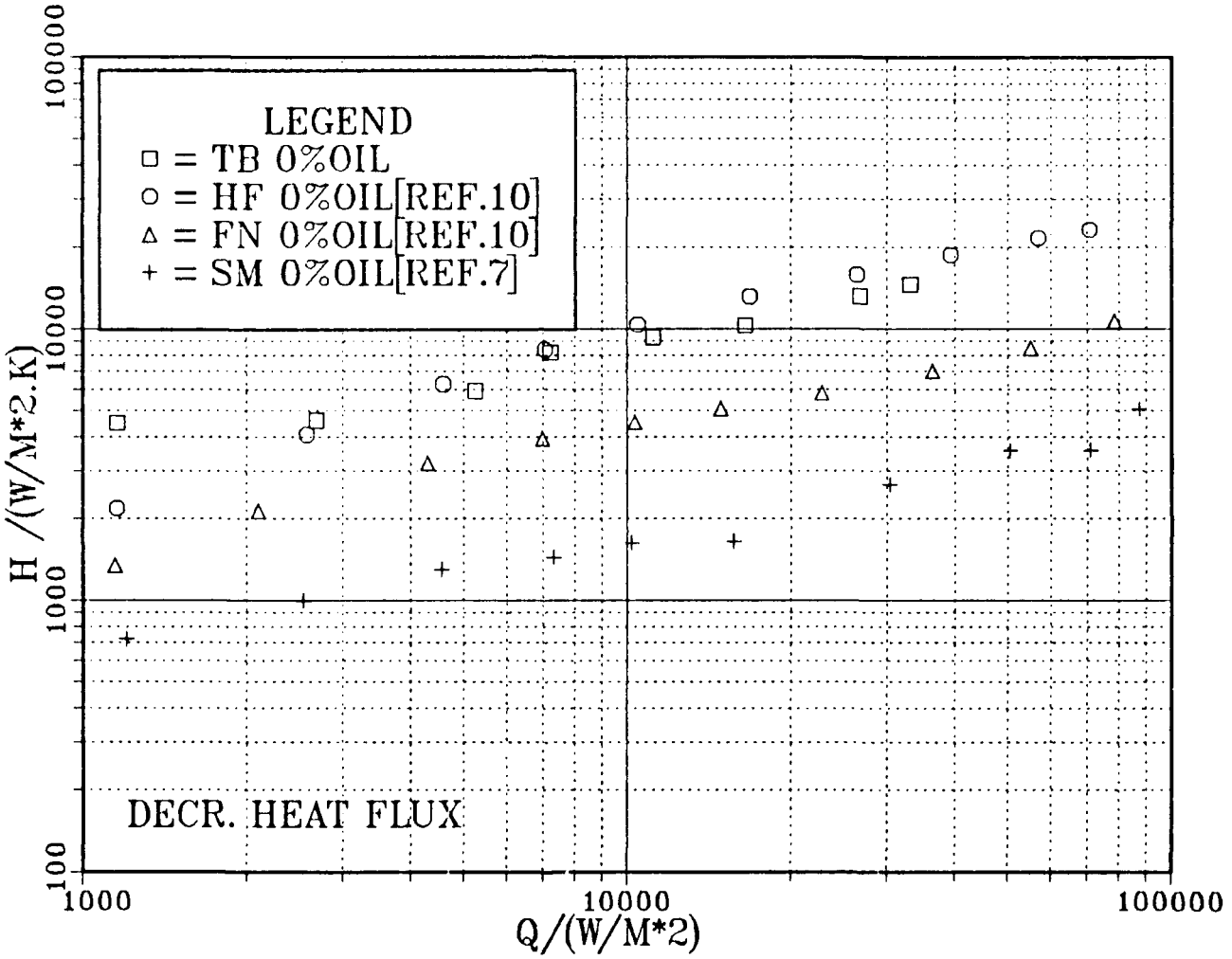

Figure 5.28. Boiling Data for High Flux, Turbo-B, Finned and Smooth Tube Bundle in Pure R-114 (Decreasing Heat Flux).

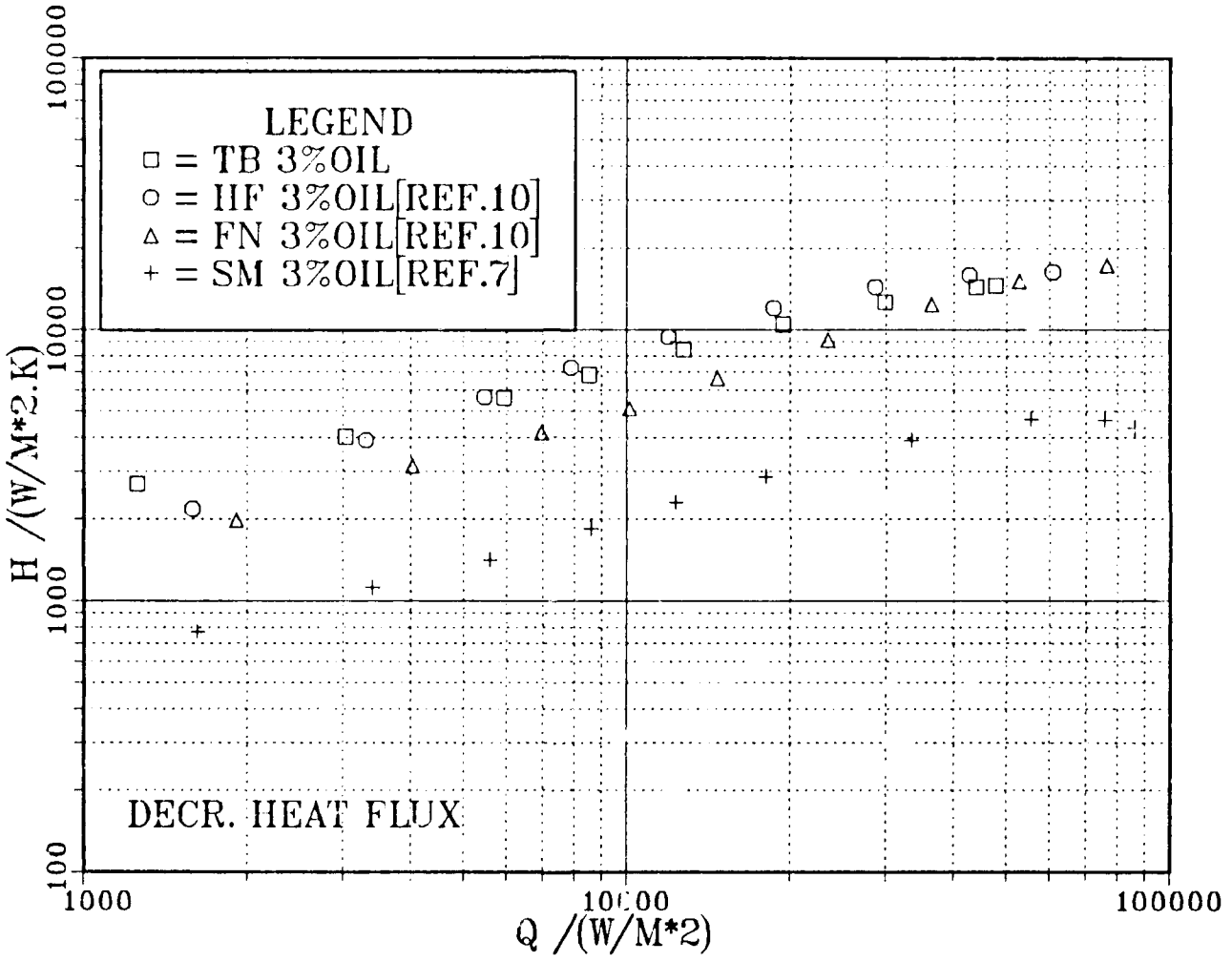

Figure 5.29. Boiling Data for High Flux, Turbo-B, Finned and Smooth Tube Bundle with 3% Oil (Decreasing Heat Flux)

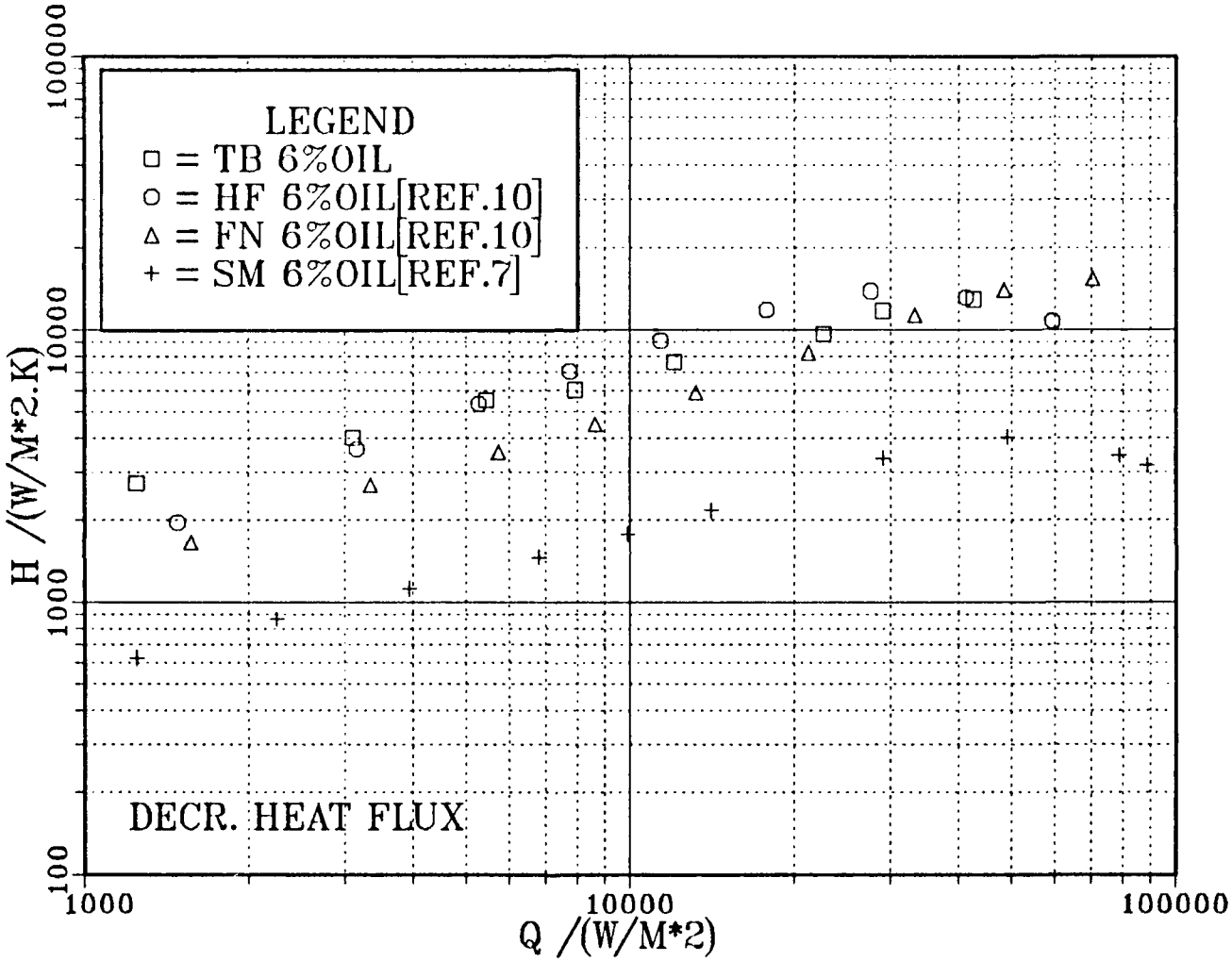

Figure 5.30. Boiling Data for High Flux, Turbo-B, Finned and Smooth Tube Bundle with 6% Oil (Decreasing Heat Flux).

VI. CONCLUSIONS AND RECOMMENDATIONS

A. CONCLUSIONS

Nucleate pool boiling data of pure R-114 and R-114/oil mixtures were obtained using a small bundle of High Flux and Turbo-B tubes. The data were taken using surface preparation-C (to simulate start-up of an air-conditioning system) for increasing heat flux and surface preparation-D (to simulate a continuously operating air conditioning system) for decreasing heat flux. The analysis of the data taken during this thesis study led to the following conclusions.

1. The presence of lower heated tubes in a High Flux tube bundle does not noticeably affect the performance of upper tubes for both increasing and decreasing heat flux.

2. Onset of nucleate boiling for the upper tubes in a bundle enhances the heat transfer coefficient of lower non-nucleating tubes within a High Flux tube bundle.

3. In natural convection regime, since the convective contribution is highest toward the top of the tube bundle due to increased velocities and flow acceleration, the nearest tube to the top of the bundle, namely tube 1, always has the best heat transfer performance.

4. After the onset of nucleate pool boiling, tube 2 exhibits the best performance presumably owing to the height of the R-114 liquid level inside the evaporator section.

5. Similar to smooth tube bundle experiment results [Ref. 20], in a High Flux tube bundle experiencing nucleate boiling, the chaotic two phase bubble motion may create favorable conditions for secondary nucleation.

6. Use of the simulation heaters at the bottom of the High Flux tube bundle to provide an inlet vapor quality does not eliminate "boiling hysteresis" in contrast to the smooth tube bundle (see [Ref. 20]). "Hysteresis" patterns exist between increasing and decreasing heat flux for the High Flux tube bundle.

7. The presence of additional activated tubes slightly enhances the heat-transfer capability of the Turbo-B bundle in nucleate boiling regime for both increasing and decreasing heat flux. However, behavior of the Turbo-B tube bundle does not have a regular pattern in the natural convection regime. Natural convection in a tube bundle is a complex phenomenon and deserves further investigation.

8. Activation of the simulation heaters does not eliminate "boiling hysterisis" for the Turbo-B tubes (similar to High Flux tubes behavior). The additional vapor quality helps to reduce the temperature overshoot of tube 1 only.

9. The effectiveness of the Turbo-B tube bundle degraded with increased amounts of oil. At a practical heat flux of $q''=30$ kW/m^2 a 9% and 15% degradation from pure R-114 was observed for 3% and 6% oil concentrations respectively.

B. RECOMMENDATIONS

1. The High Flux tube bundle experiments should be repeated with a new set of High Flux tubes, preferably soldering the instrumented tubes in a vacuum oven to provide a better tube wall temperature distribution.

2. The effect of pool height in the evaporator should be investigated.

3. A more detailed study of circulation characteristics within the bundle should be made to explain the anomalies seen, especially in the natural convection region.

4. The reasons for the poor performance of the condenser tubes in the condenser section should be thoroughly investigated and rectified.

5. The main and auxiliary condenser pumps should be overhauled to eliminate noise.

6. Taking into consideration the side effects of R-114 (and other refrigerants), the ventilation system of the laboratory should be improved.

APPENDIX A. LISTING OF DATA FILES

TABLE A.1. DATA FILE NAMES OF THE TURBO-B AND HIGH FLUX TUBE RUNS.

File Name	File Name	Number of Data Points	Number of Heated Tubes	Percent Oil	Number of Active Pairs	Number of Simulated Tubes
TBHC01	TBHD01	32/18	1	0	0	0
TBHC02	TBHD02	27/17	2	0	0	0
TBHC03	TBHD03	31/20	3	0	0	0
TBHC04	TBHD04	28/20	4	0	0	0
TBHC05	TBHD05	34/18	5	0	0	0
TBHC06	TBHD06	29/14	5	0	5	0
TBHC07	TBHD07	23/14	5	0	5	5
TBHC11	TBHD11	27/15	1	1	0	0
TBHC12	TBHD12	22/12	2	1	0	0
TBHC13	TBHD13	19/18	3	1	0	0
TBHC14	TBHD14	17/18	4	1	0	0
TBHC15	TBHD15	24/18	5	1	0	0
TBHC16	TBHD16	18/16	5	1	5	0
TBHC17	TBHD17	15/14	5	1	5	5
TBHC21	TBHD21	19/18	1	2	0	0
TBHC22	TBHD22	20/20	2	2	0	0
TBHC23	TBHD23	19/20	3	2	0	0
TBHC24	TBHD24	21/20	4	2	0	0
TBHC25	TBHD25	20/20	5	2	0	0
TBHC26	TBHD26	17/16	5	2	5	0
TBHC27	TBHD27	13/16	5	2	5	5
TBHC31	TBHD31	20/19	1	3	0	0
TBHC32	TBHD32	19/18	2	3	0	0
TBHC33	TBHD33	15/18	3	3	0	0
TBHC34	TBHD34	17/18	4	3	0	0
TBHC35	TBHD35	18/19	5	3	0	0
TBHC36	TBHD36	19/17	5	3	5	0
TBHC37	TBHD37	15/14	5	3	5	5

File Name	File Name	Number of Data Points	Number of Heated Tubes	Percent Oil	Number of Active Pairs	Number of Simulated Tubes
TBHC61	TBHD61	20/20	1	6	0	0
TBHC62	TBHD62	17/18	2	6	0	0
TBHC63	TBHD63	14/16	3	6	0	0
TBHC64	TBHD64	18/20	4	6	0	0
TBHC65	TBHD65	17/18	5	6	0	0
TBHC66	TBHD66	15/18	5	6	5	0
TBHC67	TBHD67	14/15	5	6	5	5
(1) HFHD01	-	10	1	0	0	0
(1) HFHD02	-	10	2	0	0	0
(1) HFHD05	-	20	5	0	0	0
(1) HFHD07	-	17	5	0	5	5
HFHD32	-	20	2	3	0	0
HFHD35	-	20	5	3	0	0
HFHB01	-	10	1	0	0	0
HFHB02	-	26	2	0	0	0
HFHCD01	-	38	1	0	0	0
HFHC02	HFND02	30/22	2	0	0	0
HFHC03	HFHD03	26/8	3	0	0	0
HFHC04	HFHD04	31/15	4	0	0	0
HFHC05	HFHD05	31/19	5	0	0	0
HFHC06	HFHD06	28/14	5	0	5	0
HFHC07	HFHD07	17/12	5	0	5	5
(2) HFH1C05	HFH1CD05	20/18	5	0	0	0
(3) HFH2C01	HFH2D01	28/18	1	0	0	0
(3) HFH2C02	HFH2D02	15/16	2	0	0	0
(3) HFH2C05	HFH2D05	15/18	5	0	0	0
(3) HFH2C07	HFH2D07	18/18	5	0	5	5

(1) contamination effected
(2) new arrangement of tubes in the bundle
(3) after resoldered

APPENDIX B. SAMPLE CALCULATIONS

Data set number 15 of run "TBHC23" (Turbo-B tube, surface preparation-C, 2% oil, three tubes activated), for tube number 1 was used for the sample calculation and program validation.

1. Test tube dimensions

D_o = 14.15 mm

D_i = 12.70 mm

D_{tc} = 11.58 mm

L = 203.2 mm

L_u = 25.4 mm

2. Measured parameters

T1 = 6.44 C

T2 = 5.83 C

T3 = 5.95 C

T4 = 6.13 C

T5 = 5.86 C

T6 = 5.31 C

Tld1 = 2.21 C

Tld2 = 2.25 C

Aas = 2.79 V

Vas = 2.685 V

3. Calculations

The heater power is calculated as

$$q = Vas \times Aas \times 60 \times 1 \tag{B.1}$$

The multiplication factors of the volt and amp sensors are 60 and 1 respectively, then

$$q = 2.79 \times 2.685 \times 60 \times 1$$
$$q = 449.469\ W$$

The tube inside wall temperature is obtained from the average value of six thermocouple readings.

$$\bar{T}_{wi} = \frac{1}{6} \times \sum_{n=1}^{6} Tn \tag{B.2}$$

$$\bar{T}_{wi} = \frac{1}{6} \times (6.44 + 5.83 + 5.95 + 6.13 + 5.86 + 5.31)$$
$$\bar{T}_{wi} = 5.92\ C = 279.08\ K$$

The tube outside temperature is calculated using Fourier's conduction term and the tube inside wall temperature. Uniform radial conduction is assumed in the tube wall.

$$\bar{T}_{wo} = \bar{T}_{wi} - \frac{q \times \ln\left(\frac{D_o}{D_{tc}}\right)}{2 \times \pi \times k_{cu} \times L} \qquad \text{(B.3)}$$

where k_{cu} is thermal conductivity and is calculated at $\bar{T}_{wi}$ as follows

$$k_{cu} = 434.0 - (0.112 \times \bar{T}_{wi-K}) \qquad \text{(B.4)}$$

$$k_{cu} = 434.0 - (0.112 \times 279.08)$$

$$k_{cu} = 402.74 \frac{W}{m\,K}$$

now

$$\bar{T}_{wo} = 5.92 - \frac{449.469 \times \ln\left(\frac{14.15}{12.7}\right)}{2 \times \pi \times 402.74 \times 0.2032}$$

$$\bar{T}_{wo} = 5.83C$$

The liquid saturation temperature at the top of the tube bank is

$$T_{sat} = \frac{Tld1 + Tld2}{2} \qquad \textbf{(B.5)}$$

$$T_{sat} = \frac{2.21 + 2.25}{2}$$

$$T_{sat} = 2.23\ C$$

In order to calculate the local saturation temperature for each tube, small corrrections are needed due to the hydrostatic pressure difference between the tube location and liquid free surface. This difference is calculated for tube one by

$$\Delta P = \rho \times g \times h_t \tag{B.6}$$

$$\Delta P = 1523.12 \times 9.81 \times 0.127$$
$$\Delta P = 1897.6\,Pa$$

For 1897.6 Pa pressure difference, corrected saturation temperature is obtained by adding 0.413 C (from standard tables for R-114) to T_{sat}. Corrected T_{sat} is

$$T_{satc} = 2.23 + 0.413 \tag{B.7}$$

$$T_{satc} = 2.643\ C$$

$$\Delta T = \bar{T}_{wo} - T_{satc} \tag{B.8}$$

$$\Delta T = 5.83 - 2.643$$
$$\Delta T = 3.19\ C$$

The test tube is 12 inches long in total; only a section of 8 inches is uniformly heated leaving a 1-inch and 3-inch long unheated section at either end. The 1 and 3 inch unheated lengths behave as fins in the heat transfer process. The following procedure is applied to the unheated ends of the tubes. Calculations are shown for the one inch length only.

Heat transferred from the unheated end is calculated as heat from the base of a fin:

$$q_f = (h_b \times p \times k_{cu} \times A_s)^{0.5} \times \Delta T \times \tanh (n \times L_c) \qquad \textbf{(B.9)}$$

where

$$p = \pi \times D_o = \pi \ (14.15 \ mm) \qquad \textbf{(B.10)}$$

$$p = 44.45 \times 10^{-3} m$$

now

$$A_c = \frac{\pi}{4} \times (D_o^2 - D_i^2) \qquad \textbf{(B.11)}$$

$$A_c = \frac{\pi}{4} \times (0.01415^2 - 0.0127^2)$$

$$A_c = 30.6 \times 10^{-6} m^2$$

The corrected length of unenhanced surface at the end can be calculated as

$$L_c = L_u + \frac{t}{2} \qquad \textbf{(B.12)}$$

$$L_c = 0.0254 + \frac{(0.01415 - 0.0127)}{4}$$

$$L_c = 0.02576 \ m$$

$$n = \left(\frac{h_b \times p}{k_{cu} \times A_c} \right)^{0.5} \qquad \textbf{(B.13)}$$

h_b is the natural convection heat transfer coefficient of the finned-like ends and can be calculated using the Churchill-Chu [Ref. 21] correlation for natural convection from a smooth horizontal cylinder, as modified by Pulido [Ref. 22].

$$h_b = \frac{k}{D_o} \times \{.6 + .387 \times \frac{\left(\frac{g \times \beta \times D_o^3 \times \Delta T \times \tanh(n \times L_c)}{\nu \times \alpha \times L_c \times n} \right)^{\frac{1}{6}}}{\left[1 + \left(\frac{0.559}{Pr} \right)^{\frac{9}{16}} \right]^{\frac{8}{27}}} \}^2 \qquad \textbf{(B.14)}$$

An iteration technique is then necessary to calculate h_b. The physical properties are calculated at the vapor mean film temperature given by

$$Tfilm = \frac{T_{sat} + \bar{T}_{wo}}{2} \qquad \textbf{(B.15)}$$

$$Tfilm = \frac{2.64 + 5.83}{2}$$

$$Tfilm = 4.23\ C = 277.23\ K$$

For R-114, the physical properties are given by [Ref. 23]

$$\mu = \exp\left[-4.4636 + \left(\frac{1011.47}{Tfilm_K} \right) \right] \times 10^{-3} \qquad \textbf{(B.16)}$$

$$\mu = 443.9 \times 10^{-6} \frac{kg}{m\ s}$$

$$c_p = [\, 0.40188 + Tfilm_K \times (1.65007 \times 10^{-3} + 1.51494 \times 10^{-6} \times Tfilm_K - 6.67853 \times 10^{-10} \times Tfilm_K^2) \,] \times 10^3 \qquad \textbf{(B.17)}$$

$$c_p = 961.44 \frac{J}{kg\ K}$$

$$\rho = 16.0184533 \times (36.32 + 61.146414 \times \psi^{1/3} + 16.418015 \times \psi + 17.476838 \times \psi^{1/2} + 1.119828 \times \psi^{2})$$

where

$$\psi = 1 - \left(\frac{1.8 \times Tfilm_k}{753.95} \right) \qquad \textbf{(B. 19)}$$

$$\psi = 0.338$$

and

$$\rho = 1517.8 \frac{kg}{m^3}$$

$$k = 0.071 - (0.000261 \times Tfilm) \qquad \textbf{(B.20)}$$

$$k = 0.071 - (0.000261 \times 4.23)$$

$$k = 0.06995 \frac{w}{m\,K}$$

$$Pr = c_p \times \frac{\mu}{k} \qquad \textbf{(B.21)}$$

$$Pr = 961.44 \times \frac{443.9 \times 10^{-6}}{0.06995}$$

$$Pr = 6.10$$

$$\beta = \frac{1}{\rho 2.23} \times \frac{\rho 2.22 - \rho 2.77}{\Delta T} \qquad \textbf{(B.22)}$$

$$\beta = \frac{1}{1523.1} \times \frac{1523.12 - 1521.54}{0.556}$$

$$\beta = 1.869 \times 10^{-3} \frac{1}{K}$$

$$\nu = \frac{\mu}{\rho} \qquad \textbf{(B.23)}$$

$$\nu = \frac{443.9 \times 10^{-6}}{1517.8} = 292.46 \times 10^{-3} \frac{m^2}{s}$$

$$\alpha = \frac{k}{\rho \times C_p} \qquad \textbf{(B.24)}$$

$$\alpha = \frac{0.06995}{1517.8 \times 961.44} = 47.94 \times 10^{-9} \frac{m^2}{s}$$

Using the above physical property equations evaluated at Tfilm, h_b is obtained by iteration to an accuracy of 10^{-6}.

$$h_b = 366.21 \frac{W}{m^2 K}$$

and

$$n = \frac{(366.21)(44.45 \times 10^{-3})}{(402.74)(30.6 \times 10^{-6})} = 36.34$$

$$q_f = (366.21 \times 44.45 \times 10^{-3} \times 402.74 \times 30.6 \times 10^{-6})^{0.5} \times 3.19 \times \tanh(36.34 \times 0.02576)$$

$$q_f = 1.15W$$

The corresponding results for the three inch long end is found to be

$$h_b = 292 \frac{W}{m^2 K}$$

$$q_f = 1.38 \ W$$

The heat transferred from the heated 8-inch section is then calculated as

$$q = 449.469 - 1.15 - 1.38$$

$$q = 446.939 \ W$$

The heat flux and heat transfer coefficients are then obtained from

$$q'' = \frac{q}{A_s} \qquad \textbf{(B.25)}$$

$$q'' = \frac{446.939}{\pi \times 14.15 \times 10^{-3} \times 0.2032}$$

$$q'' = 4.95 \times 10^4 \frac{W}{m^2}$$

and

$$h = \frac{q''}{\Delta T} \qquad \textbf{(B.26)}$$

$$h = \frac{4.95 \times 10^4}{3.19}$$

$$h = 1.51 \times 10^4 \frac{W}{m^2 K}$$

APPENDIX C. UNCERTAINTY ANALYSIS

The uncertainty associated with experimental parameters is calculated from the equation suggested by Kline and McClintock [Ref. 24]. If

$$R = R(x_1, x_2, ..., x_n) \tag{C.1}$$

then

$$\delta R = \left[\left(\frac{\partial R}{\partial x_1} \delta x_1 \right)^2 + \left(\frac{\partial R}{\partial x_2} \delta x_2 \right)^2 + ... \left(\frac{\partial R}{\partial x_n} \delta x_n \right)^2 \right]^{\frac{1}{2}} \tag{C.2}$$

where δR is the uncertainty of the desired dependent variable R and δx_1, δx_2, ..., δx_n are the uncertainties associated with the n variables, x_1, x_2, ... x_n.

The boiling heat transfer coefficient is given by

$$h = \frac{q}{A_s \times (\bar{T}_{wo} - T_{sat})} \tag{C.3}$$

where

$$\bar{T}_{wo} = \bar{T}_{wi} - \frac{q \times \ln\left(\frac{D_o}{D_i}\right)}{2 \times \pi \times k_{cu} \times L} \tag{C.4}$$

In equation (C.4), the second term on the right hand side is called the Fourier conduction term. If we define this term as,

$$\phi = \frac{q \times \ln\left(\frac{D_o}{D_i}\right)}{2 \times \pi \times k_{cu} \times L} \tag{C.5}$$

and

$$\Delta T = \bar{T}_{wo} - T_{sat} \tag{C.6}$$

then the uncertainty in the heat transfer coefficient is obtained from the following equation:

$$\frac{\delta h}{h} = \left[\left(\frac{\delta q}{q}\right)^2 + \left(\frac{\delta A_s}{A_s}\right)^2 + \left(\frac{\delta \bar{T}_{wi}}{\Delta T}\right)^2 + \left(\frac{\delta \phi}{\Delta T}\right)^2 + \left(\frac{\delta T_{sat}}{\Delta T}\right)^2\right]^{\frac{1}{2}} \tag{C.7}$$

where

$$q = V \times I \tag{C.8}$$

$$\frac{\delta q}{q} = \left[\left(\frac{\delta V}{V}\right)^2 + \left(\frac{\delta I}{I}\right)^2\right]^{\frac{1}{2}} \tag{C.9}$$

where $\frac{\delta V}{V}$ and $\frac{\delta I}{I}$ are given accuracy of the sensors which were used in

experimentation. Calculation of surface area and the uncertainty of it were given as

$$A_s = \pi \times D_o \times L \tag{C.10}$$

$$\frac{\delta A_s}{A_s} = \left[\left(\frac{\delta D_o}{D_o} \right)^2 + \left(\frac{\delta L}{L} \right)^2 \right]^{\frac{1}{2}} \tag{C.11}$$

$\frac{\delta D_O}{D_o}$ and $\frac{\delta L}{L}$ are estimated quantities.[1] The uncertainty calculation of the Fourier conduction term is given below.

$$\frac{\delta \phi}{\phi} = \left[\left(\frac{\delta q}{q} \right)^2 + \left(\frac{\delta k_{cu}}{k_{cu}} \right)^2 + \left(\frac{\delta L}{L} \right)^2 \right]^{\frac{1}{2}} \tag{C.12}$$

k_{cu} was calculated using below equation

$$k_{cu} = 434.0 - (0.112 \times \bar{T}_{wi-K}) \tag{C.13}$$

so uncertainty in k_{cu} can be found as

$$\delta k_{cu} = [\,(0.112 \times \delta \bar{T}_{wi-K})^2\,]^{\frac{1}{2}} \tag{C.14}$$

$\delta \bar{T}_{wi}$ and δT_{sat} are obtained using uncertainties in the thermocouple readings. Average wall inside temperature $\bar{T}_{wi}$ was obtained taking the average of six thermocouple readings inside the tube. The uncertainty associated with this variable is

[1] Work-shop device and human error in length and diameter measurements.

$$\delta \bar{T}_{wi} = \left[6 \times \left(\frac{\delta TC}{6} \right)^2 \right]^{\frac{1}{2}} \qquad \textbf{(C.15)}$$

where δTC was obtained as $\pm$0.5 C from [Ref. 23].

Saturation temperature was obtained by taking the average of two thermocouple readings and the uncertainty in this temperature was calculated from the following equation,

$$\delta T_{sat} = \left[2 \times \left(\frac{\delta TC}{2} \right)^2 \right]^{\frac{1}{2}} \qquad \textbf{(C.16)}$$

Table C1 shows the results of the uncertainty analysis performed using data file "TBHC05." Tube number one was arbitrarily chosen for the analysis. The high heat flux and low heat flux correspond to the value of q"=68.8 kW/m^2 and q"=697 W/m^2 respectively.

As seen in Table C1, uncertainty associated with the heat transfer coefficient increases to a value of 14.1% for low heat flux despite having a value of 8.7% for high heat flux.

For both low and high heat fluxes, the major uncertainty contribution is related to the term of δT_{sat}. Since only two saturation temperature readings are taken in the refrigerant, the equation (C.16) results in the value of $\delta T_{sat} = \pm 0.3534$. Since the ΔT has a small value (2.77 C) at low heat flux, the term of $\frac{\delta T_{sat}}{\Delta T}$ causes a noticeable increase in the uncertainty associated with the heat transfer coefficient.

TABLE C1. UNCERTAINTY ANALYSIS RESULTS

Variable	High Heat Flux	Low Heat Flux
ΔT	4.05 C	2.77 C
$\bar{T}_{wi}$	6.94 C	5.03 C
T_{sat}	2.28 C	2.20 C
$\frac{\delta V}{V}$	.5%	.5%
$\frac{\delta I}{I}$	.5%	.5%
$\frac{\delta q}{q}$	.71%	.71%
$\frac{\delta D_o}{D_o}$	.1%	.1%
$\frac{\delta L}{L}$	.1%	.1%
$\frac{\delta A_s}{A_s}$	.14%	.14%
$\frac{\delta k_{cu}}{k_{cu}}$	7.6%	7.6%
$\frac{\delta \phi}{\phi}$	7.6%	7.6%
$\frac{\delta h}{h}$	8.7%	14.1%

LIST OF REFERENCES

1. Thome, J.E., 'Enhanced Boiling Heat Transfer," 1st ed., Hemisphere Publication Corporation, USA, 1990.

2. Murphy, T.J., 'Pool Boiling of R-114/Oil Mixtures from Single Tube and Tube Bundles," Master's Thesis, Naval Postgraduate School, Monterey, CA, September 1987.

3. Marto, P.J. and Memory, S., 'Nucleate Pool Boiling of R-114/Oil Mixtures from Enhanced Surfaces: Part 1, Single Tubes" to be published in 1991.

4. Yilmaz, S. and Palen, J.W., 'Performance of Finned Tube Reboilers in Hydrocarbon Service," ASME Paper No. 84-HT-91, 1981.

5. Müller, J., and Hahne, E., 'Boiling Heat Transfer in Finned Tube Bundles," *Heat Transfer - Sov. Res.,* Vol. 13, No. 6, pp. 19-25, 1981.

6. Hahne, E. and Müller, J., 'Boiling on a Finned Tube and a Finned Tube Bundle," *Int. Heat Mass Transfer,* Vol. 26, pp. 849-859.

7. Anderson, C.L., 'Nucleate Pool Boiling Performance of Smooth and Finned Tube Bundles in R-113 and R-114/Oil Mixtures," Master's Thesis, Naval Postgraduate School, Monterey, CA, June 1989.

8. Yilmaz, S., Palen, J.W., and Taborek, J., 'Enhanced Boiling Surfaces as Single Tubes and Tube Bundles," *Advances in Enhanced Heat Transfer, - 1981,* Eds. R.L. Webb *et al.*, ASME, New York, HTD - Vol. 18, pp. 123-129, 1981.

9. Reilly, J.T., 'The Influence of Oil Contamination on Nucleate Pool Boiling Behavior R-114 From a Structured Surface," Master's Thesis, Naval Postgraduate School, March 1985.

10. Akcasayar, N., 'Nucleate Pool Boiling Performance of Finned and High Flux Tube Bundles in R-1144/Oil Mixtures," Master's Thesis, Naval Postgraduate School, Monterey, CA, December 1989.

11. Fujita, Y., Ohta, H., Yoshida, K., Hidaka, S., and Nishikawa, K., "Nucleate Boiling Heat Transfer in Horizontal Tube Bundles (1st Report; Experimental Investigation on Tube Bundle Effect)," *Memoirs of the Faculty of Engineeringg,* Kyusu University, Vol. 44, No. 4, pp. 427-446, 1984.

12. Fujita Y., Ohta H., Hidaka S., and Nishikawa, K., "Nucleate Boiling Heat Transfer on Horizontal Tubes in Bundles," *Proc. 8th IHTC,* San Francisco (1986), pp. 2131-2136.

13. Stephan, K., "Influence of Oil on Heat Transfer of Boiling Freon-12 and Freon-22," *Proceedings of the XI International Congress on Refrigeration,* Vol. 1, 1963, pp. 369-379.

14. Henrici, H., and Hesse, G., "Untersuchungen uber den warmeubergang beim verdampfen vou R-114 und R-114-oil-gemmischen an einem horizontalen glattrohr," *Kaltechnik-Klimatisierrun,* Vol. 23, 1971, pp. 54-58.

15. Danilova, G.N., and Dyundin, V.A., "Heat Transfer with Freons 12 and 22 Boiling at Bundles of Finned Tubes," *Heat Transfer Soviet Research,* Vol. 4, No. 4, July-August 1972.

16. Zebrowski, D., "Condensation Heat Transfer Measurements of Refrigerants on Externally Enhanced Tubes," Master's Thesis, Naval Postgraduate School, Monterey, CA, 1986.

17. Wanniarachchi, A.S., Marto, P.J., and Reilly, J.T., "The Effect of Oil Contamination on the Nucleate Pool-Boiling Performance of R-114 from a Prous-Coated Surface, *ASHRAE Transactions,* Vol. 92, Part 2, 1986..

18. Freon Product Information, "Freon Flurocarbon Properties and Applications", by Dupont, p. 4, 1975.

19. Sawyer, L.M., Jr., "The Effects of Oil Contamination on the Nucleate Pool-Boiling Behavior of R-114 from Enhanced Surfaces," Master's Thesis, Naval Postgraduate School, Monterey, CA, December 1986.

20. Marto, P.J., and Anderson, C.L., "Nucleate Boiling Characteristics of R-113 in a Smali Tube Bundle," *ASME/JSME Thermal Engineering Joint Conference,* Reno, NV, March 1991.

21. Churcill, S.W., and Chu, F.H.S., "Correlating Relations for Laminar and Turbulent Free Convection from a Horizontal Cylinder," *International Journal Heat Mass Transfer,* Vol. 18, pp. 1049-1070, 1975.

22. Pulido, R.J., "Nucleate Pool Boiling Characteristics of Gewa-T Finned Surfaces in Freon-113," Master's Thesis, Naval Postgraduate School, Monterey, CA, September 1984.

23. "Thermophysical Properties of Refrigerants," American Society of Heating, Refrigerating and Air-Conditioning Engineers, Inc., 1973, p. 61.

24. Kline, S.J., and McClintock, F.A., "Describing Uncertainties in Single Sample Experiments," *Mechanical Engineering,* p. 3, 1953.

INITIAL DISTRIBUTION LIST

1.	Defense Technical Information Center Cameron Station Alexandria, VA 22304-6145	2
2.	Library, Code 52 Naval Postgraduate School Monterey, CA 93943-5002	2
3.	Department Chairman, Code ME Department of Mechanical Engineering Naval Postgraduate School Monterey, CA 93943-5000	1
4.	Naval Engineering Curricular Office, Code 34 Department of Mechanical Engineeering Naval Postgraduate School Monterey, CA 93943-5000	1
5.	Professor Paul J. Marto, Code ME/Mx Department of Mechanical Engineering Naval Postgraduate School Monterey, CA 93943-5000	5
6.	Mr. R. Helmick, Code 2722 David Taylor Research Center Annapolis, MD 21402-5067	1
7.	Mr. J. Hanrahan, Code 2722 David Taylor Research Center Annapolis, MD 21402-5067	1
8.	Mr. A. Smookler NAVSEA (Code 05R32) Department of the Navy Washington, D.C. 20362-5101	1

9.	Dr. J. DeCorpo NAVSEA (Code 56YB) Department of the Navy Washington, D.C., 20362-5101	1
10.	Mr. Bruce G. Unkel NAVSEA (Code 56Y15) Department of the Navy Washington, D.C., 20362-5101	1
11.	Dz. Kd., Utgm. Hakan Eraydin Selimiye Eczane Sok. No 20/16 Caner Apt. Selimiye, Istanbul, TURKEY	3
12.	Deniz Kuvvetleri Komutanligi Personel Daire Baskanligi Bakanliklar-Ankara / TURKEY	1
13.	Deniz Harp Okulu Komutanligi Tuzla - Istanbul / TURKEY	2
14.	Ortadogu Teknik Universitesi Makina Muh. Ankara / TURKEY	1
15.	Istanbul Teknik Universitesi Makina Muh. Istanbul / TURKEY	1
16.	Dokuz Eylul Universitesi Makina Muh. Izmir / TURKEY	1